ΠΑΝΕΠΙΣΤΗΜΙΟ ΚΡΗΤΗΣ
ΤΜΗΜΑ ΙΑΤΡΙΚΗΣ
ΔΙΑΤΜΗΜΑΤΙΚΟ ΠΡΟΓΡΑΜΜΑ ΜΕΤΑΠΤΥΧΙΑΚΩΝ ΣΠΟΥΔΩΝ ΕΓΚΕΦΑΛΟΣ ΚΑΙ ΝΟΥΣ

ΔΙΔΑΚΤΟΡΙΚΗ ΔΙΑΤΡΙΒΗ

ΝΕΥΡΟΦΥΣΙΟΛΟΓΙΚΗ ΜΕΛΕΤΗ ΕΓΚΕΦΑΛΟΥ ΠΙΘΗΚΟΥ ΚΑΤΑ ΤΗΝ ΕΚΤΕΛΕΣΗ ΚΙΝΗΣΕΩΝ ΠΡΟΣ ΣΤΟΧΟΥΣ

ΜΑΡΙΝΑ ΚΙΛΙΝΤΑΡΗ

ΕΠΙΒΛΕΠΟΥΣΑ: ΚΑΘ. ΕΛΕΝΗ Ε. ΣΑΒΒΑΚΗ

ΗΡΑΚΛΕΙΟ, 2010

UNIVERSITY OF CRETE
FACULTY OF MEDICINE
INTERDISCIPLINARY GRADUATE PROGRAMME IN THE BRAIN AND MIND SCIENCES

PHD THESIS

NEUROPHYSIOLOGICAL STUDY OF THE MONKEY BRAIN DURING TARGET ORIENTED MOVEMENTS

MARINA KILINTARI

SUPERVISOR: PROF. H.E. SAVAKI

HERAKLION, 2010

Ευχαριστίες

Η παρούσα διδακτορική διατριβή εκπονήθηκε στα πλαίσια του μεταπτυχιακού προγράμματος Έγκέφαλος και Νους¨. Θα ήθελα να ευχαριστήσω θερμά όλους όσους με βοήθησαν κατά τη διάρκεια αυτής της προσπάθειάς μου.

Ευχαριστώ τους καθηγητές και τους συμφοιτητές μου στο μεταπτυχιακό πρόγραμμα. Ήταν υπέροχο να συμμετέχω σε αυτό. Θα ήθελα να αναφερθώ συγκεκριμένα στους Θεοδώρου Ειρήνη, Τζάνου Αθανασία, Κωνσταντουδάκη Ξένια, Καρδαμάκη Ανδρέα, Νερομυλιώτη Λευτέρη και Παπαδουράκη Βασίλη με τους οποίους κατά διαστήματα μοιραστήκαμε κάποιους εργαστηριακούς χώρους και μέρος της καθημερινότητάς μας. Στις Μπακόλα Σοφία και Ευαγγελίου Μίνα για τη βόηθειά τους τον πρώτο καιρό στο εργαστήριο και για τη μετέπειτα φιλία τους. Στην Ερημάκη Σοφία για τις ενδιαφέρουσες συζητήσεις και τις συμβουλές της. Στις Παγωμένου Μαρία και Πανάγου Μαρία για την γραμματειακή υποστήριξη. Στην Κεφαλογιάννη Μαρία για τη βοήθειά της στα τεχνικά προβλήματα που αντιμετώπισα. Στον Στάμο Αλέξη για την καλή και αποδοτική συνεργασία που είχαμε όλα αυτά τα χρόνια. Η Μαρία και ο Αλέξης είναι τα άτομα με τα οποία έζησα τα τελευταία 4 χρόνια στο εργαστήριο και τους ευχαριστώ που έκαναν αυτόν τον καιρό ευχάριστο.

Θέλω να ευχαριστήσω τους καθηγητές Τσιλιμπάρη Μιλτιάδη, Κουγιουμουτζάκη Γίαννη, Χριστάκο Κώστα, Μοσχοβάκη Αντώνη, Ράο Βασίλη και την καθηγήτρια Γρηγορίου Γεωργία που δέχτηκαν να συμμετάσχουν στην Επταμελή Εξεταστική Επιτροπή. Επιπλέον, θα ήθελα να ευχαριστήσω τον κο. Χριστάκο Κώστα γιατί η αμεσότητα με την οποία αντιμετωπίζει τους φοιτητές, μου έδωσε το θάρρος να εκφράσω την επιθυμία μου να συμμετάσχω στο μεταπτυχιακό πρόγραμμα Έγκέφαλος και Νους¨, τον κο. Δαλέζιο Γιάννη για την ανιδιοτελή βοήθειά του, την κα. Γρηγορίου Γεωργία για τη βοήθειά της κατά την συγγραφή της διδακτορικής μου διατριβής και την επίλυση των αποριών μου, τον κο. Μοσχοβάκη Αντώνη γιατί αποτέλεσε για μένα πρότυπο καθηγητή και επιστήμονα και τον κο. Ράο Βασίλη γιατί ήταν η κινητήρια δύναμη του εργαστηρίου όλα αυτά τα χρόνια.

Πάνω από όλους θα ήθελα να ευχαριστήσω την καθηγήτριά μου κα. Σαββάκη Ελένη που με εμπιστεύτηκε και μου ανέθεσε αυτό το διδακτορικό. Με στήριξε πάντα σε όλες τις προσπάθειές μου, ακόμα και σε αυτές που δεν αφορούσαν αυστηρά την παρούσα διδακτορική διατριβή. Μου μετέδωσε τις γνώσεις της με υπομονή και ενθουσιασμό. Την ευχαριστώ για την καθοδήγησή της και την ασφάλεια που αυτή μου παρέχει. Η μαθητεία δίπλα της είναι μοναδική εμπειρία. Είναι τιμή μου να την έχω δασκάλα μου.

Τίποτα από ότι έχω επιτύχει ως τώρα, δεν θα ήταν δυνατό αν δεν είχα την στήριξη της οικογένειάς μου. Τους είμαι ευγνώμων.

Funding:
Greek Secretariat of Research and Technology (PENED grant 03ED803)
European Union (FP6 grant IST-027574)

Article in press:
Kilintari M, Raos V, Savaki HE. Grasping in the dark activates early visual cortices. Cereb Cortex 2010; doi: 10.1093/cercor/bhq175

Contents

Ευχαριστίες **iii**

Περίληψη **xi**

Summary **xv**

Glossary & List of Abbreviations **xvii**

1 Introduction **1**

Visual Areas . . . 6

Visual area V1 (primary visual or striate cortex) . . . 6

Visual area V2 . . . 10

Visual area V3 . . . 14

Visual area V3A . . . 17

Visual area V4 . . . 18

Connections . . . 24

Connections of visual area V1 . . . 24

Connections of visual area V2 . . . 26

Connections of visual area V3 . . . 28

Connections of visual area V3A . . . 28

Connections of visual area V4 . . . 29

Functional Streams . . . 30

2 Aim of the Study **33**

3 Methods **35**

Subjects . . . 35

Animal Preparation . . . 35

Experimental Set-up . . . 36

Behavioural Tasks . . . 36

Grasping in the light (Gl) . . . 36

Grasping observation (O) . . . 37

Motion control (Cm) . . . 37
Fixation control (Cf) . . . 37
Grasping in the dark (Gd) . . . 38
Control in the dark (Cd) . . . 38
[^{14}C]-Deoxyglucose Method in Brain Imaging . . . 38
Theoretical basis . . . 38
[^{14}C]-deoxyglucose experiment . . . 43
Analysis of arterial plasma 2DG and glucose concentrations . . . 43
Tissue processing . . . 44
Analysis of autoradiographs . . . 44
Two-dimensional reconstructions . . . 44
Geometrical normalisation and activity plots . . . 45
Histology . . . 46

4 Results **49**

5 Discussion **67**

References **79**

List of Figures

1.1 Schematic representation of the two cortical visual pathways. 32

3.1 Schematics of behavioural paradigms and task events. 39
3.2 Theoretical basis of the radioactive deoxyglucose method for measurement of local cerebral glucose utilisation 41
3.3 Operational equation of the radioactive deoxyglucose method 43
3.4 2D reconstruction of metabolic and anatomical maps of the occipital cortex. 47

4.1 3D histograms of the dwell time of the line of sight as a function of eye position. . . 50
4.2 2D spatial reconstruction of the LCGU values (μmol/100g/min) of the metabolic activity in the occipital cortex of the four hemispheres of the two monkeys reaching-to-grasp in the light (Gl). 53
4.3 Quantitative 2D-maps of metabolic activity in the occipital cortex of the grasping light monkeys and percent LCGU difference from the motion control. 54
4.4 2D spatial reconstruction of the metabolic activity in the occipital cortex of the six hemispheres of the three observation monkeys (O). 55
4.5 Quantitative 2D-maps of metabolic activity in the occipital cortex of the observation monkeys and % LCGU difference from the motion control. 57
4.6 Differential activations induced by the Gl and O tasks. 58
4.7 2D spatial reconstruction of the LCGU values (μmol/100g/min) in the occipital cortex of the four hemispheres of the two grasping-in-the-dark monkeys (Gd). 59
4.8 Quantitative maps of activity in the occipital cortex of monkeys in complete darkness. 60
4.9 Effects of fixation and biological motion. 62
4.10 Plots of % LCGU differences along areas V3d and V4. 65

List of Tables

4.1 Average LCGU values from the two motion control (Cm) monkeys. 51
4.2 Metabolic effects in occipital cortical areas of the monkey brain. 63

Περίληψη

Οι μηχανισμοί με τους οποίους τα άτομα αντιλαμβάνονται τις ενέργειές τους είναι ιδιαίτερα σημαντικοί γιατί τους επιτρέπουν να καθορίσουν τον εαυτό τους ανεξάρτητα από το εξωτερικό τους περιβάλλον. Συνεπακόλουθα, η αναγνώριση του εαυτού είναι προαπαιτούμενο για την απόδοση μιας συμπεριφοράς στον σωστό φορέα και τελικά για τη δημιουργία κοινωνικής συμπεριφοράς. Η διάκριση εαυτού/άλλου όσον αφορά στην αναγνώριση μιας κινητικής συμπεριφοράς μπορεί να φαίνεται σχετικά απλή όταν οι εκτελούμενες κινήσεις είναι ορατές. Η διάκριση όμως κατά την παρατήρηση κινήσεων που εκτελούνται από κάποιον άλλον καθώς και κατά την νοητική προσομοίωση φανταστικών κινήσεων αποτελεί πρόκληση. Παρόλο που οι δύο προαναφερθείσες καταστάσεις φαίνονται ανόμοιες, έχει δειχθεί ότι ενεργοποιούν κοινούς νευρωνικούς πληθυσμούς. Μελέτες λειτουργικής απεικόνισης εγκεφάλου, με τη χρήση της ποσοτικής αυτοραδιογραφικής μεθόδου της δεοξυγλυκόζης ([^{14}C]-δεοξυγλυκόζη), έδειξαν ότι πολλές κινητικές, σωματαισθητικές και συνειρμικές περιοχές του φλοιού των εγκεφαλικών ημισφαιρίων, ενεργοποιούνται τόσο κατά την εκτέλεση όσο και κατά την παρατήρηση κινήσεων σύλληψης. Δηλαδή, τα αποτελέσματα των μέχρι τώρα μελετών αποδεικνύουν ότι προκειμένου να καταλάβουμε μία πράξη που εκτελείται από ένα άλλο υποκείμενο, υποδυόμαστε αυτήν την κινητική συμπεριφορά μέσα μας και την επαναλαμβάνουμε νοερά, μία διαδικασία που ονομάζεται νοητική προσομοίωση.

Η παρούσα μελέτη διερευνά τη συμμετοχή των οπτικών περιοχών V1,V2, V3, V3A και V4 του φλοιού, στο νευρωνικό κύκλωμα που ενεργοποιείται κατά την παρατήρηση κινητικών συμπεριφορών που εκτελούνται από άλλα υποκείμενα και κατά την εκτέλεση κινήσεων σύλληψης απουσία οπτικής πληροφορίας από το ίδιο το υποκείμενο.

Με τη χρήση της ποσοτικής αυτοραδιογραφικής μεθόδου της [^{14}C]-δεοξυγλυκόζης χαρτογραφήθηκε η μεταβολική δραστηριότητα στην ινιακή καλύπτρα, στη μηνοειδή αύλακα και στην κάτω ινιακή αύλακα πιθήκων που εκτελούσαν τις παρακάτω δοκιμασίες: (α) εκτέλεση κίνησης σύλληψης τρισδιάστατου αντικειμένου με την άκρα χείρα παρουσία οπτικής πληροφορίας, (β) εκτέλεση κίνησης σύλληψης απομνημονευμένου τρισδιάστατου αντικειμένου με την άκρα χείρα στο σκοτάδι και (γ) παρατήρηση κίνησης σύλληψης τρισδιάστατου αντικειμένου με την άκρα χείρα από τον πειραματιστή.

Για την αποκάλυψη των εμπλεκόμενων φλοιϊκών περιοχών αναδομήθηκε δισδιάστατα ο οπτικός φλοιός σε όλη τη ραχιαίο-κοιλιακή και προσθιοπίσθια διάστασή του. Η δισδιάστατη αυτή αναδόμηση της μεταβολικής δραστηριότητας κάθε εγκεφαλικής περιοχής πραγματοποιήθηκε με τη μέτρηση της τοπικής εγκεφαλικής κατανάλωσης γλυκόζης, pixel ανά pixel (διακριτική ικανότητα 45-55 μm/pixel), κατά την προσθιοπίσθια έκταση 1300 οριζόντιων τομών εγκεφάλου και κατά μήκος μιας γραμμής παράλληλης στην επιφάνεια του φλοιού. Για κάθε τομή υπολογίστηκε μία σειρά τιμών κατανάλωσης γλυκόζης που

αντιστοιχούσε στην προσθιοπίσθια κατανομή λειτουργικής δραστηριότητας της υπό ανάλυση περιοχής του φλοιού. Ο μέσος όρος από τις σειρές τιμών 5 διαδοχικών τομών αντιστοιχεί σε 1 γραμμή του δισδιάστατου χάρτη στην προσθιοπίσθια διάσταση. Η ευθυγράμμιση των σειρών όλων των οριζόντιων τομών ανέδειξε το ραχιαιοκοιλιακό επίπεδο. Με τον τρόπο αυτό παράχθηκαν δισδιάστατοι χάρτες, των οποίων η διακρισιμότητα τόσο στην προσθιοπίσθια όσο και στην ραχιαιοκοιλιακή διάσταση ήταν 100 μm. Οι χάρτες αυτοί επιτρέπουν τη σύγκριση της κατανομής της μεταβολικής δραστηριότητας στις υπό μελέτη περιοχές.

Η σύγκριση του μέσου λειτουργικού χάρτη των πειραματόζωων που εκτελούσαν κινήσεις σύλληψης στο φως, με τον αντίστοιχο μέσο λειτουργικό χάρτη των πειραματόζωων ελέγχου, αποκαλύπτει σημαντική ενεργοποίηση στο ραχιαίο τμήμα της οπτικής περιοχής 3 (τόσο στο ινιακό-κροταφικό κομμάτι όσο και στο ινιακό-βρεγματικό), στην οπτική περιοχή 3A και στο τμήμα της οπτικής περιοχής 4 που βρίσκεται στην μηνοειδή αύλακα.

Η σύγκριση του μέσου λειτουργικού χάρτη των πειραματόζωων, τα οποία είχαν εκπαιδευτεί στην παρατήρηση κίνησης σύλληψης τρισδιάστατου αντικειμένου από τον πειραματιστή, με τον αντίστοιχο χάρτη των πειραματόζωων ελέγχου, αποκαλύπτει σημαντική ενεργοποίηση στην περιοχή αντιπροσώπευσης του κεντρικού οπτικού πεδίου του πρωτοταγούς οπτικού φλοιού, στο ραχιαίο τμήμα της οπτικής περιοχής 3 (τόσο στο ινιακό-κροταφικό κομμάτι όσο και στο ινιακό-βρεγματικό) και στην οπτική περιοχή 3A.

Τέλος, η σύγκριση του μέσου λειτουργικού χάρτη των πειραματόζωων που εκτελούσαν κινήσεις σύλληψης απομνημονευμένου τρισδιάστατου αντικειμένου στο σκοτάδι με αυτόν των αντίστοιχων πειραματόζωων ελέγχου, αποκαλύπτει σημαντική ενεργοποίηση στον πρωτοταγή οπτικό φλοιό στην ινιακή καλύπτρα, στον πρωτοταγή οπτικό φλοιό στην περιοχή της αντιπροσώπευσης του περιφερικού οπτικού πεδίου, στο τμήμα της οπτικής περιοχής 2 που βρίσκεται εντός της μηνοειδούς αύλακας στην περιοχή της αντιπροσώπευσης του περιφερικού οπτικού πεδίου και στο τμήμα της οπτικής περιοχής 2 που βρίσκεται εντός της κάτω ινιακής αύλακας. Επίσης ενεργοποίηση παρατηρήθηκε στο ινιακό-βρεγματικό τμήμα της ραχιαίας οπτικής περιοχής 3 και στο τμήμα της οπτικής περιοχής 3 που βρίσκεται εντός της κάτω ινιακής αύλακας και στην οπτική περιοχή 3A.

Σύμφωνα με τις λειτουργικές ιδιότητες των νευρώνων, την λειτουργική οργάνωση και τις συνδέσεις των οπτικών περιοχών 3 (V3) και 3A (V3A) προτείνουμε ότι η ενεργοποίηση αυτών των περιοχών για τις δοκιμασίες της παρατήρησης κίνησης σύλληψης από τον πειραματιστή και της σύλληψης απομνημονευμένου τρισδιάστατου αντικειμένου στο σκοτάδι αντιστοιχεί στην επεξεργασία πληροφορίας σχετική με την νοητική προσομοίωση της κίνησης. Οι περιοχές αυτές πιθανότατα κωδικοποιούν οπτικοχωρικές πληροφορίες που απαιτούνται για τη φάση προσέγγισης της κίνησης, τη θέση του αντικειμένου και την τρισδιάστατη απεικόνισή του, οι οποίες είναι απαραίτητες για τον κατάλληλο προσανατολισμό του χεριού και την αλληλεπίδραση με το αντικείμενο. Είναι γνωστό ότι οι περιοχές V3 και V3A αποτελούν τμήμα του ραχιαίου οπτικού μονοπατιού, το οποίο είναι υπεύθυνο για την αντίληψη των χωρικών σχέσεων και την πραγματοποίηση οπτοκινητικών μετασχηματισμών. Στη μελέτη μας, η ενεργοποίηση των περιοχών V3 και V3A μπορεί να αντικατοπτρίζει την είσοδο απομνημονευμένης οπτικοκινητικής πληροφορίας από τις ανώτερες βρεγματομετωπιαίες περιοχές του ραχιαίου οπτικού μονοπατιού προς τις κατώτερες οπτικές φλοιϊκές περιοχές. Προτείνουμε ότι κατά την παρατήρηση της κίνησης σύλληψης και την κίνηση σύλληψης απομνημονευμένου τρισδιάστατου αντικειμένου στο σκοτάδι, οι περιοχές V3 και V3A ενεργοποιούνται λόγω της εσωτερικής προσομοίωσης της παρατηρούμενης ή της απομνημονευμένης πράξης. Κατά την συνθήκη παρατήρησης, μέσω της

οπτικής νοητικής προσομοίωσης ανακαλούνται απομνημονευμένες οπτικοχωρικές πληροφορίες, οι οποίες αντικατοπτρίζουν την κίνηση και τις αισθητικές συνέπειές της. Κατά την συνθήκη της κίνησης στο σκοτάδι, μέσω της οπτικής νοητικής προσομοίωσης είναι πιθανό να ανακαλούνται απομνημονευμένες οπτικοχωρικές πληροφορίες απαραίτητες για τον έλεγχο των κινήσεων με την άκρα χείρα.
Συνοψίζοντας, κατά αντιστοιχία με την ενεργοποίηση των κινητικών, σωματαισθητικών και βρεγματικών περιοχών, η οποία παρέχει στην νοητικά προσομοιωμένη πράξη την κινητική και σωματαισθητική της αναπαράσταση, η ενεργοποίηση των οπτικών περιοχών κατά την εκτέλεση κινήσεων στο σκοτάδι και κατά την παρατήρηση κινήσεων παρέχει την οπτική αναπαράσταση στοιχείων της κίνησης.

Summary

In the past, we demonstrated that the neural system which supports both the generation of an action and the perception of the same action performed by another subject encompasses widespread areas in a parieto-frontal cortical network. In the present study we examined whether this system that helps match action perception to action generation extends beyond these areas to early visual cortices. We applied the quantitative autoradiographic method of [^{14}C]-deoxyglucose, combined with cytoarchitectonic identification of cortical areas, to explore early visual cortical areas throughout the cortex of the occipital operculum, lunate and inferior occipital sulci of twelve adult female monkeys (*Macaca mulatta*) performing three behavioural tasks: (a) grasping-in-the-light (Gl), (b) grasping-observation (O), and (c) grasping-in-the-dark (Gd). In order to disambiguate the effects of the purposely reaching/grasping action from the effects of (a) the non-goal-directed biological-motion elicited by a purposelessly moving forelimb in front of the monkey, and (b) the visual stimulation induced by mere presentation of the 3D-object, we compared the functional activity in the Gl and O monkeys with that in two arm-motion control (Cm) monkeys. To reveal the effects induced by reaching-to-grasp in the dark, we compared the functional activity in the two Gd monkeys with that in two control-in-the-dark monkeys (Cd). In order to reveal the effects induced by the behavioural tasks, we produced and compared two-dimensional reconstructions (2D-maps) of the spatio-intensive pattern of metabolic activity (LCGU values in μmol/100 g/min) throughout the full extent of the visual areas V1, V2, V3, V3A, and V4.

During grasping-in-the-light increased metabolic activity was evident in extrastriate areas V3d, V3A and V4 with the two segments of area V3d, the occipito-parietal reflecting peripheral vision and the occipito-temporal reflecting central vision being equally activated. During grasping-observation, area V4 was not activated, marginal activation was displayed in the representation of the central visual field of area V1 and significant activation was displayed in areas V3d and V3A with the occipito-temporal region of area V3d being more activated than the occipito-parietal. During grasping-in-the-dark activation was observed in areas V1, V2, V3A, and V3v. Area V3d was markedly activated in its occipito-parietal segment, contrary to the occipito-temporal which was not activated.

According to our previous proposal, the activations induced by grasping-observation in the parietal and motor cortex imply that observation of an action corresponds to simulation of its overt counterpart. Based on our present findings, we suggest that the activation of areas V3d and V3A for action-observation and for action-execution in the dark reflects the processing of visual information

related to the mental simulation of the action. Area V3 may relay to the motor system, via the parieto-frontal visuo-motor stream, visuospatial information required for the reaching component of the action and 3D-object-related information useful for the grasping constituent. Therefore, as the somatotopic activation of the primary somatosensory cortex during action-observation in our previous study supported an introspective kinesthetic feeling of the movement by the observer in a first person perspective, the activation of the early visual cortices during action-generation in the dark in the present study supports an internalized visual representation of the spatial-location and the 3D-form of the invisible object to be reached and grasped, i.e. visual imagery during action control.

Glossary & List of Abbreviations

2D	two dimensional	δισδιάστατος
3D	three dimensional	τρισδιάστατος
2DG or ^{14}C-DG	[^{14}C]-deoxyglucose	[^{14}C]-δεοξυγλυκόζη
2DG-6-P	[^{14}C]-deoxyglucose-6-phosphate	[^{14}C]-δεοξυγλυκόζη-6-φωσφορική
LCGU	local cerebral glucose utilization	τοπική κατανάλωση γλυκόζης στο φλοιό
afferent		προσαγωγός
claustrum		προτείχισμα
CO	metabolic enzyme cytochrome oxidase	ένζυμο κυτοχρωμική οξειδάση
corpus callosum		ακτινοβολία μεσολοβίου
efferent		απαγωγός
extrastriate		εξωταινιωτός
fMRI	functional magnetic resonance imaging	λειτουργική απεικόνιση μαγνητικού συντονισμού
TMS	transcranial magnetic stimulation	διακρανιακός μαγνητικός ερεθισμός
op	occipito-parietal	ινιακοβρεγματικό
ot	occipito-temporal	ινιακοκροταφικό
operculum		καλύπτρα
occipital operculum		ινιακή καλύπτρα
pons		γέφυρα
pulvinar		προσκέφαλο θαλάμου
splenium		σπληνίο μεσολοβίου
striate		ταινιωτός
superior colliculus		άνω διδύμιο
dorsal visual pathway		ραχιαία οπτική οδός
ventral visual pathway		κοιλιακή οπτική οδός

continued

Areas

area 8	area 8 of the prefrontal cortex	περιοχή 8 του προμετωπιαίου φλοιού
area prestriata		προταινιωτή περιοχή
BA17	Brodmann area 17	κυτταροαρχιτεκτονικό πεδίο 17 του Brodmann
BA18	Brodmann area 18	κυτταροαρχιτεκτονικό πεδίο 18 του Brodmann
BA19	Brodmann area 19	κυτταροαρχιτεκτονικό πεδίο 19 του Brodmann
CITd	central inferotemporal dorsal area	κεντρική κάτω κροταφική περιοχή, ραχιαίο τμήμα
CITv	central inferotemporal ventral area	κεντρική κάτω κροταφική περιοχή, κοιλιακό τμήμα
DL	dorsolateral area	ραχιοπλάγια περιοχή
DM	dorsomedial area	ραχιομέση περιοχή
DLr	rostral half of the DL	πρόσθιο ήμισυ της ραχιοπλάγιας περιοχής
DLc	caudal half of the DL	οπίσθιο ήμισυ της ραχιοπλάγιας περιοχής
DP	dorsal prelunate area	ραχίαια προμηνοειδής περιοχή
FEF	frontal eye fields	πρόσθια οφθαλμικά πεδία
FST	fundus of the superior temporal area	επί του πυθμένα της άνω κροταφικής αύλακας περιοχή
cIP	caudal intraparietal area	περιοχή στο οπίσθιο τμήμα της ενδοβρεγμάτιας αύλακας
LIP	lateral intraparietal area	περιοχή στο πλάγιο τμήμα της ενδοβρεγμάτιας αύλακας
MST	medial superior temporal area	έσω άνω κροταφική περιοχή
MSTd	medial superior temporal area, dorsal	έσω άνω κροταφική περιοχή, ραχιαία
MT (or V5)	middle temporal area (or visual area 5)	έσω κροταφική περιοχή / οπτική περιοχή 5

continued

MTp	far peripheral projection zone from V1 and V2 of MT	προβλητική ζώνη περιφερικής όρασης από τις V1 και V2 στην οπτική περιοχή 5/MT
PIP	posterior intraparietal area	οπίσθια ενδοβρεγματική περιοχή
PITd	posterior inferotemporal dorsal area	οπίσθια κάτω βρεγματική περιοχή, ραχιαία
PITv	posterior inferotemporal ventral area	οπίσθια κάτω βρεγματική περιοχή, κοιλιακά
PO	parieto-occipital area	βρεγματοϊνιακή περιοχή
TE	cytoarchitectonic area TE in anterior temporal cortex	κυτταροαρχιτεκτονική περιοχή TE στον κροταφικό φλοιό
TEO	area temporoccipital (cytoarchitectonic area TEO in posterior inferior temporal cortex)	κροταφική-ινιακή περιοχή
TF	cytoarchitectonic area TF on the parahippocampal gyrus (temporal area F)	κυτταροαρχιτεκτονική περιοχή TF στην παραϊπποκάμπεια έλικα
V1	visual area 1 or primary visual cortex or striate cortex	οπτική περιοχή 1 ή πρωτοταγής οπτικός φλοιός ή ταινιωτή περιοχή
V2	visual area 2	οπτική περιοχή 2
V3	visual area 3	οπτική περιοχή 3
V3d	dorsal part of visual area V3	ραχιαίο τμήμα οπτικής περιοχής 3
V3v (or VP)	ventral part of visual area V3	κοιλιακό τμήμα οπτικής περιοχής 3
VP	ventral posterior area (i.e. V3v)	κοιλιακό τμήμα οπτικής περιοχής 3
V3A	visual area V3A	οπτική περιοχή 3A
V4	visual area V4	οπτική περιοχή 4
V4a	visual area 4a	οπτική περιοχή 4a
V4t	transitional visual area 4	μεταβατική οπτική περιοχή 4t
VIP	ventral intraparietal area	κοιλιακή ενδοβρεγματική περιοχή
VOT	ventral occipitotemporal area	κοιλιακή ινιακοκροταφική περιοχή
VTF	visually responsive portion of temporal visual area F	οπτικά αποκρινόμενο τμήμα της κροταφικής οπτικής περιοχής F

continued

Sulci

As	arcuate sulcus	τοξοειδής αύλακα
Cs	central sulcus	κεντρική αύλακα
Cas	calcarine sulcus	πληκτραία αύλακα
IOs	inferior occipital sulcus	κάτω ινιακή αύλακα
Ls	lunate sulcus	μηνοειδής αύλακα
OTs	occipitotemporal sulcus	ινιακοκροταφική αύλακα
POs	parieto-occipital sulcus	βρεγματικοϊνιακή αύλακα
STs	superior temporal sulcus	άνω κροταφική αύλακα

Cortices

cingulate cortex		φλοιός του προσαγωγίου
frontal cortex		μετωπιαίος φλοιός
insular cortex		νησιδιακός φλοιός
occipital cortex		ινιακός φλοιός
parahippocampal cortex		παραϊπποκάμπειος φλοιός
parietal cortex		βρεγματικός φλοιός
prefrontal cortex		προμετωπιαίος φλοιός
primary visual cortex		πρωτοταγής οπτικός φλοιός
polysensory cortex		πολυαισθητικός φλοιός
temporal cortex		κροταφικός φλοιός

Nuclei

amygdaloid nucleus		αμυγδαλοειδής πυρήνας
intralaminar nuclei		ενδοπετάλιοι πυρήνες θαλάμου
nucleus basalis of Meynert		βασικός πυρήνας του Meynert
LGN	lateral geniculate nucleus	έξω γονατώδης πυρήνας

end of list

CHAPTER 1

Introduction

A fundamental cognitive process is to acquire and retain knowledge about the external world. This perceived information is used by the agent to interact with the environment, to develop behavioural strategies and probably to match individual dispositions with that of his companions. It is evident that knowledge and skills are built and learned in collaborative social activity. Yet a fundamental question remains to be explored. How knowledge and skills sharing is achieved, how a joint experience of the world and of the existing objects is communicated and how the detection and understanding of purposeful strategies is accomplished.

Communication and understanding is present even in newborns. Within minutes of birth a baby can enter into a dialogue of expressions with another person, in which the taking of turns is expected. At the time, the infant imitation is intentional and his/her provocation when he/she seeks communication is attentive (Fiamenghi 1997; Kugiumutzakis 1998; Nagy and Molnar 2004). Among other researchers, neuroscientists vigilantly try to clarify the processes that signal the direction and the aim of the interest of people and mediate sequences of actions which convey their intentions and goals. Therefore the discovery of the neural bases of action understanding is of utmost importance. These processes are achieved, up to a significant level, by readily exchanging information with other agents. The discovery of mirror neurons in F5 boosted this premise and augmented the argument that action understanding is based on mechanisms that match observation and execution of goal-related motor actions (Gallese et al. 1996; Rizzolatti et al. 1996; Gallese and Goldman 1998). Mirror neurons are activated during object-oriented actions, whether they are performed or observed by the recording monkey. This finding was among the first that revealed a direct correspondence between a neural substrate and the visual perception of an action, although very early in the imagery study such a correspondence has been assumed. Hebb had wittily remarked that first order and higher order cell assemblies are the foundation for the specific and less specific imagery processes respectively (Hebb 1968).

It has been proposed that the observation, perception and imitation of actions executed by others, and the planning of actions executed in due course by the subjects themselves can be accomplished through the formation of mental images and the implementation of mental simulation. Mental imagery gained quite early the attention of the scientific community, and its functional constituents

were explored. Imagery was regarded to have a mnemonic role (Bower 1970; Paivio 1975), to function as a cognitive strategy (Huttenlocher et al. 1972) or to be a similar process to perception (Segal and Fusella 1970). Imagery can be recruited in two conditions: when the subject voluntarily forms a mental image or action and when the subject observes other agents. In the latter case the perceiver can rehearse the representation of an action and the simulation can provide a frame for the recognition of this action.

A visual mental image can be formed in the absence of an immediate appropriate sensory input. It is an internal representation similar to that created during the initial phases of perception, without the stimulus actually being perceived. Researchers have expressed different opinions regarding the form of internal representations for imagery. The two main theories are the propositional interpretation and the depictive interpretation. The propositional interpretation supports that images are memorized as propositions (nodes/points) linked to each other constructing a network. In the propositional theory, the mental representations are processed in a serial ordered way in which people search the nodes and links of the network to find the feature of interest. The propositional format is a symbolic amodal representation that simplifies the mental process and provides a common framework for all mental representations [(e.g. visual, linguistic etc (Pylyshyn 1973, 2002; Pylyshyn 2003)]. The depictive interpretation argues that many properties of the images are embodied in the mental representation of the perceived image (Kosslyn et al. 2006b). The notion that the visual images parallel the internal structures of their referents and exhibit some of the same spatial properties as do the original percepts can be supported by several experimental results. Findings which imply that mental representations are processed in a picture-like way were presented from the beginning of the mental imagery debate. Well-known experiments are those of mental rotation (Cooper and Shepard 1973; Bethell-Fox and Shepard 1988). For example, in one of the original studies, the subjects had to compare a test object visually presented in different orientations, with another reference object presented in another orientation and had to determine if the portrayed 2D objects corresponded to the same 3D objects. The subjects reported that the process they employed was to rotate one end of one object into congruence with the corresponding end of the other object and examine whether the rest parts were also coinciding (Shepard and Metzler 1971). Other influential experiments are those of visual scanning. Kosslyn demonstrated that people can scan the distances embodied in images. Scanning times increased when subjects had to scan larger images, and consequently reaction times were bigger because subjects had to scan further distances across the visual images. Kosslyn described visual representations as quasi-pictorial mental images which seem to embody information about actual interval spatial extents (Kosslyn et al. 1978). Shepard and Metzler (1971) had also demonstrated that the reaction time of the subjects increased as a linear function of the angular difference between the two compared objects. The well-established behavioural effect of compatibility between physically presented stimuli and overt responses was also reported in more recent studies regarding imagery; e.g. it was demonstrated that in imagery, as in perception, response times are slower for stimuli and responses which are on opposite sides of the image (Tlauka and McKenna 1998).

When imagery involves voluntary control on part of the imager as an agent, then the internal representations are conceived as ”motor imagery” (Annett 1995). Motor imagery refers to internal motor schemas from a first person perspective (Jeannerod 1994) or similarly to an image that the participant experiences as if he or she were performing the action voluntarily (Annett 1995).

The varieties of imaginary actions include both the voluntary manipulation of imaginary objects and the imaginary manipulation of physically present objects (Annett 1995). Motor imagery has become an important topic in the areas of rehabilitation, e.g. in promoting the recovery of motor function following stroke (Stevens and Stoykov 2003; Sharma et al. 2006; Zimmermann-Schlatter et al. 2008), in mental practice (Driskell et al. 1994), in sport psychology and athletic training and performance (Mahoney and Avener 1977; Driskell et al. 1994; Cumming and Hall 2002; Gregg and Hall 2006), and in bodily preparation for action and in action control, where the neural bases and temporal characteristics of motor imagery can be explored to aid our understanding of action (Jeannerod 1997). Motor imagery [or mental practice: the systematically repeated imagination (covert rehearsal) of the movement pattern in the absence of any muscular movements] can also be employed in observational learning and mental training, without any physical realization of the task (Elliott and Khan 2010).

As in the case of visual imagery, several parameters that are encoded in real actions are found in motor images. Experimental data underscore that mental and overt actions have prominent similarities. First of all, the time needed to execute them is very similar. In a classic experiment the subjects were asked to walk a certain distance both overtly and mentally to targets located at different distances. It was found that walking times were the same in both cases. Moreover, in both conditions the walking time increased when the walking distance increased too (Decety et al. 1989). Here we would like to mention that similar results were demonstrated in a visual imagery study (Kosslyn et al. 1978). In another study, where the subjects were tested in graphic tasks, it was shown that a mental execution of a writing or drawing task entails temporal information processes similar to those used when the movement is actually performed (Decety and Michel 1989). Another well-known experiment investigated mentally simulated actions in a virtual reality environment (Decety and Jeannerod 1996). The participants had to walk mentally through gates of different widths positioned at different distances within a virtual environment. Mental walking time was found to increase with increasing gate distance and decreasing gate width. Therefore Fitts law (Fitts 1992), which states that more difficult physical movements take more time to be executed than do easier ones, also applies to imagined movements. Similar results were obtained in a previous experiment, where subjects were asked either to actually walk or imagine themselves walking on four beams which had the same length but varied in width. Indeed the results were consistent with an inverse relationship between the difficulty of a movement and the speed with which it can be performed. The beam width was a factor of difficulty of the task, such that it took longer to walk on a narrower beam (Decety 1991). Another study, exemplifying the fact that motor imagery uses same processes that are used in motor execution, examined the time needed by the subjects to configure their hand from one resting posture to another, when they executed the task physically or mentally. It was revealed that the time to imagine the movement was highly correlated with the time to actually perform the movement and the time for two conditions was usually equal when the actions were related to familiar hand postures. This finding indicates that not only time, but also kinematic constraints, are similarly represented in the two cases(Parsons 1994). In another noteworthy study, the researchers examined how a perceptual variable known to affect grip selection, the orientation of a manipulandum, affected internally represented actions and the prospective action judgments. The participants were required either to actually grasp a visually presented dowel or judge how they would grasp it under comparable circumstances. It was found

that the time taken by the subjects to give the response increased as a function of the angle at which the bar was presented (Johnson 2000). Thus, in motor imagery as in real grasping, the selection of the final hand position is dictated by the biomechanical demands and the awkwardness of the final posture and is accomplished through the shortest biomechanically plausible trajectory (Rosenbaum et al. 1995). These and other results, e.g. (Adams et al. 1987; Decety et al. 1991; Decety et al. 1993; Sirigu et al. 1996; Cerritelli et al. 2000; Paccalin and Jeannerod 2000; Papaxanthis et al. 2002a; Papaxanthis et al. 2002b; Papaxanthis et al. 2003) suggest that processes underlying mental movements within internally represented space are similar to those underlying actual movements within physical space.

In general, both visual and motor imagery should be considered as processes which rely on the same mechanisms and use much of the same cortical areas employed in perception and overt generation of actions, and which result in internal representations that convey, store and assemble information regarding an external stimulus.

There is a growing body of evidence suggesting that motor imagery involves a subsystem of that involved in motor planning and/or control. Imagining movements activates areas involved in motor planning and control including the supplementary and pre-motor areas (Rao et al. 1993; Decety et al. 1994; Stephan et al. 1995; Deiber et al. 1998; Lotze et al. 1999; Gerardin et al. 2000; Hanakawa et al. 2003; Iseki et al. 2008), the parietal cortex (Stephan et al. 1995; Sirigu et al. 1996; Deiber et al. 1998; Gerardin et al. 2000; Hanakawa et al. 2003), the cerebellum and the basal ganglia (Decety et al. 1988; Decety et al. 1990; Ryding et al. 1993; Gerardin et al. 2000; Hanakawa et al. 2003). Although there has been some controversy in the neuroimaging literature regarding involvement of the primary motor cortex (MI) during motor imagery, experiments often reveal activity increases in MI during motor imagery and in some cases in somatosensory cortex (Hallett et al. 1994; Porro et al. 1996; Roth et al. 1996; Hari et al. 1998; Gerardin et al. 2000; Porro et al. 2000).

Furthermore, we have also demonstrated that the neural system which supports both the generation of an action and the perception of the same action performed by another subject encompasses widespread areas in a parieto-frontal cortical network. We have shown that it involves several premotor and cingulate areas as well as the primary motor and somatosensory cortices, which are somatotopically activated when subjects observe object-related hand actions, as they are for execution of the same actions (Raos et al. 2004, 2007). We have also demonstrated that this resonant system, which helps action-perception to match action-generation, involves extensive regions of the lateral, medial and intra-parietal cortex of the primate brain (Evangeliou et al. 2009). Our findings complement the results of other studies reporting activation of parts of this parieto-frontal cortical network not only by execution but also by mere observation of goal directed hand actions (Grafton et al. 1996; Decety et al. 1997; Hari et al. 1998; Buccino et al. 2001; Avikainen et al. 2002; Cisek and Kalaska 2004; Filimon et al. 2007; Tkach et al. 2007).

Evidently, there is general agreement that several higher-order cortical areas are involved in both visual and motor imagery processes. However, the possible involvement of lower-order visual areas in imagery is intensely debated (Kosslyn and Thompson 2003). Several studies have shown that the primary visual cortex can become activated when people visualise objects with their eyes closed, e.g. (Le Bihan et al. 1993a; Kosslyn et al. 1995; Sabbah et al. 1995; Chen et al. 1998; Thompson et al. 2001). Yet, other reports did not detect any activity in V1 and adjacent visual areas such as V2 and V3 (e.g. (Roland et al. 1987; Charlot et al. 1992; Fletcher et al. 1995; Mellet et al. 1995; Mellet et al. 1996; Mellet et al. 2000). It has been argued that lower-order visual areas are predominantly

computational and not representational and, as such, are not obligatory in recreation of an already computed representation (Roland and Gulyas 1994).
In the present study we explored whether the proposed neural substrate of mental simulation of an action extends beyond the parieto-frontal motor/kinesthetic network, to the striate and extrastriate occipital cortical visual areas. Our analysis focused on striate area V1 and the extrastriate cortices V2, V3, V3A, and V4, which occupy the occipital operculum and both banks of the lunate (Ls) and the inferior occipital (IOs) sulci.
In the following section an attempt is made to briefly present the knowledge about the boundaries of visual areas V1, V2, V3, V3A, and V4 in striate and extrastriate visual cortex, their functions and their connectivity. Moreover, the hierarchical processing of information and the segregation of form, motion, depth, and colour along the visual pathways will be discussed.

Visual Areas

A basic step towards the understanding of perception through sight is the identification of the brain areas that mediate this function and their connectivity. Brodmann (Brodmann 1909) was the first to establish functionally distinct visual domains, 17, 18, and 19. Later on other researchers such as von Economo (von Economo 1929) and von Bonin and Bailey (von Bonin and Bailey 1947) studied the visual cortex and characterised the "well" defined visual areas. In recent years, the advent of new advanced, elaborate, and refined techniques enabled scientists to readdress the question on the determination of visual areas, and to revise those early findings. The organisation of the visual cortex, with the exception of striate cortex, was utterly rearranged and the investigators proposed new schemes regarding the location and the connections of visual areas. An impressive number of new visual areas emerged, areas that do not lie within the classical subdivisions of the occipital lobe but extend further frontally (Desimone and Ungerleider 1986; Felleman and Van Essen 1991). Nevertheless, the variety of cytoarchitectonic, physiological, anatomical and behavioural studies failed to provide sharp boundaries and distinct functions in visual areas. Clearly, there has been a deeper understanding of the visual cortex. However, questions regarding connectivity, functions of areal subdivisions and their interaction, and even the existence of certain visual areas and their boundaries, remain unanswered.

Visual area V1 (primary visual or striate cortex)

As shown in early studies (Brodmann 1909; von Bonin 1942) but also as verified by new high resolution imaging techniques both in monkey and human brains (Brewer et al. 2002; Hinds et al. 2008), most of visual area V1 (or primary visual cortex or striate cortex) is located along the medial surface of the occipital lobe or folded within the calcarine fissure. The portion of V1 that is exposed posteriorly on the brain and extends over the lateral surface of the occipital lobe forms a dome-shaped operculum. The operculum extends to the Ls, which separates the visual cortex from the parietal and temporal lobes. On the medial surface, the striate area is closely associated with the calcarine fissure, which forms a T-shaped figure at the occipital tip divided into the superior and inferior branch. Several studies have estimated the area V1 occupies and its cortical thickness. The average V1 area has been found to vary between 1320 mm^2 (Daniel and Whitteridge 1961) and 1450 mm^2 (Clark 1942). In a more recent report the average surface was found to be 1195 mm^2. However, in the latter report the measurements exhibited a large degree of variability (690-1560 mm^2) (Van Essen et al. 1984). A contemporary study with that of Van Essen measured a significantly smaller area of 841 mm^2 with the average total thickness of V1 layers being 1.592 mm (O'Kusky and Colonnier 1982). An even more recent study in adult *Macaca mulatta* (Purves and LaMantia 1990) showed that the striate cortex may range from 1148 to 1246 mm^2. Despite the substantial variability of the extent of primary visual cortex demonstrated in all these studies, V1 is evidently the largest visual area (Brewer et al. 2002).

In stained preparations of the primate visual cortex, area V1 is prominent because of its distinct and unique lamination, which has been the object of studies from early years on (Brodmann 1905; von Bonin 1942). The primary visual cortex is one of the most easily distinguishable areas due to its well developed and differentiated *lamina granularis interna (lamina IV).* The results of anatomical and physiological investigations led different investigators to adopt different lamination schemes. The

numbering scheme which is most commonly used, is the one proposed by Brodmann (1905).[1] For a review of the lamination in area V1 in primates see (Clark 1925) and of the *Macaca mulatta* see (Billings-Gagliardi et al. 1974). Another feature that makes primary visual cortex one of the most easily recognizable areas in the primate brain is a prominent white band, running tangentially in the middle of the cortex, *the stria of Gennari* or *the outer stripe of Baillarger*, consisting of heavily myelinated axons. This feature is one of only a few histological features that can be investigated using current MRI technology (Clark et al. 1992; Hinds et al. 2005). It is the presence of this stripe that led to the V1 cortex being called *striate cortex*.

When stained for the metabolic enzyme cytochrome oxidase (CO), another distinctive histological feature of V1 is revealed; a periodic distribution of darker staining zones or "*blobs*", most prominent in layer II and III, expressing high levels of CO. The heavily staining regions of blobs in this repeating dot-like pattern are separated by unstained regions, the "*interblobs*" (Horton and Hubel 1981; Horton 1984; Hendrickson 1985; Purves and LaMantia 1990; Farias et al. 1997). These blobs have been regarded as the functional cytoarchitectonic unit of the primary visual cortex (Horton 1984; Horton and Hedley-Whyte 1984), with the CO-rich and CO-poor zones possessing different functional properties (Tootell et al. 1988a; Tootell et al. 1988b; Tootell et al. 1988c; Ts'o and Gilbert 1988; Silverman et al. 1989; Ts'o et al. 1990; Edwards et al. 1995). Blobs are centered above ocular dominance columns and contain unoriented neurons predominantly sensitive to colour, which prefer lower spatial frequencies than the surrounding interblob regions (Livingstone and Hubel 1984; Silverman et al. 1989; Born and Tootell 1991; Edwards et al. 1995). Cells selective for stimulus orientation and therefore involved with the processing of form vision, that respond at higher frequencies are found between the blobs (Livingstone and Hubel 1984; Ts'o and Gilbert 1988). Evidence from anatomical studies exists that these functional units are added gradually to the developing primate brain from birth to maturity (Purves and LaMantia 1990).

Like other cortical areas, such as the somatosensory cortex (Mountcastle 1957), the primary visual cortex exhibits columnar organisation. It is organised in at least two columns of cells, anatomical and functional, extending vertically from surface to white matter. These two overlapping and independent systems of vertical bands are the *orientation columns* and the *ocular dominance columns* (Hubel and Wiesel 1968). In the first system, cells are assembled into groups which respond to similarly oriented line segments. Following a sequence from one column to another, a precise gradual shift in the axis of orientation was revealed, followed by a sudden shift in direction preference (Hubel and Wiesel 1968). In the second system, cells are grouped into columns that are driven most effectively by the left or the right eye. The bands tend to course perpendicular to the V1/V2 border as they approach the border, and this tendency becomes more apparent in parts of the cortex representing peripheral and paracentral vision, than parts representing central and foveal vision (Florence and Kaas 1992). Hubel and Wiesel (Hubel and Wiesel 1974) introduced the term

[1] *I. Lamina zonalis:* the narrow cell-free cortical border. II. *Lamina granularis externa:* very feebly developed and hardly separable from the adjacent pyramidal layer. III. *Lamina pyramidalis* - pyramidal cells are located superficially; somewhat larger pyramidal cells are found only in deeper parts. IV. (a) *Lamina granularis interna superficialis:* stands out in the photographs as a distinct dark cell stripe. At higher magnification many little round cells (so-called granules) can be recognized, apart from larger slender star- and pyramid-shaped cells. (b) *Lamina (granularis interna) intermedia:* contains the stripe of Gennari in fibre preparations. (c) *Lamina granularis interna profunda:* this is the most cell-rich and, because of this, the darkest, most prominent layer in any cortical cross section. *V. Lamina ganglionaris:* the most cell-poor and therefore the lightest layer of area 17. VI. *Lamina multiformis* - can be more clearly subdivided than in man into two subdivisions: (a) *Lamina triangularis*: a darker outer layer containing mostly larger cells, and (b) *Lamina* fusiformis: the lighter cell-poor inner layer, or the true spindle-cell layer, which stands out sharply against the white matter.

hypercolumn to refer to a complete array of columns that correspond to all values of a given variable. For the orientation system this is a full set of columns responsive to lines of all orientations from a particular region in space, while for the ocular dominance system it is a group of a left-eye and a right-eye column. A complete sequence of ocular dominance columns and orientation columns is repeated regularly and precisely over the surface of the primary visual cortex, and this organisation seems to imply that such entities are required to analyse the multidimensional visual field into a two-dimensional surface (Hubel and Wiesel 1968).

An array of functional columns of cells in the visual cortex (and generally in any other area) that contains the neural machinery necessary to analyse a discrete region of the visual field can be thought of as a *functional module* (Mountcastle 1997). Therefore, each module contains one complete set of orientation columns, one set of ocular dominance columns (right and left eye), and several blobs (regions of the cortex associated with colour processing). The entire visual field can be represented in the visual cortex by a regular array of such modules.

The layout of the orientation columns was demonstrated with autoradiographic, optical and differential imaging methods (Wiesel et al. 1974; Hubel et al. 1978; Blasdel and Salama 1986; Ts'o et al. 1990; Blasdel 1992a, 1992b). These metabolic maps revealed the orderly pattern of active and inactive stripes which are related to the various functional columns, that include orientation, binocular interaction, colour, and spatial frequency (Horton and Hubel 1981; Michael 1981; Horton 1984). Accordingly, the pattern of ocular dominance columns was also reconstructed (LeVay et al. 1985). Earlier studies have tried to interpret how the scheme of the alternating bands arises. Attempts to model stripe development and order were based on the idea that they result from the repulsive force between afferents from different eyes and/or from the geometry of geniculocortical projections (LeVay et al. 1985). Later experiments (in ferrets) indicate that the initial appearance of ocular dominance columns occurs at an early stage of cortical development (Crowley and Katz 2000), before the onset of cortical visual responses and well before the critical period (Issa et al. 1999). A study in prenatally enucleated monkeys showed normal size and distribution of CO blobs, indicating that cues from retinal photoreceptors are not essential for the development of the blobs (Kuljis and Rakic 1990). It is proposed that ocular dominance columns is the first component of modular circuitry that emerges in visual cortex, and that the early presence of ocular dominance columns may constrain the subsequent organisation of orientation columns, perhaps explaining why the centers of orientation pinwheels are aligned with the centers of ocular dominance columns (Obermayer and Blasdel 1993; Crair et al. 1997).

Visual information passes sequentially from the retina to the lateral geniculate nucleus (LGN) (Leventhal et al. 1981; Perry et al. 1984), and to the striate cortex, where the visual field is represented. One of the first detailed studies on localization of the projections of the retina in the geniculate body in apes was carried out by Brouwer and Zeeman (Brouwer and Zeeman 1925). Ganglion cells project to LGN in an orderly manner, so that each LGN has a retinotopic representation of the contralateral visual hemifield. V1 accepts a topographically organised point-to-point input from the LGN, which is reflected functionally in the detailed analysis that area V1 performs.

In primary visual cortex, the fundamental pattern of retinotopic organization has been described as a *first-order transformation* of the visual hemifield (Allman and Kaas 1971). It is best described as a one-to-one mapping in which adjacent points in the hemifield are always represented at adjacent points on the cortical surface. V1 has a complete representation of the contralateral visual field

in a continuous way (Hubel and Wiesel 1968; Van Essen et al. 1984). The upper visual field is represented in the ventral part of V1 and the lower visual field in its dorsal part (Van Essen et al. 1984). The vertical meridian forms the anterior border of V1 with visual area V2 in the posterior crown of Ls (Daniel and Whitteridge 1961; Tootell et al. 1982). The representation of the visual field in area V1 exhibits a distortion as revealed by the calculation of the magnification factor. The fovea is represented in the region of acute curvature of the V1/V2 border (Tootell et al. 1988d) and there is an over-represenation of the retinal fovea corresponding to the central visual field as compared with the peripheral visual filed (Daniel and Whitteridge 1961; Dow et al. 1981; Tootell et al. 1982; Van Essen et al. 1984). The peripheral visual field is represented towards the calcarine fissure (Daniel and Whitteridge 1961). Van Essen et al. (1984) and Tootell et al. (1988d) have suggested that the inferior visual field is overrepresented relative to the superior field. In measurements from the striate cortex representing peripheral vision, these investigators showed that the striate area devoted to the inferior visual field was, on average, about 1.2 times that devoted to the superior field. Moreover an anisotropy of 1.5:1 in vertical/horizontal magnification in foveal striate cortex was also reported (Dow et al. 1985). Moving towards the periphery, the topographic representation becomes coarser and the receptive fields larger (Hubel and Wiesel 1968). In owl monkeys, data obtained from recording experiments indicate that the temporal periphery of the V1 visual field does not share a common border with area V2. Moreover, it was shown that much of the upper visual field is represented on the upper bank of the calcarine sulcus (Cas)(Allman and Kaas 1971). The anisotropies and differences in V1 retinotopy have been studied in detail (Van Essen et al. 1984; Blasdel and Campbell 2001).

The most effective stimulus for many of the striate cortex units in the awake monkey is an elongated slit of light (Wurtz 1969). V1 neurons are classified into three categories: simple, complex and hypercomplex cells (Hubel and Wiesel 1962, 1968; Wurtz 1969), according to their receptive field structure. Simple cortical cells are built up due to convergence of geniculate cells with concentric fields. Simple cells in turn converge upon complex cells, and complex on hypercomplex resulting in these receptive field types (Hubel and Wiesel 1962). Most V1 cells show two principle functions: orientation selectivity and binocularity. Orientation selectivity refers to the preference of most cortical cells for edges at certain orientations. Binocularity results from the convergence of inputs from both eyes to the same simple cell. Moreover, neurons in macaque V1 can often be driven through either eye, but rarely are the two eyes equally effective (Hubel and Wiesel 1968). Binocularly driven neurons in V1 could provide a substrate for stereopsis, may be through the horizontal misalignment of the two receptive fields (Barlow et al. 1967; Poggio and Fischer 1977). Early studies reported an absence of disparity selectivity in anesthetized monkeys (Hubel and Wiesel 1968), but more recent studies demonstrated that a large proportion of V1 cells are tuned for disparity in the awake behaving animals (Poggio and Fischer 1977; Poggio and Talbot 1981; Poggio et al. 1988). However, the notion that these cells could support judgements of stereoscopic depth was questioned. Evidence was provided that disparity-selective neurons in macaque V1 are selective for absolute, but not for relative disparities, and cannot provide reliable cues to binocular stereoscopic depth (Cumming and Parker 1997, 1999).

Furthermore, V1 encodes information related to many other aspects of the visual stimulus such as form, colour, depth, and motion.V1 neurons exhibit direction selectivity, and some are selective for the length of the optimal stimulus (Hubel and Wiesel 1968; Wurtz 1969; De Valois et al. 1982b).

Studies have demonstrated the presence of cells sensitive to colour (Dow and Gouras 1973; Gouras and Kruger 1979; Zeki 1983b; Livingstone and Hubel 1984; Thorell et al. 1984), speed of movement (Orban et al. 1985; Orban et al. 1986), spatial frequency (Schiller et al. 1976; Poggio et al. 1977; De Valois et al. 1982a), luminosity (Kayama et al. 1979; Thorell et al. 1984), or cells sensitive to even more particular stimuli, such as textured backgrounds (Hammond and MacKay 1977; Hammond 1981) and contextual modulations (i.e. stimuli presented in the receptive field, the surround of which may modulate the response of the cells) (Lamme 1995; Zipser et al. 1996). The output of the V1 neurons is a representation that Marr (Marr 1982) has called *primal sketch*.

Visual area V2

Area V2 occupies the medial surface of the occipital operculum and extends to the caudal bank of the Ls. In more ventral parts it extends to the posterior and anterior bank of inferior occipital sulcus (IOs) (Gattass et al. 1981). The lamination of area V2 has been studied in detail (Valverde 1978). V2 surrounds the striate area along its lateral and anterior margins and is smaller than V1 (Gattass et al. 1981).

The representation of V2 is not a mirror image of that in V1. The first relevant findings were reported by Hubel and Wiesel for the cat (Hubel and Wiesel 1965). Using a number of medio-lateral microelectrode penetrations, they found that close to the V1/V2 border, the receptive fields were located near the vertical meridian of the visual field, but moving laterally across V2, the receptive fields proceeded to only 15° from the vertical meridian. Later studies showed that V2 has a reduced representation of the temporal periphery, the portion of the visual field furthest from the vertical midline (Gattass et al. 1981).

By the use of lesions in striate cortex and sections of the callosum, Zeki studied the topographic organisation of this extrastriate area in rhesus monkeys (Zeki 1969a). The analysis of interhemispheric connections is a particularly useful method, based on the finding that callosal fibers terminate preferentially in regions representing the vertical midline of the visual field (Choudhury et al. 1965; Berlucchi 1972; Zeki 1983a). The upper and the lower visual quandrants in V2 are represented is separate regions that are contiguous only along a short segment near the representation of the center of gaze (Zeki 1969a). This type of representation in which neighboring points of the visual field on opposite sides of the horizontal meridian are represented in separate loci in the visual cortex has been described as a *second order transformation* of the visual hemifield (Zeki 1969a; Allman and Kaas 1974b).

Zeki found a representation of the vertical meridian just anterior to the striate-prestriate border at the lip of the operculum (V1/V2 border). The representation of the vertical meridian in V2 is adjacent to that in V1 throughout the extent of the latter, i.e. on the lateral surface, on the medial surface, and within the Cas, and forms the posterior border of V2. Lesions of the striate cortex limited in the region of representation of the horizontal meridian revealed that the horizontal meridian in Ls is represented between the two representations of the vertical meridian, one at the striate-prestriate border and the other in the medial one-sixth of the sulcus. Therefore, the representation of the horizontal meridian, in the depth of the Ls, forms the anterior border of V2. Subsequently, other researchers studied in detail V2 topography. It was confirmed that the central parts of the lower visual quadrant are represented in dorsolateral V2 and more peripheral parts of the lower quadrant are represented in the extension of V2 on the medial wall and the upper bank of

the Cas. The central parts of the upper visual quadrant are represented in the extension of V2 on the ventral surface (IOs) and the peripheral parts in the lower bank of the Cas (Allman and Kaas 1974b). Moving down the upper bank of the Cas (in V1) and along its floor, the receptive fields move towards the horizontal meridian. Continuing along the floor and up the lower bank of the calcarine towards the medial V2/V1 border near the lower lip of the Cas, the receptive fields move from the horizontal meridian the vertical meridian. Crossing the border of V1 with V2 in the lower bank of the Cas and moving around the ventral convexity, the progression of the receptive fields reverses and moves away from the vertical meridian in the upper visual field. It then curves back and moves towards the horizontal meridian near the fovea at the border with striate cortex on the lateral surface. The foveal representation is located laterally in the occipital operculum (Gattass et al. 1981). In V2, an overrepresentation of a few degrees above and below the horizontal meridian is apparent. Receptive fields at the anterior border of dorsal V2 extend above the HM and those at the anterior border in ventral V2 extend below the HM (Van Essen and Zeki 1978; Gattass et al. 1981). Additionally, there is an increase in receptive field size and scatter in V2 relative to V1 (Van Essen and Zeki 1978). At corresponding eccentricities near the fovea, receptive fields in V2 are two or three times larger than in V1 (Gattass et al. 1981; Foster et al. 1985).

The visuotopic organisation of V2 seems to be dictated by the need of immediate connectivity with V1. This organisation ensures that any part of the visual field is represented in proximal parts of V1 and V2. A non distorted organisation of the visual field in V2 would result in longer connections between V1 and V2 (Allman and Kaas 1974b). Apart from this irregular representation of the horizontal meridian, other irregularities in the point-to-point mapping of the visual field were also found. V2 departs considerably from the traditional assumption that a single visual area should contain a complete and orderly representation of the visual field, and eventually will be evident that it is not the only exception to this notion.

V2, when stained with cytochrome oxidase, exhibits a similar histological feature with V1 blobs, a series of stained bands known as *stripes* (Tootell et al. 1983; Tootell and Hamilton 1989; Olavarria and Van Essen 1997). These bands are alternatively dark *thin* and *thick* stripes separated by lightly stained *pale* stripes, which are organised sequentially as thin/pale/thick with the triplet repeating cyclically along its length (Tootell et al. 1983). They extend orthogonally from the V1/V2 border, and in ventral V2 some stripes curve away from V1 to run almost parallel to the anterior border of V2 with V3 (Olavarria & Van Essen 1997). The definitions thin and thick do not correspond always to the actual size of the stripes (Hubel and Livingstone 1987). Anatomical and physiological studies support that this organisation serves a functional system specialised for the processing of different visual submodalities (Hubel and Livingstone 1987; Roe and Ts'o 1995).

Several studies support a multiple and discontinuous representation of visual space across the three types of functional stripes in V2. This mode of representation is characterised by a continuity within stripes, by discontinuities at stripe borders, and by continuity from one stripe to the next similar stripe (Roe and Ts'o 1995; Shipp and Zeki 2002b). Electrophysiological (DeYoe and Van Essen 1985; Shipp and Zeki 1985; Hubel and Livingstone 1987; Shipp and Zeki 2002a), ^{14}C-deoxyglucose (Tootell and Hamilton 1989; Vanduffel et al. 2002), and optical imaging studies (Ts'o et al. 1990; Roe and Ts'o 1995, 1999; Ts'o et al. 2001) have suggested that the visual map of V2 consists of three distinct interleaved maps, where each locus of visual space is represented at least three times: once in the colour domain, once in the orientation domain, and once in the disparity domain. The thick

stripes contain cells processing disparity and motion, the thin stripes contain cells processing colour, and the pale stripes are processing form and orientation. However, one should not infer uniformity among any single stripe. In fact, it is clear that each stripe contains a mixture of response types (Levitt et al. 1994b; Gegenfurtner et al. 1996; Ts'o et al. 2001; Shipp and Zeki 2002a). Neuronal responses are multimodal in nature but there is a significant degree of form, colour, and disparity integration in V2. It is also important to note that there is substantial individual variation in this defined alteration of thin/pale/thick, and even more a prominent dorsoventral asymmetry in their compartmental organisation (Olavarria and Van Essen 1997).

The most significant difference between V1 and V2 neurons is that almost all neurons in V2 are excitable through either eye or both together and most of them are equally excitable through either eye (Hubel and Wiesel 1970; Burkhalter and Van Essen 1986). They respond best to concurrent stimulation by the two eyes with a very narrow range of disparities (Hubel and Wiesel 1970; Poggio and Fischer 1977), but most seem indifferent to whether they are driven by either eye alone or both together over a broad range of phases (Hubel and Livingstone 1987). Some of these binocular neurons are disparity-selective (Poggio et al. 1988). Binocular "depth" cells are present in the posterior bank of the Ls (Hubel and Wiesel 1970; Poggio and Fischer 1977) and may process information for stereoscopic depth discrimination. Using dynamic random-dot stimuli, in which the relative disparity between center and surround was manipulated, it was recently found that a proportion of V2 neurons are sensitive to relative disparity (Thomas et al. 2002). This specialisation may provide reliable information for processing binocular stereoscopic depth.

The properties of V2 neurons regarding orientation, spatiotemporal frequency and colour have been studied in detail (Levitt et al. 1994a). Most neurons in V2 are orientation-selective (Zeki 1978c; Levitt et al. 1994a) though perhaps slightly less sharply than neurons in V1 (Levitt et al. 1994a). Cells without orientation selectivity are also found in considerable numbers (Orban et al. 1986; Levitt et al. 1994a). Direction selective cells are found in fewer numbers than orientation-selective cells (Zeki 1978c; Burkhalter and Van Essen 1986; Orban et al. 1986). V2 neurons exhibit spatial frequencies slightly lower than that of V1 (De Valois et al. 1982a; Foster et al. 1985; Levitt et al. 1994a), but almost exactly the same with that in V4 (Levitt et al. 1994a). In early studies, a considerable percentage of the cells in the posterior bank of the Ls was found to be excited by some colours and inhibited by others (Baizer et al. 1977; Zeki 1978c). All these cells exhibited spatially coextensive colour opponent responses, and some of them had in addition a suppressive surround for the same wavelength that excited the center (Baizer et al. 1977; Moutoussis and Zeki 2002). The existence of colour-sensitive cells was confirmed by later studies (Burkhalter and Van Essen 1986; Hubel and Livingstone 1987; Levitt et al. 1994a; Gegenfurtner et al. 1996; Kiper et al. 1997). V2 colour-sensitive cells do not exhibit any eye preference, and seem to be quite similar to the ones described in V1, although V2 cells exhibit greater range of colour preference (Roe and Ts'o 1995) than V1 cells (Ts'o and Gilbert 1988). In a later study it was delineated that V2 cells respond to the wavelength composition reflected by an object and not to its real colour, suggesting that colour constancy is not achieved in V2 (Moutoussis and Zeki 2002). Other types of colour cells have also been described in V2, such as spot cells (Roe and Ts'o 1995), colour border cells and colour disparity cells (Burkhalter and Van Essen 1986).

V2 neurons exhibit a tendency to cluster in a certain CO compartment. However, this tendency is not strict. Orientation sensitivity is common everywhere, but mainly in the thick stripes and

interstripes. Direction-selective cells are common, though not predominant, in the thick stripes, but more rare in the thin and pale stripes. Colour-selective cells (often not orientation-selective) are found most often in the thin stripes, but they do not predominate anywhere. Cells that prefer binocular stimulation are most often found in the thick stripes (DeYoe and Van Essen 1985; Shipp and Zeki 1985; Hubel and Livingstone 1987; Levitt et al. 1994a; Gegenfurtner et al. 1996; Moutoussis and Zeki 2002; Shipp and Zeki 2002a). Disparity-sensitive neurons in V2 were found segregated in zones extending through the depth of the cortex (Poggio et al. 1988) or restricted to the thick stripes (Hubel and Livingstone 1987), however other researchers report that they are found in all compartments (Peterhans and von der Heydt 1993). Observations by Tootell and Hamilton suggest that there might be also some systematic mapping of spatial frequency (Tootell and Hamilton 1989).

In most respects, neurons in V1 and V2 are not remarkably different (Baizer et al. 1977; Hubel and Livingstone 1987) and this may imply that they do not make different contributions to visual processing. Broadly, they have similar direction and orientation selectivities, similar distributions of chromatic preferences, and they even exhibit similar responses in functions that are thought to require more complex properties or processing, such as contextual segmentation and detection of illusory contours (von der Heydt et al. 1984; Peterhans and von der Heydt 1989; von der Heydt and Peterhans 1989; Grosof et al. 1993; Marcus and Van Essen 2002). Hence, it would be reasonable to argue that V2 is simply an intermediate station between V1 and "higher" visual areas. However, this is not the case.

It is believed that one of the important transformations achieved in V2 is the representation of disparity information. Within the thick stripes there is a clustering of disparity cell types, with tuned excitatory, tuned inhibitory, and near and far disparity cells (Poggio and Fischer 1977; LeVay and Voigt 1988). Each one of these cell types is segregated into its own set of patches within a single thick stripe (Ts'o et al. 1990b) and can provide reliable cues for stereoscopic depth. Intermodular interactions are also present in V2. Qualitatively different groups of cells do seem to cluster into different stripe compartments, yet results suggest that the correlation between histology and physiology is not strict (Roe and Ts'o 1995). The organisation of V2 may promote integration across stripes, since the range of visual overlap, and intrinsic connections, exceeds a single set of stripes (Shipp and Zeki 2002b). Hence, the results suggest that both segregating and integrating mechanisms are implemented at this early level of processing. Moreover, lesion studies reveal the distinct role of V2. It is generally known that V1 lesions have devastating effects on vision (Kluver 1941; Humphrey and Weiskrantz 1967), and V1 inactivation results in the cessation of the majority of V2 neurons (Girard and Bullier 1989). However, other studies provide evidence that V2 can process information in the absence of V1 input. Studying the visual performance after V2 lesions (in the posterior bank of the dorsal Ls) reveals that V2 does not participate only in basic visual functions such as visual acuity and contrast sensitivity, but is also important for visual discrimination tasks which require more complex processing (Merigan et al. 1993). Additionally, a recent fMRI study reports that after V1 lesion the BOLD signals in area V2 are retained at 20-30% of the pre-lesion levels indicating that other subcortical inputs or feedback projections from higher areas may drive V2 (Schmid et al. 2009). In conclusion, area V2 is more than a relay station.

Visual area V3

The third visual area, V3, is located within Brodmann area 18 and receives a direct, point-to-point input from V1 with the consequence that the retina is also topographically mapped into it (Cragg 1969; Zeki 1969b, 1969a; Zeki and Sandeman 1976; Van Essen and Zeki 1978; Zeki 1978b). The myeloarchitecture pattern of V3 differs from that of V2. V2 shows a homogeneous, broad, dark band of fibers that extends from layer VI through layer IV and fades out in the bottom of layer III (Gattass et al. 1981). In V3 this band becomes less homogeneous, more stratified and the inner band of Baillarger becomes visible. In the region of representation of the center of gaze however it is often difficult to distinguish V3 and V2 (Gattass et al. 1988).

V3 was originally described in cats. Hubel and Wiesel (Hubel and Wiesel 1965) while recording the progression of the receptive fields in penetrations across the visual cortex of the cat, found a gradual shift of the receptive fields from the vertical meridian in the V1/V2 border, to the periphery of the visual field moving laterally across V2 and back towards the vertical meridian in more laterally placed penetrations. They considered the site of reversal in the progression of receptive fields as the border between V2 and another area located lateral to V2, area V3. Bilge et al. (Bilge et al. 1967) reported that most of the border between V2 and V3 in the cat corresponds to a representation of the horizontal meridian. In monkeys, V3 was first identified by Zeki (Zeki 1969a) and Cragg (Cragg 1969) on the basis of the pattern of degeneration found after making discrete lesions in various parts of V1. In particular, their evidence suggested that V3 was a narrow strip adjoining both dorsal (lower field) and ventral (upper field) subdivisions of V2. These and later studies confirmed that in Ls, the border between V2/V3 is the representation of horizontal meridian and the anterior border of V3 is the representation of vertical meridian (Zeki and Sandeman 1976). Callosal terminations in cortex rostral to V2 were also thought to mark the representation of the vertical meridian and the anterior border of V3 (Zeki 1977b; Van Essen and Zeki 1978). Later, microelectrode mapping results verified the posterior and anterior borders of V3, however they illustrated a discontinuity in the dorsal and ventral portions of V3 (Gattass et al. 1988). These parts are called V3d and V3v respectively. V3d is the part of V3 which lies in the fundus and in the anterior bank of the Ls and in the posterior portion of the annectant gyrus. V3v extends across both banks of the inferior occipital and occipitotemporal sulci. V3d contains a representation of about the central 40° of the lower visual field. The horizontal meridian forms its posterior border, and the representation of the lower vertical meridian forms the anterior border of V3d. The receptive fields of V3 in the Ls move inferiorly as one moves dorsally in the sulcus (Zeki and Sandeman 1976). However, in some cases, there was a partial split in the representation of the vertical meridian. The anterior border of V3d was found to be divided into two portions, with a piece of the visual field intercalated between these portions. The representation of the displaced portion of the visual field abuts V3A. The remainder of the representation of the vertical meridian is adjacent to area PO. A representation of the central 4°-8° of the vertical meridian borders with dorsal V4. V3v contains a representation of about the central 35° of the upper visual field. The horizontal meridian forms the posterior border of V3v and the vertical meridian the anterior border of V3v. Receptive field size in V3 increases markedly with increasing eccentricity. However, even at the more peripheral fields they do not extend across the ventral meridian into the contralateral field by more than 3°-4°. As a consequence, with increasing eccentricity, the vertical meridian is not represented by fields centered at the meridian. Instead, it

is represented by the nasal portion of the receptive fields whose centers are located away from the meridian (Gattass et al. 1988).

As for the unity of extrastriate divisions V3d and V3v, it was claimed that the dorsal and ventral portions of V3 are valid visual areas by themselves, even though each represents only one (the lower or upper correspondingly) visual quadrant. The dorsal portion was called area V3. The corresponding ventral V3 region was considered a separate visual area, the ventral posterior area (VP) (Burkhalter et al. 1986). One of the first indications that supported this conclusion came from an observed dorsoventral asymmetry in the projections of V1 (Weller and Kaas 1983; Burkhalter et al. 1986; Van Essen et al. 1986). Results indicated that dorsal V1 was reciprocally connected with V3 (i.e. V3d) but no detectable projection to VP (i.e. V3v) from ventral V1 was found. Part of the problem was that projections from dorsal V1 to the region of dorsal V3 could be interpreted as connecting to another area, the DM, along the rostral border of V2, which contained the representation of both upper and lower visual field (Allman and Kaas 1975; Stepniewska and Kaas 1996). The second argument came from the difference in myeloarchitecture (Burkhalter et al. 1986). In myelin-stained sections through dorsal extrastriate cortex, V3 (i.e. V3d) was identified on the basis of its heavy myelination, similar to that of area MT (middle temporal) in the superior temporal sulcus (STs). In ventral prestriate cortex, VP consistently lacked heavy myelination. For those investigators who were against a unified V3 these observations on cortical myeloarchitecture strongly supported the idea that V3 is restricted to dorsal extrastriate cortex. Another key argument for the existence of two different visual areas came from the study of visual topography and callosal inputs. It is well known that the dorsal and ventral parts of area V3 have representations of different parts of the visual field. V3d represents only the lower part of the visual field, and the ventral half, V3v (or VP), represents only the upper part of the visual field [old world monkeys (Van Essen et al. 1982; Newsome et al. 1986; Gattass et al. 1988) and new world monkeys (Allman and Kaas 1975; Newsome and Allman 1980)]. Regarding the callosal inputs, the pattern of degeneration following transections of the splenium (Van Essen et al. 1982) revealed a pronounced asymmetry in the organisation of callosal recipient zones. A single long strip of callose inputs was demonstrated ventrally in contrast to a more irregular array of inputs dorsally. However, the asymmetry of callosal inputs alone was weak evidence as to whether separate areas adjoined dorsal and ventral V2. A more robust documentation came from the comparison of these findings with those from owl monkeys. It was shown that the pattern of callosal inputs in the owl monkey is practically the same as in the macaque. This homology urged the investigators to suggest that VP area exists also in macaque (Burkhalter et al. 1986). Another argument against a unitary V3 was the asymmetries observed in physiological properties of neurons. Major differences were found between the two areas regarding colour selectivity, direction selectivity, and receptive field size. V3d cells were highly direction selective but not strongly colour sensitive. On the contrary, the incidence of colour-selective cells was three times higher in V3v than in V3d and the number of direction-selective cells in V3v was one-third of that encountered in V3d. Additionally, receptive field areas in V3v were approximately twice as large as those at a corresponding eccentricity in V3d (Burkhalter et al. 1986). Finally, evidence supports that V3d and V3v differ in their connections with other areas and not only in their connections with V1. Specifically, V3d has connections with V4 transitional area (V4t) that are absent for V3v; V3v has connections with ventral occipitotemporal area (VOT),

dorsal prelunate area (DP), and visually responsive portion of temporal visual area F (VTF) that are absent or occur only rarely in V3d (Burkhalter et al. 1986; Felleman et al. 1997a).

All these findings were sufficient to support a distinction between V3d and V3v. Nonetheless, some of the previous evidence has been disputed. The notion that there is an asymmetric anatomical input from V1 to upper and lower V3 has been questioned. In *Cebus* monkeys, a direct input from V1 to lower V3 was found (Pinon et al. 1998) and recording experiments showed that there is a continuous representation of visual fields in V3 from lower to upper quadrants as one proceeds dorsoventrally (Rosa et al. 2000). Other supporting evidence came from the Old World macaque monkey, when a direct input from V1 to V3 was found (Lyon and Kaas 2001, 2002). This finding has led Lyon and Kaas to conclude that V3 is one continuous area, not two separate areas, with dorsal and ventral halves, in which both upper and lower fields are represented. The retinotopic scheme of V3 with dorsal and ventral halves, where the lower and the upper visual fields are represented correspondingly, was confirmed also in humans using PET (Shipp et al. 1995). Zeki has called these partial representations "improbable areas", and he has noted that one should neither be willing to accept easily and uncritically such segregations which impose ambiguous issues in functional organisation nor should be led to conclusion for other cortical areas by accepting questionable evidence (Zeki 2003).

The functional properties of V3 neurons were briefly aforementioned. The vast majority of V3 cells were found to be binocularly driven (Zeki 1978b) (this is referred to the part of V3 which lies in the depth and anterior bank of Ls and in the parieto-occipital sulcus (POs) medially, and corresponds to V3d). V3 is included in motion sensitive areas (Vanduffel et al. 2001). V3d cells show strong orientation and direction selectivity, however exhibiting great variety in the range of directions to which they respond (Zeki 1978b; Felleman and Van Essen 1987; Gegenfurtner et al. 1997; Adams and Zeki 2001). Previous studies reported a smaller number of these group of cells (Baizer 1982) and direction selectivity was thought to be uncommon (Zeki 1978b). Cells that lacked sensitivity to orientation (non-oriented cells) were also encountered (Baizer 1982). In one study several cells displaying multi-peaked orientation and/or direction tuning curves were observed (Felleman and Van Essen 1987), however this finding was not verified by another study (Gegenfurtner et al. 1997). V3d neurons are also tuned for the speed of the stimulus, showing an optimum response at a mean speed of 16°/sec. A significant fraction consists of disparity selective cells (Adams and Zeki 2001), with the group exhibiting excitatory response being larger than that with inhibitory response (Felleman and Van Essen 1987). Although earlier reports failed to record any colour opponency (Zeki 1978c, 1978b; Baizer 1982), a considerable proportion of V3d cells show selectivity for colour (Felleman and Van Essen 1987; Gegenfurtner et al. 1997), and exhibit contrast sensitivity (Gegenfurtner et al. 1997). Additionally, end-stopping and pattern cells have been encountered (Gegenfurtner et al. 1997). Many V3 cells were found to exhibit selectivity to combinations of stimulus characteristics, but a statistical significant association between different stimulus attributes was not detected (Gegenfurtner et al. 1997). V3v neurons show a significant incidence of disparity selectivity (Burkhalter and Van Essen 1986), and, like V3d neurons, exhibit preference for specific rates of motion, but with different preferred speeds (32°/sec) (Burkhalter and Van Essen 1986; Felleman and Van Essen 1987). Burkhalter and Van Essen (1986) found the incidence of each type of selectivity in V3v to be largely independent of other types of selectivities. Finally, receptive fields of cells in V3 are larger than fields of V2 cells at comparable eccentricities

(Zeki 1978c; Baizer 1982; Burkhalter and Van Essen 1986), and especially receptive fields in V3v are approximately twice as large as those at a corresponding eccentricity in V3d (Burkhalter et al. 1986).

Based on the properties of its neurons, area V3 is suggested to be involved in dynamic form (Zeki 1993) and orientation (Zeki 1978b). The existence of disparity-selective cells in V3 led scientists to propose that this area participates in the analysis of three-dimensional form, processing the 3D shape of an object and the global 3D layout (Adams and Zeki 2001; Tsao et al. 2003). On the other hand, there is no consensus regarding the process of colour in V3. Some researchers, due to the substantial chromatic signal in area V3d and its parvocellular inputs, argue that V3d seems to play an important role in the processing of motion and colour stimuli (Gegenfurtner et al. 1997). In contrast, other researchers found a very small percentage of colour selective or colour biased cells and postulate that V3 is not involved in colour processing. Some researchers, who have compared the percentage of colour-selective cells in V3v encountered in their study (Burkhalter and Van Essen 1986) with the lower percentage of colour-selective cells in V3d demonstrated in previous studies (Baizer 1982; Zeki 1978a; 1978b), suggested that this information is processed asymmetrically in V3. However, other studies have found higher percentage (54%) of colour-selective cells in V3d (Gegenfurtner et al. 1997). Therefore such a suggestion cannot be confirmed. Nonetheless, the functional properties of V3v cells led the researchers to suggest that this area plays an important role in both form and colour vision (Burkhalter and Van Essen 1986). In general V3 is considered part of the dorsal visual stream areas which is engaged in motion processing.

Visual area V3A

V3A lies in the Ls, anterior to V3. It also extends over the annectant gyrus into the POs. V3A was identified mainly on the basis of the pattern of callosal inputs in these sulci. It was illustrated that the region adjacent to V3 consists of a central callosal-free zone surrounded by a ring of callosal-recipient cortex. Within this region there is a representation of both superior and inferior visual quadrants that are distinct from V3 medially and V4 laterally (Van Essen and Zeki 1978; Zeki 1978b). Initially Zeki (Zeki 1978b) reported that V3A did not receive a direct input from V1 as V3 does. However, a later study by the same scientist demonstrates that more peripheral parts of V1 project directly to V3A (Zeki 1980a).

V3A has a complex and irregular topographic organisation. The anterior border of V3d with V3A represents the inferior vertical meridian (Van Essen and Zeki 1978; Zeki 1978b; Van Essen et al. 1986; Gattass et al. 1988). The superior vertical meridian is represented along the V3A/V4 border and along the zone of degeneration in the parieto-occipital sulcus, and the horizontal meridian within the degeneration-free portion of V3A (Van Essen and Zeki 1978). The central visual fields may be represented at least twice in V3A: once in Ls, where receptive fields are reasonably small, and once again in the fundus of the POs, where receptive fields are large even when they overlap the fovea (Van Essen and Zeki 1978). This relatively large size of the receptive fields of V3A neurons may account for the absence of a strong preference for central foveal signals in a fMRI study, in which the most central portion of eccentricity representation in V3A responded best to signals near 5° of eccentricity, and did not extend into the central fovea (Brewer et al. 2002).

Judging from its proposed location, area V3A appears to correspond to the dorsomedial visual area DM. Area DM was defined in owl monkeys as a systematic representation of the contralateral

hemifield within a field of moderately dense myelination (Allman and Kaas 1975), with major connections with V1 (Lin et al. 1982), MT and adjoining posterior parietal (intraparietal) cortex (Wagor et al. 1975).

V3A is distinguished from V1 and V2 by the lack of simple-like cells (Gaska et al. 1987), and by larger receptive fields at similar eccentricities (Zeki 1978b, 1978c; Gaska et al. 1987, 1988). Almost all cells in V3A were found to be binocularly driven. As with area V3, the most commonly encountered type of cell is the orientation selective (Zeki 1978b, 1978c). Direction selective cells are also present, though in smaller numbers (Zeki 1978c; Gaska et al. 1988). Cells with orientation preference and binocularly driven cells are often grouped together, although abrupt changes between successive cells can be encountered (Zeki 1978b). In both humans and monkeys, area V3A is found activated for disparity (Poggio et al. 1988; Tsao et al. 2003). Furthermore, V3A is characterized by absence of colour opponency (Zeki 1978b, 1978c), and colour bias (Conway and Tsao 2006). V3A neurons exhibit spatial and temporal frequency selectivity (Gaska et al. 1988), but not to all colour modulations (Liu and Wandell 2005).

The studies on the role of V3A in motion processing lead to conflicting evidence. It is found that more than 40% of V3A neurons are real-motion cells, i.e. cells that can distinguish an actual movement in the visual field from a retinal stimulation caused by an eye movement (Galletti et al. 1990). Such cells have also been reported in areas V1 and V2 (Galletti et al. 1984; Galletti et al. 1988). Using fMRI in humans, V3A was found to have high motion and contrast sensitivity and to be more sensitive to motion than in non human primates (Tootell et al. 1997). Other interesting properties regarding motion processing have also been reported. It was suggested that V3A uses contour cues (contour curvature) to extract information about form and motion interaction (Caplovitz and Tse 2007). Additionally, V3A cells, do not respond well to extended sine-wave gratings, in the same way as V1 and V2 cells. The inhibition in V3A is not evident only for gratings extending beyond the receptive field, but V3A cells exhibit intra-field suppression which is far stronger. These properties imply that V3A cells are driven by spatially distributed, nonlinear (complex-like) inputs (Gaska et al. 1987). Furthermore, human V3A is found to be more activated by coherent motion than by incoherent, random motion (Braddick et al. 2001; Moutoussis et al. 2005), while it appears to encode information related to for both chromatic and luminance defined motion (McKeefry et al. 2010). However, evidence from other studies indicates that macaque V3A plays no significant role to motion perception. Using fMRI in awake monkeys, the investigators did not observe significant motion-sensitive voxels in V3A, and comparing motion sensitivity in humans and monkeys they observed absence of motion sensitivity in simian V3A (Vanduffel et al. 2001; Orban et al. 2003).

Therefore, studies reveal that V3A holds contradicting properties. As we shall witness, V3A has connections with areas of both dorsal and ventral stream, which may account for these observations. Overall, area V3A along with area V3 are primarily considered part of the motion cortical pathway.

Visual area V4

V4 was originally described by Zeki who examined the projections from areas 18 and 19 of upper and lower prestriate cortex (Zeki 1971b). Zeki proposed that the anterior bank of the Ls (beyond area 19) consists of more than one area. He named these two areas visual area 4 (V4) and visual area 4a (V4a). In subsequent studies V4a was replaced by the name V4t. He suggested that the

upper areas 18 and 19 project to the anterior bank of the Ls and spread onto the prelunate gyrus. The projections from lower areas 18 and 19 exhibited a more complex pattern. The ventral portions of V4 and V4a was reported to fall in the posterior bank of the IOs, however a weak projection from lower V2 and V3 to the anterior bank of the IOs was also noticed. Following studies have placed the ventral part of V4 only in the anterior bank of the IOs (Gattass et al. 1988). The latter study described in detail the extent of V4. It was proposed that dorsally V4 runs from the anterior bank of the Ls across the prelunate gyrus onto the lip of the posterior bank of the STs. Ventrally, V4 extends across the inferior occipital and occipitotemporal sulci (Gattass et al. 1988). Taking into consideration the change in the sulcal and gyral pattern from dorsal to ventral, where the area of interhemispheric degeneration in the anterior part of the prelunate gyrus moves to the posterior part of the inferior occipital gyrus or the anterior part of the inferior occipital sulcus, this complicated pattern of projection of lower areas 18 and 19 in the posterior bank and anterior bank of IOs reported in the initial study can be explained (Zeki 1970).

V4 is distinguishable from V2, V3, and V3A by the presence of much more prominent inner and outer bands of Baillager. Areas V4t, TEO (temporoccipital area), and VF which constitute the anterior border of V4, differ from V4 in their myeloarchitecture, enabling V4 differentiation (Gattass et al. 1988). In owl monkeys, the area between V2 and MT (most probably the area homologous to V4) which was named dorsolateral area, DL, contains the representation of the contralateral visual hemifield (Allman and Kaas 1974a). Later studies of connections provided evidence of a rostral and a caudal half of the DL, DLr and DLc respectively. DLc, receives the most dense projections from V2, whereas the rostral subdivision is more densely connected with MT and DM (Cusick and Kaas 1988; Steele et al. 1991; Stepniewska and Kaas 1996). Functional studies have highlighted that some properties of V4 neurons resemble those of neurons in area DL, supporting the notion that DL is homologous to V4 (Petersen et al. 1980; Desimone and Schein 1987).

Initial studies had argued that V4 has a multiple representation of the same part of the visual field at distant points within the cortex (Van Essen and Zeki 1978). Other reports suggested that the prelunate gyrus has a complex organisation with evidence for several distinct subdivisions (Maguire and Baizer 1984). Van Essen and Zeki proposed three possible explanations for this complex topography. The first explanation implies that such a visual topography is a feature of a visual area defined not only by its anatomical connections, but by other criteria as well. The other two notions imply that V4 consists of a number of distinct subparts or alternatively that V4 is the sum of different areas, with different functions and different inputs. Each of the subparts may represent only a portion of the visual hemifield or each of the several distinct areas may contain a complete map of the visual hemifield, yet the authors thought this latter possibility to be most unlikely (Van Essen and Zeki 1978). The study of Gattass led to the conclusion that V4 contains a single representation of the visual field (Gattass et al. 1988). Gattass et al. proposed that we can comprehend the failure to discover a systematic representation of the visual field in the first attempt of Van Essen and Zeki, if we consider that those recordings were restricted only to a very small portion of the central visual field. They claim that such a small sample could not be either representative or informative about the actual topography.

According to Gattass et al. (1988) (in *Macaca fascicularis*) V4 contains a single, rather organised and somewhat disorderly representation of the contralateral visual field of about 35°- 45°. The representation of the upper visual field is located ventrally. Most of the representation of the lower

visual field is located dorsally, but a small and variable portion is located close to the anterior border of ventral V4. This portion of the lower field located ventrally includes the region adjacent to the horizontal meridian beyond an eccentricity of about 5°. Thus, in V4 the split of the representation of the contralateral visual field does not take place entirely along the horizontal meridian. Rather, beyond an eccentricity of about 5° it takes along a line oblique to the horizontal meridian (Gattass et al. 1988). Later, based on projections from V2, it was found that V4 contains a representation of up to 50° eccentricity (Gattass et al. 1997).
Dorsally, the posterior border of V4 corresponds to the representation of the central portion of the vertical meridian (2°-8°) adjoining V3 and more medially V3A (Zeki 1969a; Gattass et al. 1988). The anterior border of dorsal V4 lies next to area V4t, where there is a representation of the horizontal meridian with the centers of the receptive fields located at 4°-8° and the temporal borders at up to 18° along the horizontal meridian. Therefore, as one moves anteriorly up the bank of the Ls from the border of V3/V3A with V4 in the prelunate gyrus, towards the anterior border of V4, the receptive fields shift from the vertical meridian towards the horizontal. Moving from lateral to medial, the receptive fields shift from near the center of gaze into the periphery (Gattass et al. 1988).
Area V4t (t for transitional) appears to correspond to part of the colour coding area of the STs described by Zeki (Zeki 1977a). It is a narrow area (1-3 mm wide) which lies in the lateral bank of the STs, between areas V4 and MT from which is myeloarchitectonically distinct. The medial border of V4t forms part of the posterior border of area MT and has the tendency to represent the vertical meridian. The lateral border of V4t with V4 lies near the representation of the horizontal meridian. This visuotopic organization of V4t is thought to serve as a transitional zone between the representation of these two meridians in areas V4 and MT (Desimone and Ungerleider 1986; Ungerleider and Desimone 1986b). V4t contains a representation of the lower visual field (Desimone and Ungerleider 1986), and receives a projection from MT, same way as V4 (Ungerleider and Desimone 1986a).
Ventrally, the posterior border of V4 corresponds to the representation of the vertical meridian and is adjacent to and congruent with that in V3, up to an eccentricity of about 20°. Ventrolaterally, V4 borders with TEO. At or near the border of V4/TEO there is a representation of the horizontal meridian. However, due to the partial representation of the inferior visual field in ventral V4, the entire horizontal meridian is not represented in both dorsal and ventral V4. Rather, the entire horizontal meridian is represented in ventral V4 except for the central portion, which is also represented in dorsal V4 (Gattass et al. 1988). A similar topography is observed in V2, where within the dorsal part of V2 some receptive fields are distinctly superior to the horizontal meridian [only a small portion of the superior contralateral quadrant was represented in dorsal V2 as there were no V2 receptive fields in the Ls more than 1°-2° superior to the horizontal meridian (Van Essen and Zeki 1978)]. In the ventral portion of V4, as one moves anteriorly from the border V3/V4 to the anterior border of V4, the receptive field centres move from the vertical meridian towards the horizontal meridian. Moving from lateral to medial the centres of the receptive fields move from the center of the visual field to the periphery. Medial to the occipitotemporal sulcus (OTs), V4 borders with visual cortex that it was previously named VF (Gattass et al. 1988).
Maguire and Baizer examined the topographic organisation of the prelunate gyrus and adjacent cortex in the Ls and in the STs, an area partially coextensive with the V4 complex, in awake behaving monkeys (Maguire and Baizer 1984) and found a different topography, which was depicted

also in a quite recent study (Youakim et al. 2001). They subdivided this area into two portions, area AL which extends from the prelunate gyrus into the posterior bank of STs, and area PM which occupies part of the prelunate gurys and extends into the anterior bank of the Ls. PM corresponds to a portion of V4 dorsomedially (Gattass et al. 1988). AL is also part of V4 in the prelunate gyrus and mast probably occupies part of V4t. Both PM and AL have a representation of the contralateral lower visual quadrant and share a common representation of the vertical meridian. This vertical meridian runs from the anterior crown of the Ls to the posterior crown of STs and separates PM from AL dorsoventrally. Area PM dorsomedially and area AL anteriorly are bordered by a representation of the horizontal meridian (Baizer and Maguire 1983; Maguire and Baizer 1984). A following study explored the homogeneity in the dorsal part of V4 in prelunate gyrus (Youakim et al. 2001) and concluded that the prelunate gyrus exhibits at least two different subregions one laterally and one medially, which share a single representation of the vertical meridian that outlines the change in topography between these two areas.

The topography and extent of V4 was also demonstrated in *Cebus* monkey, and was comparable with those of area V4 defined in *Macaca fascicularis* by Gattass. It was found that V4 in *Cebus* monkey contains a topographically organised representation of 50° of the contralateral hemifield, in which the lower quadrant is represented dorsally and the upper quadrant ventrally, the vertical meridian represented along its posterior border, and the horizontal meridian along its anterior border (Pinon et al. 1998).

Overall, the visuotopic organisation of V4 is coarser than that in V3, V2 and V1. Several factors lead to that conclusion. Two different topographic representations are found in V4 among individuals (Baizer and Maguire 1983; Maguire and Baizer 1984; Gattass et al. 1988; Youakim et al. 2001). Receptive fields in V4 are several times larger than those in V1, V2 and V3 cortices. Their structure resembles that of V1 simple and complex cells (Schein et al. 1982; Desimone et al. 1985; Desimone and Schein 1987). They exhibit significant scatter and reversals in their systematic progression, while receptive fields in the same location in the visual field can be found at distant recording sites (Zeki 1970; Van Essen and Zeki 1978; Gattass et al. 1988; Youakim et al. 2001). According to the interconnections between V4/V4t and V2 or V3, scientists have deduced that the receptive fields of cells in areas V4/V4t can extend into the ipsilateral visual field because these areas are heavily interhemispherically interconnected (Zeki 1971b; Van Essen and Zeki 1978). Finally, the representation of the center of gaze corresponds to what has been termed a *point-to-line* transformation as opposed to the *point-to-point* organisation found in V1 (Palmer et al. 1978). In other words, the center gaze is represented by an elongated strip of cortex rather than by a circular region (Gattass et al. 1988).

Early cell recordings suggested that area V4 is specialised for colour (Zeki 1973, 1977a), a notion inferred by the extremely high occurrence of colour cells in these recordings. The colour specific neurons preferring a particular wavelength had the tendency to cluster in a penetration normal to the cortical surface. This interesting organisation was thought to be implied by the functional properties of the neurons rather than the topographic representation of the visual field in this area (Zeki 1973). Subsequent reports by the same author have presented varying results for the incidence of colour selectivity in V4 complex, ranging from 32% to 87% in V4, while in V4t the percentage of colour coding cells was lower (Zeki 1977a; Van Essen and Zeki 1978; Zeki 1978c; Zeki 1983d). These results made obvious that colour-coding became more emphasised in V4 than it was

in previous areas. Nonetheless, later reports questioned the specialisation of V4 in colour analysis since V4 cells lacking colour selectivity were also encountered in significant numbers (Kruger and Gouras 1980; Schein et al. 1982). V4 cells process other stimulus qualities as well. V4 cells are highly sensitive to the stimulus form and exhibit orientation preference. Direction-selectivity is less prominent, yet a significant group of such neurons is present in V4 (Zeki 1973, 1977a; Desimone et al. 1985; Desimone and Ungerleider 1986; Desimone and Schein 1987; Schein and Desimone 1990). Other stimulus features processed in V4 include the length and width of the stimulus (i.e. bar), the spatial frequency and the phase of the stimulus (i.e. a moving grating). V4 cells exhibit quite similar orientation bandwidths and directional indices to those of V1 neurons, and they also exhibit spatial sensitivity with frequencies comparable with those of V1 and V2 neurons (Fischer et al. 1981; Schein et al. 1982; Desimone et al. 1985; Desimone and Schein 1987). It was also found that the response of many V4 cells to a receptive field stimulus was influenced by the spectral and spatial characteristics of the stimuli presented in the surround of the receptive field (suppressive surround) (Desimone and Schein 1987; Schein and Desimone 1990). V4 cells were found binocularly driven (Zeki 1977a; Fischer et al. 1981; Schein et al. 1982).

The properties of V4 colour cells were studied extensively by Zeki, who classified them into two main categories, wavelength-selective (WL) and colour-coded (CO). The first category of cells respond to the amount of their preferred wavelength reflected from an area in their receptive field, while the second category includes cells whose responses correlate with perceived natural colours (Zeki 1983b). Zeki proposes that WL cells cannot code colour, since their response depends on the reflectance from a surface which is obvious that alters constantly under different lighting conditions (Zeki 1983b). However, another crucial role was assigned to WL cells. It was shown that WL cells are sensitive to the changes in the wavelength composition of the light reflected from a surface. It was supported that this ability serves as an informative cue for the nervous system in order to maintain colour stability (Zeki 1983c). Regarding the spectral properties, initial studies have reported that colour cells respond poorly to white stimuli (Zeki 1973; Zeki 1980b, 1983b). Even though, ensuing studies report a vigorous response to white light of about 58% of that to the best wavelength (Schein and Desimone 1990). Moreover, few cells presented opponent surround properties (Zeki 1973, 1977a; Schein et al. 1982; Zeki 1983b, 1983c). This lack of overt colour opponency, contrary to that encountered in colour-opponent ganglion and geniculate cells, led to the conclusion that most V4 cells selectively sum half-wave rectified cone opponent signals (Schein and Desimone 1990).

Conclusively, area V4 is undoubtedly a cortical area in which colour is analysed. It was proposed that V4 is important for higher level aspects of colour processing, thus its spectral interactions reflect a mechanism for colour constancy (i.e. colour constancy refers to the persistence of the colour of objects or of surfaces when viewed in lights of different spectral composition), crucial for accurate colour identification (Zeki 1983c; Desimone et al. 1985; Schein and Desimone 1990). Basic processes such as construction of perceptual colour categories are probably formed at earlier stages of visual process (Walsh et al. 1992). Several studies have tested the effects of V4 lesions on colour constancy of the experimental animals. Partial lesions of V4 representing the lower visual field produce little if any impairment of hue discrimination but result to impaired colour constancy (Wild et al. 1985), a result demonstrated by another study in which monkeys after V4 ablation exhibited reduced colour constancy abilities but regained their pre-operative performance in hue discrimination (Walsh et al.

1993). Yet, hue discrimination deficit has been reported after a bilateral removal of V4 (Heywood and Cowey 1987). The authors commenting on the results of Wild *et al.* argue that their sample size was not adequate to enable any secure statistical comparison. Nonetheless, colour is not the only feature functionally analysed in this area. Results from other studies introduce a significant role for V4 as a form area, participating in the functional stream of object recognition (Desimone and Schein 1987; Schein and Desimone 1990).

Connections

The general approach of brain function implies that neurons belonging to different cortical areas or to different sub-compartments in a single area are in a high degree specialised for a specific function. However, these neurons are not isolated. All brain areas, including those analysed previously, are connected through afferent, efferent and inter-hemispheric connections in networks, exchanging information and modulating their responses for handling the various parameters of vision. Thus, areas interconnected with each other usually serve the same or similar function.
Below we shall review a series of studies regarding brain connectivity and we will attempt to clarify the complex relationships emerging from this scheme.

Connections of visual area V1

The pulvinar, together with the LGN, are the main thalamic centers of the primate visual system. Other extrageniculate projections to V1 have also been reported from structures such as the claustrum and the intralaminar nuclei, the basal amygdaloid nucleus, the pons and others (Mizuno et al. 1981; Kennedy and Bullier 1985; Perkel et al. 1986; Fries 1990).
The inferior pulvinar and the adjacent ventral portions of the lateral pulvinar, which show well-defined receptive fields arranged in precise retinotopic maps (Bender 1981; Ungerleider et al. 1983; Petersen et al. 1985) are connected with the area V1 and extrastriate areas V2, V3 and V4 (Benevento and Davis 1977; Ungerleider et al. 1983; Boussaoud et al. 1992; Gutierrez and Cusick 1997). In contrast, most of medial pulvinar (PM) and the dorsomedial visual portion of the lateral pulvinar (Pdm), seem to have a crude retinotopic organisation (Petersen et al. 1985) and do not have connections with striate cortex or area V2 (Ungerleider et al. 1983; Kennedy and Bullier 1985), but connect with other extrastriate visual areas including V4, inferotemporal, and areas in posterior parietal cortex (Selemon and Goldman-Rakic 1988; Baleydier and Morel 1992; Baizer et al. 1993; Yeterian and Pandya 1997). Moreover, PM interconnects with auditory and somatosensory cortical areas, as well as with insular, superior temporal polysensory, prefrontal, parahippocampal, and cingulate cortex (Burton and Jones 1976; Baleydier and Mauguiere 1985; Acuna et al. 1990; Barbas et al. 1991; Romanski et al. 1997; Hackett et al. 1998).
The organisation of the receptive field of the LGN neurons and their response properties are well established. The LGN contains six layers of cell bodies separated by intralaminar layers of axons and dendrites. The layers are numbered from 1 to 6, ventral to dorsal. Three classes of LGN neurons were found: the *parvocellular P* (X-like), *the magnocellular M* (Y-like) and the (W-like) *koniocellular K* neurons, occupying interlaminar regions (Stone and Fukuda 1974; Dreher et al. 1976; Sherman et al. 1976; Hendry and Yoshioka 1994; Hendry and Reid 2000). LGN neurons have concentric receptive fields, with an antagonistic center-surround organisation. The parvocellular (P) and magnocellular (M) layers of the LGN receive separate projections from the populations of midget and parasol ganglion cells of the retina (Leventhal et al. 1981), and like the retinal ganglion cells, they respond best to small spots of light in the center of their receptive field. Any individual layer in the nucleus receives input from one eye only (Wiesel and Hubel 1966). Layers 1, 4, and 6 (named V1, D3, and D1 respectively in the study of Hubel and Wiesel) receive input from the contralateral nasal hemiretina and layers 2, 3, and 5 (V2, D4, and D2 respectively) receive input from the ipsilateral temporal hemiretina (Wiesel and Hubel 1966). Cells in M and P divisions of

the LGN have different physiological properties (Wiesel and Hubel 1966; Dreher et al. 1976; Schiller and Malpeli 1978; Kaplan and Shapley 1982; Hicks et al. 1983; Derrington and Lennie 1984) and their responses to variations in stimulus parameters like size, shape, wavelength and spatiotemporal properties vary. These and other studies revealed that the LGN neurons exhibit properties crucial for the analysis of both spatial and chromatic qualities of the retinal image.

The main inputs to V1 from the LGN are conveyed through these three distinct pathways: the parvocellular (P), the magnocellular (M), and the koniocellular (K). These pathways terminate in different layers of the primary visual cortex (Callaway 1998). The magnocellular fibers innervate principally layer 4Ca and have a weaker projection to layer 6. Parvocellular neurons project mostly to 4Cb, with weaker projections to layers 4A and 6, and koniocellular neurons terminate in the CO rich blobs in layers 2 and 3, as well as in layer 1. Using the retrograde transport of horseradish peroxidase, efferent cells in area V1 projecting to the LGN have been identified. The projection to the parvocellular division arises preferentially from the upper half of lamina 6, while that to the magnocellular division from the lower part of the lamina (Lund et al. 1975).

The main cortical output of V1 is area V2 (Zeki 1969a, 1978a; Rockland and Pandya 1979; Lund et al. 1981; Rockland and Pandya 1981; Weller and Kaas 1983; Perkel et al. 1986). The rostrally directed efferents from area V1 to area V2 originate from neurons in the supragranular layers (II and III) (Spatz et al. 1970; Lund et al. 1975; Wong-Riley 1978) and terminate mainly in layer IV (Cragg 1969; Spatz et al. 1970). In contrast, the caudally directed efferents from V2 to area V1 originate from neurons in the supragranular layers and terminate mainly in layer I in the squirrel monkey (Tigges et al. 1974).

There is evidence that the P, M and K pathways remain segregated in V1 and extrastriate area V2. V1 cytochrome oxidase blobs from layers 2/3, which are mainly driven by the parvocellular layers of the LGN and contain cells selective for the colour of the stimulus, project to thin stripes of V2 (Livingstone and Hubel 1983, 1984; Tootell et al. 1988b; Ts'o and Gilbert 1988; Born and Tootell 1991; Sincich and Horton 2002a; Sincich and Horton 2005; Shipp 2006), which project mainly to V4 (DeYoe and Van Essen 1985; Shipp and Zeki 1985; Zeki and Shipp 1989; Nakamura et al. 1993; Felleman et al. 1997b; Xiao et al. 1999), an area specialised in colour processing. The output from V1 which arises from cells in interblob columns in layer 3 terminates primarily within the CO pale stripes (Livingstone and Hubel 1984) and CO thick stripes of V2 (Sincich and Horton 2002b, 2002a), whereas the main input to the thick stripes from area V1 arises from layer 4B (Livingstone and Hubel 1987).

Thus in V2, the M-pathway can coincide with the thick CO-rich bands, the P-pathway with the pale interbands and the thin CO-rich bands, and the K-pathway with the thin CO-rich bands. In that scheme, the three anatomical channels are shown to be distinct and parallel (Hubel and Wiesel 1972; Lund 1973) and have a functional counterpart, with motion and depth being treated in the thick bands, form in the pale, and colour in the thin bands (Hubel and Livingstone 1987; Livingstone and Hubel 1987; Livingstone and Hubel 1988). However, the segregation of pathways has been questioned. Studies have shown that there is a great degree of connectivity between the pathways as early as in area V1 (Lund and Boothe 1975; Blasdel et al. 1985; Fitzpatrick et al. 1985; Lachica et al. 1992; Nealey and Maunsell 1994; Yoshioka et al. 1994), and to an even larger degree in area V2 (Rockland 1985; Levitt et al. 1994b; Xiao and Felleman 2004). Beyond V2, signals carried by these pathways give rise to the "what" and "where" functional streams described in extrastriate cortex (Ungerleider and Mishkin 1982).

A second target of V1 is area V3 (both V3d and V3v). The projection from V1 arises from layer III and possibly IVB (Zeki 1978a, 1978b; Rockland and Pandya 1979; Zeki 1980a; Weller and Kaas 1983; Burkhalter et al. 1986; Van Essen et al. 1986; Felleman et al. 1997a; Lyon and Kaas 2002). Area V3 in macaque monkeys differs from area DM in owl monkeys. Injections of tracers in V1 label reciprocal connections with area DM (Lin et al. 1982; Krubitzer and Kaas 1990; Krubitzer and Kaas 1993). Moreover, parts of V1 representing peripheral eccentricities project directly to area V3A (Zeki 1978b; Zeki 1980a). A study in New World monkeys, demonstrated that V1 connections to area 19DM (probably the homologous of area V3A in Old World monkeys) arise from cells in layer III and IV (vogt Weisenhorn et al. 1995). V1 also projects to area V4, the main output of which is the inferior temporal cortex (Perkel et al. 1986; Ungerleider et al. 2008). This projection to V4 may depend on eccentricity since reports showed that the foveal projection from V1 to V4, which originate in both CO-rich blobs and CO-poor interblob regions, is consistent whereas extrafoveal V1 projects to V4 sparsely or even not at all (Zeki 1971b, 1978a; Yukie and Iwai 1985; Perkel et al. 1986; Van Essen et al. 1986; Nakamura et al. 1993). It has also been shown that V4 projects back to V1 (Perkel et al. 1986).

Another cortical target of V1 is MT (Zeki 1971a; Weller and Kaas 1983; Perkel et al. 1986; Ungerleider and Desimone 1986a; Van Essen et al. 1986) [an area selectively involved in the analysis of visual motion (Newsome et al. 1985)]. V1 is reciprocally connected with MT. The projections from area V1 to MT originate from layers IVB and VI, and terminations in MT are concentrated in layer IV and extend into inner layer III (Lund et al. 1975; Spatz 1977; Seltzer and Pandya 1978; Maunsell and van Essen 1983; Weller and Kaas 1983; Shipp and Zeki 1989a), while the feedback connections from MT are more diffusely spread than the origins of the forward projection and terminate mainly in supragranular and infragranular layers (Spatz 1977; Weller and Kaas 1983; Shipp and Zeki 1989a). However, it should be noted that after partial or total ablations of striate cortex, cells in MT remain visual responsive (Rodman et al. 1989). In a detailed study of the projection pattern of V1 to areas in the STs, it was found that the central representation of V1 projects to MT whereas the far peripheral representation to a region termed MTp. The investigators used the term MT only for the heavily myelinated projection portion of the striate projection zone in STs and applied the term MTp to far peripheral projection zone. These two portions should be regarded as distinct parts of a single area, rather than two different areas (Desimone and Ungerleider 1986; Ungerleider and Desimone 1986b). Other cortical projections of V1 include areas PO (parieto-occipital area or V6) (Colby et al. 1988) to which V1 projects retinotopically, and MST (medial superior temporal area) which connects with the far peripheral field representations of V1 (Boussaoud et al. 1990). Finally V1 receives backward projections from area TE (Suzuki et al. 2000).

Connections of visual area V2

The cortical area V2, like V1, has a distinct connection profile with subcortical structures such as the pulvinar and the LGN. It has been shown that the projections from the pulvinar terminate within the thick and thin CO stripes of V2, mainly in the lower part of layer III (at the border with layer IV) and in layer IV (Ogren and Hendrickson 1977; Kennedy and Bullier 1985; Levitt et al. 1995), while projections from the LGN to V2 arise mainly from its interlaminar zones (Bullier and Kennedy 1983), although earlier studies failed to report a direct projection from dLGN to area

V2 e.g. (Ogren and Hendrickson 1977). Other subcortical structures connected with V2 include the intralaminar nuclei, the nucleus basalis of Meynert, and the amygdala. However, the latter afferents to V2 are more weak (Kennedy and Bullier 1985).
As it was previously discussed in detail, the main input to V2 originates from the primary visual cortex, with V2 sending back projections to it (Kennedy and Bullier 1985; Gattass et al. 1997; Anderson and Martin 2005). Additionally, area V2 is connected with many other cortical areas. Initially, a lesion study in the part of V2 representing the lower half of the central visual field demonstrated anterograde degeneration in areas V3, V4 and MT (Zeki 1971b). Subsequent reports (Zeki 1978b; Rockland and Pandya 1979; Lund et al. 1981; Rockland and Pandya 1981) confirmed these connections and studied them more comprehensively. Accordingly, V3 (both dorsal and ventral parts) and V4 were found to receive topographically organised V2 projections. Also projections to area MT seem to retain a topographic organization (Ungerleider and Desimone 1986a) but are overlapping, indicating a coarser topography of MT in comparison with that of V2 (Gattass et al. 1997). Layer IV is the major target of the V2 projection in MT. V2 projection also extends in layers I and II of MT and does not form synapses in layer VI (Anderson and Martin 2002). As in V1, the back projections from MT to V2 exhibit reciprocal asymmetry, i.e. they are more widespread in visuotopic and functional terms than the origin of feedforward projection (Shipp and Zeki 1989b). Yet, it has been shown that inactivation of V1 results in a correspondent inactivation of area V2, indicating that the direct input from LGN and the feedback projections from MT cannot drive V2 but rather modulate the information send to V2 from area V1 (Girard and Bullier 1989).
Area V2 is also connected with area V3A. An initial study (Kennedy and Bullier 1985) showed that there was a strong input to V2 from the anterior bank of the lunate sulcus and the prelunate gyrus. However, these authors had not defined functionally the visual areas in this part of the cortex. Yet, it is known that within its extent three visual areas are included (V3, V3A, and V4) indicating V2 connection with those areas (Kennedy and Bullier 1985). Later, other investigators (Gattass et al. 1997) showed that only in rare cases V2 projects to V3A. Recently, a detailed study affirmed that V2 sends an excitatory, feedforward connection to area V3A, with the majority of terminations ending in layer IV (Anderson and Martin 2005).
Area V2 demonstrates heterogeneity in the connections of its stripes. It has been found that cells in both the thin and the pale stripes project to V4 (DeYoe and Van Essen 1985; Shipp and Zeki 1985; Zeki and Shipp 1989; Nakamura et al. 1993), whereas thick stripes project to MT (DeYoe and Van Essen 1985; Shipp and Zeki 1989b). However, the back projections from MT and V4 to V2 are more widespread than the origin of the forward projections and extend beyond the clusters of efferent cells within the thick and thin/pale stripes respectively (Shipp and Zeki 1989b; Zeki and Shipp 1989). In addition, it was found that V2 projects to V4t, and that the peripheral, but not central, field representation of V2 projects to a number of other visual areas located in the occipitoparietal cortex, including PO, MST and VIP (ventral intraparietal area), as well as to a portion of area TF (on the parahippocampal gyrus) (Colby et al. 1988; Gattass et al. 1997). Moreover, area V2 is reciprocally connected with area TEO (Distler et al. 1993), it receives projections from area TE (Suzuki et al. 2000) and in one or two cases V2 projections were found in area prestriata and area 8 of the prefrontal cortex (Gattass et al. 1997).
It has been suggested that the bypass routes from V2 directly to temporal and parietal areas (TEO and PO), and from V1 directly to V4 may allow coarse information regarding form/colour and

spatial information to arrive quickly in the temporal and parietal cortices enabling an elementary analysis of the stimulus (Nakamura et al. 1993; Gattass et al. 1997).

Connections of visual area V3

As it was previously discussed, there was a controversy regarding delineation of area V3. It was considered that its dorsal and ventral halves differ in their connections with V1, their myeloarchitecture, their callosal inputs, their receptive field properties, and their outputs to higher areas (please refer to the V3 section on page 14). Now, it is well established that both parts of V3 receive projections from V1 (please refer to the V1 section on page 6), and that after V1 inactivation visual responsiveness of almost all V3d neurons is ceased (Girard et al. 1991). Nonetheless, V3d and V3v have similar but not the same connections with other cortical areas. Hence, V3d has connections with areas V4t and FST (fundus of the superior temporal area) [reciprocal in (Boussaoud et al. 1990) and not reciprocal in (Felleman et al. 1997a)], that are absent or rare for VP (Boussaoud et al. 1990; Felleman et al. 1997a). VP has connections with the ventral occipitotemporal area (VOT), the DP area, and the visually responsive portion of temporal visual area F (VTF) that are absent or occur only rarely for V3 (Felleman et al. 1997a). On the contrary, both V3d and V3v are reciprocally connected with V2 (Felleman et al. 1997a) (please refer also to the V2 section on page 10). It should be noted that thick stripes are the major source of output to V3 (DeYoe and Van Essen 1988; Felleman and Van Essen 1991; Shipp 2002; Shipp 2006).
Moreover, V3d and V3v have reciprocal connections with areas V4 (Felleman et al. 1997a; Ungerleider et al. 2008) and MT (Ungerleider and Desimone 1986a; Felleman et al. 1997a) in a topographically organised way, and areas V3A, posterior intraparietal area (PIP), dorsal MST (MSTd), VIP (Felleman et al. 1997a) and frontal eye fields (FEF) (Barbas and Mesulam 1981; Barbas 1988). Furthermore, area V3 (d and v) is reciprocally connected with PO (Colby et al. 1988; Shipp et al. 1998), an area in the anterior bank of the parieto-occipital sulcus involved in sensory motor integration of reaching arm movements (Galletti et al. 1997) and in the spatial encoding of extrapersonal visual space (Galletti et al. 1995). This projection from V3 is also topographically organised.
Other projections directly from V3 and indirectly via V3A terminate to the posterior parietal lobule (PPL) within the extent of the DP area (Andersen et al. 1990), the caudal intraparietal area (cIP) (Sakata et al. 1997) and the lateral intraparietal area (LIP) (Andersen et al. 1990; Blatt et al. 1990). In addition, area V3 sends feedforward, topographically organised inputs to area TEO and receives a feedback projection from it (Distler et al. 1993).

Connections of visual area V3A

Area V3A is richly connected to surrounding cortical areas. It receives feedforward connections from caudal cortical areas, including a direct projection from peripheral parts of V1 (Zeki 1978b; Zeki 1980a; Van Essen et al. 1986), and a strong input from V2 (Gattass et al. 1997) and V3 (Zeki 1978b; Felleman et al. 1997a). If V1 is cooled, in contrast to V3 neurons that stop responding to visual stimulation, many neurons in V3A continue responding (Girard et al. 1991). Therefore, other connections than that with V1 are also capable to drive V3A neurons. These may include the pulvinar (Benevento and Rezak 1976), the LGN (Fries 1981; Yukie and Iwai 1981), or the MT.

V3A is reciprocally connected with MT (Ungerleider and Desimone 1986a), and residual activity is found in MT after V1 inactivation (Rodman et al. 1989). Moreover, MT is also found to be extensively connected to subcortical structures (Ungerleider et al. 1984; Sincich et al. 2004).
In addition to MT in the dorsal stream, V3A is also connected to LIP (Cavada and Goldman-Rakic 1989; Andersen et al. 1990; Blatt et al. 1990; Baizer et al. 1991; Nakamura et al. 2001), area DP (Andersen et al. 1990), MST, FST (Boussaoud et al. 1990) and PO (Colby et al. 1988; Shipp et al. 1998). V3A also has reciprocal connections with areas of the ventral stream including V4 (Ungerleider et al. 2008) and the peripheral field representation of TEO (Distler et al. 1993; Webster et al. 1994). V3A has reciprocal connections with the FEF too (Schall et al. 1995; Stanton et al. 1995).

Connections of visual area V4

Both the central and peripheral parts of V4 are connected with occipital areas V1, V2, V3, and V3A (please refer to corresponding sections). It should be noted that while there is good evidence that cells in both the thin and the pale stripes (which are predominantly fed by the parvocellular system) project to V4 (DeYoe and Van Essen 1985; Shipp and Zeki 1985; Zeki and Shipp 1989; Nakamura et al. 1993), it has been further shown through inactivating selected layers of V4 that it receives about equally strong magnocellular and parvocellular inputs (Ferrera et al. 1994).
V4 is connected with areas in the temporal cortex. It projects to superior temporal areas V4t, MT, and FST (Ungerleider and Desimone 1986a; Boussaoud et al. 1990; Ungerleider et al. 2008). Yet, its major output is to areas TEO and TE in the inferior temporal cortex (Desimone et al. 1980; Weller and Kaas 1985, 1987; Distler et al. 1993) which contains neurons selective for many object features, such as colour, shape, and texture (Desimone et al. 1984; Tanaka et al. 1991; Fujita et al. 1992; Tanaka 1996). V4 receives backward projections from these areas (Distler et al. 1993; Suzuki et al. 2000). V4 displays dense reciprocal connections with several subdivisions of inferotemporal cortex including the posterior inferotemporal ventral area [(PITv), part of the temporal-occipital transition region (TEO)], the central inferotemporal ventral area (CITv), the posterior inferotemporal dorsal area (PITd), and the central inferotemporal dorsal area (CITd). The retinotopic organisation of TEO is less precise than that in area V4, but clearly different from that described in area TE where retinotopy is absent (Desimone and Gross 1979; Boussaoud et al. 1991). The peripheral field representations of V4 are mainly connected with occipitoparietal areas DP, VIP, LIP, PIP, and MST (Andersen et al. 1990; Ungerleider et al. 2008). V4 is also reciprocally connected with PO, with the projections from V4 to PO being retinotopically organised (Colby et al. 1988; Ungerleider et al. 2008). Furthermore, V4 is connected with the parahippocampal area TF (Ungerleider et al. 2008) and the FEF (Barbas and Mesulam 1981; Ungerleider et al. 2008).

Functional Streams

It is evident that the numerous visual areas described previously are richly interconnected with many direct corticocortical pathways and have different functions. A question that has always engaged the interest of the researchers is whether this obvious specialisation is evident in the organisation of the brain through the configuration of specific networks. Two principles have been proposed for the visual processing in the cortex. The first view is that referred as *hierarchical processing*. According to it, visual areas are sequentially organised into well-defined pathways which serve the serial processing of visual information. The other classical model, *parallel processing*, supports that visual information is simultaneously sent by the primary visual cortex and also by other subcortical sources (e.g. the thalamic nucleus of the pulvinar and the LGN) bypassing V1, to many visual areas which process the various features of the stimuli in parallel (Van Essen and Maunsell 1983). This concurrent handling of the perceptual load reduces the necessary "computational" time. On the other hand, hierarchical processing is beneficial since the different cortical elements that analyse distinct constituents of the visual information can be transmitted to sequentially higher order areas, eliminating the need to process the same visual components in multiple visual areas.

These organisation principles provided the framework to construct an orderly scheme for the process of visual information. A number of studies have provided evidence that visual process is segregated into two streams, each transforming visual information in a discrete way. This notion stemmed from initial studies on the different properties and connections of LGN neurons, on the physiological parameters of cortical areas and on the visual deficits following temporal and parietal lesions in monkeys (Ettlinger 1959; Pohl 1973). Among the first who supported the view that vision is mediated by two functionally specialised processing pathways, the dorsal and the ventral one, were Ungerleider and Mishkin (Ungerleider and Mishkin 1982). Each pathway has the striate cortex as the source of initial input and processes different attributes of the visual scene. The dorsal pathway connects V1 with the posterior parietal cortex and has been suggested to be responsible for spatial vision i.e. motion and disparity information. The ventral pathway extends from V1 to the inferior temporal cortex and is thought to be responsible for visual identification of objects i.e. form and colour perception (Fig.1.1).

This segregation seems to start as early as the output of the retina. The P/ventral pathway arises in the midget retinal ganglion cell and ascends through the parvocellular LGN, to layers 4Cb and 4A in V1, the thin and pale stripes of V2, V4, and the inferior temporal cortex. The M/dorsal pathway begins with the parasol retinal ganglion cell and continues to magnocellular LGN, layers 4Ca and 4B in V1, thick stripes in V2, to V3, and MT, and the parietal cortex. These processing streams are broadly referred as "*what*" and "*where*" pathways, respectively (Livingstone and Hubel 1988; Zeki and Shipp 1988; Goodale and Milner 1992; Merigan and Maunsell 1993; Ungerleider and Haxby 1994; Goodale 1998; Goodale and Humphrey 1998; Shipp 2006).

Although this concept of parallel and hierarchical processing of different types of visual information is interesting, obviously it is not an absolute rule. Numerous studies have demonstrated that there is interaction between the two pathways. For instance, there is substantial convergence of P and M signals in the upper layers of V1 (Lachica et al. 1992; Martin 1992; Merigan and Maunsell 1993; Yoshioka et al. 1994). It is shown that thick, thin and pale stripes all receive projections from the same V1 layers: heaviest from layer 2/3 and less from layers 4A, 4B, and 5/6 (Sincich and Horton 2002b). In V2, it was shown that the different CO compartments are extensively

interconnected. The thin stripes project more frequently to the thick stripes than to other thin stripes, the thick stripes project more frequently to the thin stripes than to other thick stripes and the pale stripes project almost equally to CO-rich and pale stripes (Levitt et al. 1994b). Another possible mechanism for P/M convergence could be the back projections to V2 from V4 and MT. Although distinct V2 subregions provide ascending outputs to these areas, the feedback connections to V2 terminate less specifically over all stripe divisions (Shipp and Zeki 1989b; Zeki and Shipp 1989). It is already mentioned that M input reaches area V4, and that area V1 is connected with both V4 and V5, while these areas have projections to parietal and temporal cortex. Hence, it is evident that another aspect of cortical organisation is functional integration.

These findings which point to anatomical and functional coupling between the two functional streams are neither odd nor unexpected. These various lines of evidence can evoke substantial objections against functional specialisation in the visual system (Merigan and Maunsell 1993). However they should be considered as significant components subserving the construction of a unified percept of the visual image, which is processed in two relatively independent, albeit interacting cortical pathways in the brain (Zeki and Shipp 1988; Shipp 1995). This last scheme seems plausible. On one hand segregation enables the representation of selected features of the external world on an edifice with limited spacing abilities, and on the other hand integration ensures that these networks provide as much an accurate and complete representation of external world as it could be.

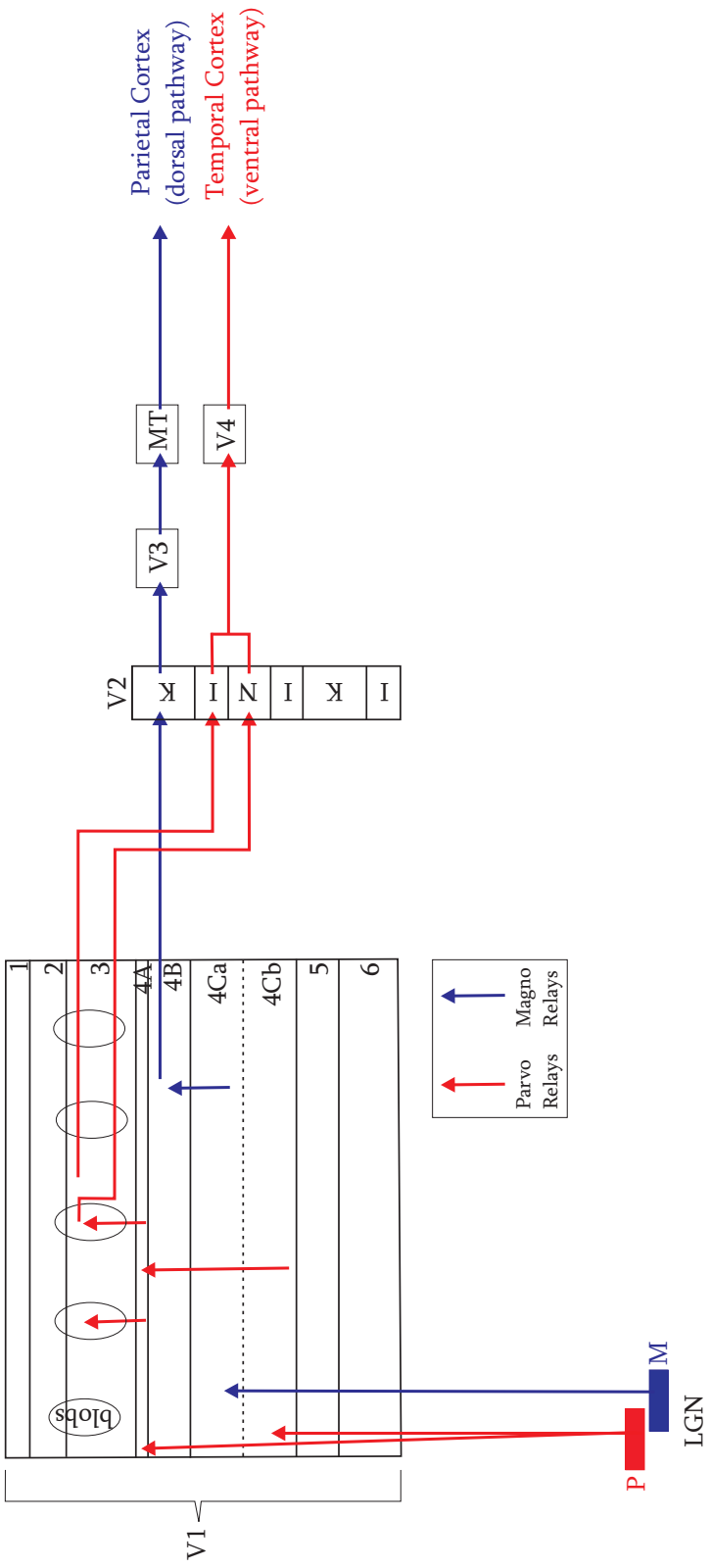

Figure 1.1: A schematic representation of the two cortical visual pathways. The dorsal pathway directed to visual areas of the posterior parietal cortex through areas V3 and MT, begins from the magnocellular layers of the LGN, and continues to layers 4Ca and 4B in V1 and to thick stripes of V2. The ventral pathway directed to visual areas of the inferior temporal cortex through area V4, begins from the parvocellular layers of the LGN, and continues to layers 4Cb and 4A in V1, and to thin and pale stripes of V2. LGN: Lateral Geniculate Nucleus; M: magnocellular layers of LGN; P: parvocellular layers of LGN; I: interstripes; K: thick stripes; N: thin stripes; red: parvocellular inputs; blue: magnocellular input.

CHAPTER 2

Aim of the Study

The findings of our laboratory, so far, have demonstrated that we perceive the actions of others by recruiting virtually the same parieto-frontal cortical circuits which are responsible for the generation of the same actions (Raos et al. 2004, 2007; Evangeliou et al. 2009). In other words, observation of an action stimulates the motor controller used to execute the same action. Indeed, action-execution, action-observation and action-recognition share cerebral and physiological correlates with 'motor imagery', also known as 'mental practice' or 'mental simulation of action', i.e. the faculty whereby we mentally rehearse voluntary movements without bodily executing them (Decety et al. 1994; Jeannerod 1995; Stephan et al. 1995; Porro et al. 1996; Roth et al. 1996; Sirigu et al. 1996; Deiber et al. 1998).

The aim of the present study was to examine whether the network of interconnected areas subserving action cognition also includes early visual cortical areas. Research data has delivered new and often contradicting results regarding the contribution of early visual areas in imagery processes. In the present study we explored whether the proposed neural substrate of mental simulation of an action extends beyond the parieto-frontal motor/kinesthetic network, to the striate and extrastriate occipital cortical visual areas representing the object to be reached and manipulated and its spatial location, information useful for guiding the arm and shaping the hand to interact with the object. We used the [^{14}C]-deoxyglucose (^{14}C-DG) quantitative autoradiographic method (Sokoloff et al. 1977) to obtain high-resolution functional images of the monkey occipital visual cortical areas activated for grasping small 3D-objects in the light and in the dark, as well as for observation of the same grasping movements executed by another subject. We reconstructed two-dimensional (2D)-maps of metabolic activity of the striate area V1 and the extrastriate cortices V2, V3, V3A, and V4, which occupy the occipital operculum and both banks of the lunate (Ls) and the inferior occipital (IOs) sulci. Specifically, we addressed the questions whether particular early visual cortical areas are activated (a) for grasping in the dark, i.e. for the voluntary manipulation of an invisible/imaginary object and (b) for observation of grasping performed by another subject, involving mental simulation of the action, i.e. for the imaginary manipulation of a visible object. Based on previous findings and on the information flow in the networks responsible for imagery, involving the parietal and temporal areas which are connected to the occipital areas, our hypothesis

was that early visual cortical areas may be activated during action in the dark and during action-observation.

CHAPTER 3

Methods

Subjects

Twelve adult female monkeys (*Macaca mulatta*) weighing between 3 and 6 kg were used in the present study. All animals were purpose-bred by authorised suppliers (Deutsches Primatenzentrum, Göttingen, Germany; R. Hartelust, Nederlands). Food access was unrestrained for the animals, ensuring an enriched, varied diet which complied with the nutrition requirements of the animals. Water access during the training process was controlled, yet the animals received the necessary fluids during the daily experimental sessions. On weekends water access was unhampered. The weight and well-being of the animals were carefully monitored and, if necessary, supplementary fruit, water and caregiving were provided. Housing, experimental and surgical procedures were approved by the Greek Veterinary Authorities and the Foundation of Research and Technology-Hellas animal use committee, complying with European Council Directive 86/609/ECC.

Animal Preparation

Upon arrival, the animals were accommodated in their cages (Crist Instrument Co, Hagerstown, MD, USA). Introducing animals to the new facility, with associated changes in their living environment, social groups, and new personnel, produced a stress response that necessitated the acclimatisation of animals before they were used in the research protocol. During this acclimatisation period, animals had free access to food and water, and their behaviour was carefully assessed by observation and during interactions with the researcher. Animals were presented with enrichment stimuli such as toys and music and allowed to familiarise themselves with the new conditions. Animals participated in the experimental procedure only after a stable physiological state was reached. This ensured the well being of the animals and eliminated the risk of unwanted responses that would influence the experimental procedure.

Prior to behavioural training, a metal bolt (Crist Instrument Co, Hagerstown, MD, USA) embedded in dental cement (Resivy, Vence, France) was stereotactically implanted on each monkeys' head with

the use of mandibular plates (Synthes, Bettlach, Switzerland), secured on the cranium with titanium screws (Synthes, Bettlach, Switzerland) for head immobilization. All surgical procedures were performed under aseptic conditions and anesthesia (ketamine hydrochloride, Imalgene 1000, Merial, France, 20mg/kg, i.m and sodium pentobarbital 25mg/kg, i.m), with the aid of a stereomicroscope. Systemic antibiotics (Rocephin, Roche, Switzerland, 60-70 mg/kg/day i.m) and analgesics (Apotel, Uni-Pharma, Hellas) were administered pre- and post- operatively. The animals were allowed to recover from surgery for at least three weeks before beginning of training sessions.

Experimental Set-up

The behavioural apparatus for the grasping and the observation tasks contained a PC-controlled rotating turntable, into which a 3D geometrical solid horizontally oriented ring of 15mm diameter was accommodated. The behavioural apparatus was placed in front of the monkeys, at shoulder height, at a distance depending on whether the experimenter or the monkey performed the requisite movements. The ring was grasped with the digging out grip (index finger inserted into the ring). A sliding circular window of 8° diameter, at the front side of the behavioural apparatus allowed or prohibited sight the object and access to it. EMG (gainx2000, band-pass filter 0.3-3000KHz) recordings were performed using Ag-AgCl surface electrodes. The digitised electromyograms (1000Hz) were recorded from the biceps and wrist extensor muscles and were aligned at the end of the movement, rectified and averaged over 150 movements in each case.
The behavioural apparatus for the fixation task was a 21 inch video monitor (Philips, the Netherlands) placed 23 cm in front of the monkey. Visual targets were red spots of 1.5° diameter. Eye position for all monkeys was recorded with an infrared oculometer (Dr. Bouis) and is illustrated in 3D-histograms of the dwell time of the line of sight (Fig.4.1).
During training sessions and ^{14}C-DG experiments, the animals were seated in a primate chair (Crist Instrument Co, Hagerstown, MD, USA) with their head immobilized, and their lower limbs and one or both forelimbs restrained with Velcro tapes, depending on the special features of the task. Training was based on operant conditional techniques and successful completion of each trial was rewarded with water, delivered by a tube placed close to the animal's mouth. Monkeys were trained on a daily basis for at least an hour over a period of 4-11 months, until their performance displayed a 95% success rate. On the day of the ^{14}C-DG experiment, monkeys performed their tasks continuously during the entire experimental period of 45 min and received the custom reward.

Behavioural Tasks

The number of monkeys employed in the present study is the minimum possible that allows for solid conclusions.

Grasping in the light (Gl)

Two grasping-in-the-light (Gl) monkeys were trained to reach and grasp with the left forelimb and under visual guidance, while the right forelimb was restricted. They were required to fixate the illuminated object behind the opened window for 0.7-1 s, until a dimming of the light would signal reaching, grasping and pulling the ring with the left forelimb. The maximum latency to grasp

the object was set to 1 s, although the movement was usually completed within 500-600 ms. The monkeys had to maintain fixation (within the 8° diameter circular window) until the end of the movement. The Gl monkeys were allowed to move their eyes outside the window only during the intertrial intervals (ranging between 2 and 2.5 s).

Grasping observation (O)

Three grasping-observation (O) monkeys were first trained to perform the task of the Gl monkeys (grasping-training), and later on to observe the same grasping movements executed by the experimenter (observation-training). In order to eliminate any possible inter-hemispheric differences in the effects due to the earlier grasping-training, the first monkey was trained to grasp with its left hand, the second one with its right hand and the third one with both hands consecutively. During the observation-training and during the ^{14}C-DG experiment, both forelimbs of the O monkeys were restricted. The experimenter was always standing on the right side of the monkey and was using the right arm/hand for reaching/grasping. Both reaching and grasping components of the movement were visible to the monkey.

Motion control (Cm)

In order to disambiguate the effects of the purposely reaching/grasping action, i.e. the components of reaching-to-grasp, hand preshaping, and object-hand interaction from (a) the non-goal-directed biological-motion effect, elicited by a purposelessly moving forelimb in front of the monkey (arm-motion effect), and from (b) the visual stimulation effect induced by mere presentation of the 3D-object to the monkey (object-presentation effect), we compared the effects on the Gl and O monkeys with those on two arm-motion control (Cm) monkeys. Each Cm monkey had both hands restricted, had no previous grasping training, and was trained to maintain its gaze straight ahead, within the 8° diameter circular window, during the opening of the window of the apparatus, the presentation of the illuminated object behind the opened window, the closure of the window, and while the experimenter was reaching with extended hand towards the closed window (for a total period of 2.7-3 s per trial). The direction of motion and velocity of the experimenter's arm were the same as in the observation task. At this point it should be noted that monkey and human movements share striking kinesiological similarities. Both species have almost identical prehension characteristics, and reaching and grasping components of the movement e.g. accuracy appears to be achieved in the same way by both species, the mean velocity of reach to grasp movement is equivalent and the relationship between grip aperture and object size is remarkably similar (Roy et al. 2000). Therefore, the observation of a reaching movement made by a human experimenter does not impose any bias on our study and does not have any deteriorating effect on our results. The Cm monkeys were allowed to move their eyes outside the circular window only during the intertrial intervals (ranging between 2 and 2.5 s).

Fixation control (Cf)

In order to remove the visual effect caused by plain fixation, the activations of the visual cortex of the Cm, Gl and O groups of monkeys were compared with those of the two hemispheres of a fixation-control monkey (Cf). The visual target for fixation was a red target 1.5° in diameter,

located straight ahead. The Cf monkey had both its arms restricted and was trained to maintain fixation within a circular window 2.5° in diameter, centered on the fixation target, for the duration of the trial (4 s). Intertrial intervals ranged between 0.2 and 0.3 s. The Cf monkeys maintained fixation for 75% of the ^{14}C-DG experimental time including intertrial intervals.

Grasping in the dark (Gd)

Two grasping-in-the-dark (Gd) monkeys were trained to reach and grasp with the left forelimb in complete darkness, while the right forelimb was restricted. The task took place in complete darkness, achieved by using black curtains which enclosed the primate chair together with the behavioural apparatus, and by an extra black drape positioned in front of the eyes of the monkey. A speaker, placed 25 cm in front of the monkey in the median sagittal plane below the behavioural apparatus, delivered the go-signals. The initiation signal of the grasping movement was a low frequency auditory cue (90 Hz). Following this, each Gd monkey had to look straight ahead towards the memorised location of the object for 0.7-1 s, until a second high frequency auditory cue (180 Hz) signaled the generation of the learned action (reaching, grasping and pulling the unseen, memorised ring with the left forelimb) while maintaining its gaze straight ahead within a window of 10x10 deg. The maximum latency to grasp the object was set to 1 s, although the movement was usually completed within 500-600 ms. The Gd monkeys were allowed to move their eyes outside the window only during the intertrial intervals (ranging between 2 and 2.5 s).

Control in the dark (Cd)

To reveal the effects induced by reaching-to-grasp in the dark, the metabolic maps of the four hemispheres from the two Gd monkeys were compared with those obtained from the four hemispheres of two control-in-the-dark monkeys (Cd). The Cd monkeys were allowed to move their eyes freely throughout the experiment and were presented with auditory stimuli similar to the acoustic cues presented to the Gd monkeys. Reward was delivered at random intervals to prevent association of the auditory stimuli with the reward expectancy. The total number of rewards that the Cd monkeys received matched that of the Gd monkeys. The task was held in complete darkness and the monkeys were alert and actively exploring their environment during the ^{14}C-DG experiment as it is revealed by the roughly even distribution of eye position in much of the oculomotor space (Fig.4.1 Cd).
A schematic overview of the tasks is illustrated in Fig.3.1.

[^{14}C]-Deoxyglucose Method in Brain Imaging

Theoretical basis

The required energy for all cerebral functions derives from the glucose metabolism. The primate brain is highly selective for the entry of energy substrates due to the existence of the blood-brain barrier. This protective mechanism limits the possible substrates and allows only specific substances to enter to the brain. As a result, the primate brain utilises almost exclusively D-glucose, from which it derives virtually all of the energy requirements under normal conditions.
The [^{14}C]-deoxyglucose (^{14}C-DG) functional imaging method is used for simultaneous quantitative determination of the rates of glucose consumption in all of the macroscopic structural components

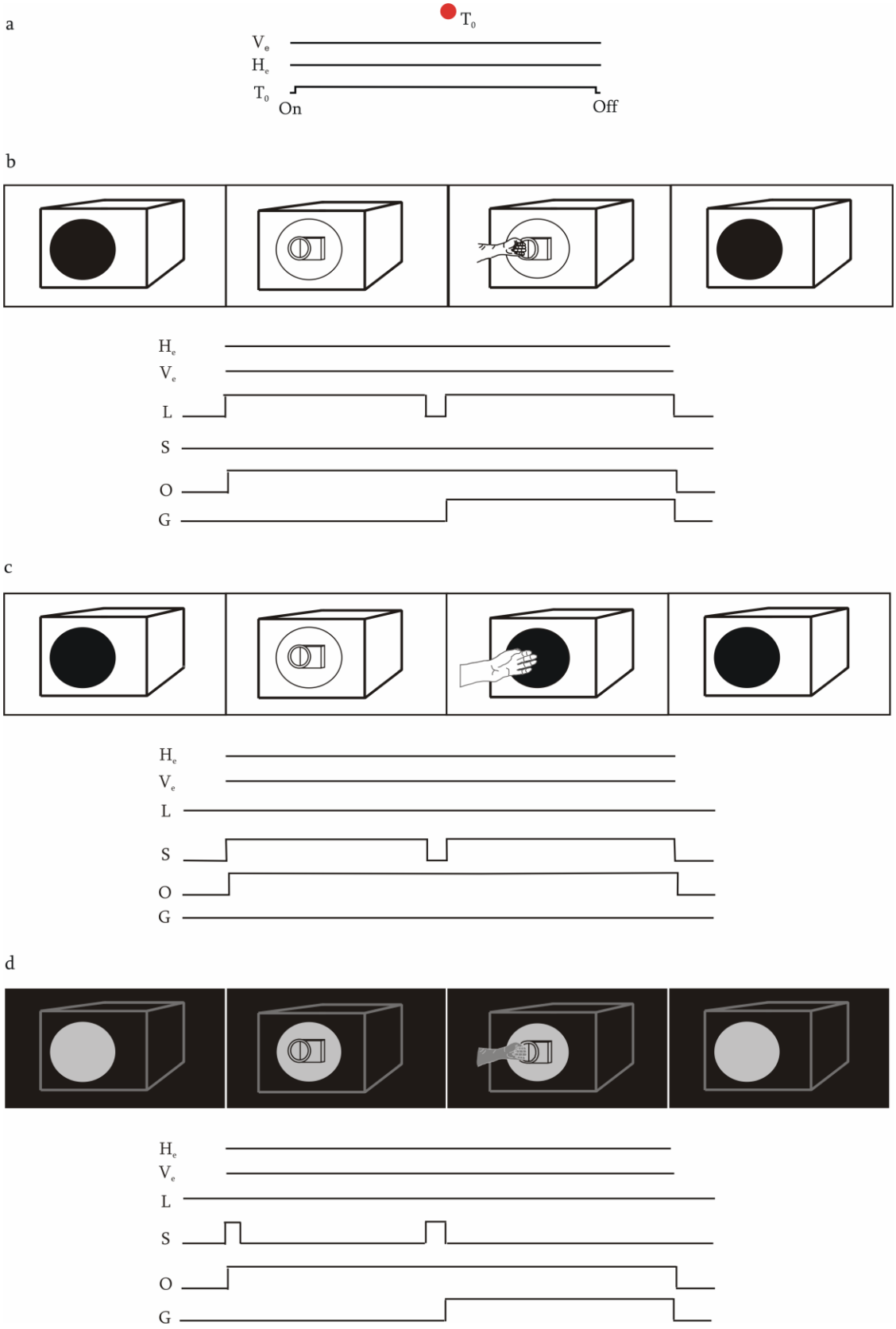

Figure 3.1: Schematics of behavioural paradigms and task events. ***a***, in the visual fixation task, the monkey was rewarded for fixating a visual target T_o centered straight ahead. ***b***, in the grasping in the light (Gl) task, the monkeys were rewarded for grasping with the left forelimb a 3D ring under visual guidance. ***c***, in the motion-control (Cm) task, the monkeys were rewarded for maintaining their gaze straight ahead, while observing the experimenter reaching with his extended hand towards the behavioural apparatus. ***d***, in the grasping in the dark (Gd) task, the monkeys were rewarded for grasping with the left forelimb a 3D ring in complete darkness. He and Ve represent the horizontal and vertical eye position, respectively. L represents the illumination of the compartment of the behavioural apparatus that made the object visible. S represents the auditory cues that signaled either the onset of the trial or the go-signal for the initiation of the movement. O stands for observation and G for execution of grasping.

of the central nervous system in conscious laboratory animals (Sokoloff et al. 1977; Kennedy et al. 1978). The impetus for employing this method is the tight coupling of energy metabolism to neuronal activity whereby local changes in brain activity can be detected by monitoring the changes in physiological properties such as blood flow, glucose utilisation or oxygen consumption. Although oxygen consumption is the most direct measure of energy metabolism, the volatility of oxygen and its metabolic products and the short half-life of its radiolabeled isotopes preclude measurement of oxidative metabolism by the autoradiographic technique. Radioactive glucose is not fully satisfactory either, because its labeled products are lost too rapidly from cerebral tissues. On the other hand, the biochemical properties of 2-deoxy-D-1[^{14}C]glucose (2DG), the labeled analogue of glucose, are such that enable its usage as a tracer for the glucose metabolism and make it an appropriate tool for the measurement of the local cerebral glucose utilisation (LCGU) by the autoradiographic technique.

The tenet of the method derives from the biochemical properties of 2DG in the brain and the kinetics of the exchange of 2DG and glucose between plasma and brain tissue and their phosphorylation by hexokinase. 2DG differs from glucose only in the replacement of the hydroxyl group on the second carbon atom by a hydrogen atom. This single structural difference makes 2DG suitable for this method. 2DG is bidirectionally transported between blood and brain by the same carrier that transports glucose across the blood-brain barrier (Bidder 1968; Bachelard 1971). Therefore, 2DG and glucose compete for both blood-brain transport and hexokinase phosphorylation. In the cerebral tissue, 2DG is phosphorylated by hexokinase to 2-deoxyglucose-6-phosphate (DG-6-P) just like glucose is phosphorylated to glucose-6-phosphate (G-6-P) (Sols and Crane 1954). Unlike G-6-P, which is metabolised further, eventually to CO_2 and water (and to a lesser degree via the hexosemonophosphate shunt), DG-6-P cannot be converted to fructose-6-phosphate because the lack of the hydroxyl group on the second carbon atom makes it unsuitable as a substrate for glucose-6-phosphate dehydrogenase (Sols and Crane 1954). There is relatively little glucose-6-phosphatase activity in the brain and even less deoxyglucose-6-phosphatase activity (Sokoloff et al. 1977). DG-6-P can be converted to deoxyglucose-1-phosphate, then to UDP-deoxyglucose and eventually to glycogens, glycolipids, and glycoproteins. However, reactions are slow, and also a very small fraction of the formed DG-6-P proceeds to these products in mammalian tissues (Nelson et al. 1984). In any case, these compounds are secondary, relatively stable products of DG-6-P, and all together represent the products of deoxyglucose phosphorylation. DG-6-P and its derivatives are stable substances and once formed are trapped in the cerebral tissue, at least long enough for the duration of the experimental session (Fig.3.2).

If, following the administration of 2DG, the interval of time is kept short enough (less than 1 hour), the quantity of 2DG-6-P accumulated in any cerebral tissue at any time is equal to the integral of the rate of 2DG phosphorylation by hexokinase during that interval of time. This integral is related to the amount of glucose that has been phosphorylated over the same interval, depending on the time courses of the relative concentrations of 2DG and glucose in the precursor pools, and the Michaelis-Menten kinetic constants for hexokinase with respect to both 2DG and glucose. With the cerebral glucose consumption in a steady-state, the amount of glucose phosphorylated during an interval of time equals the steady-state flux of glucose through the hexokinase-catalysed step times the duration of the interval, and the net rate of flux of glucose through this step equals the rate of glucose utilisation.

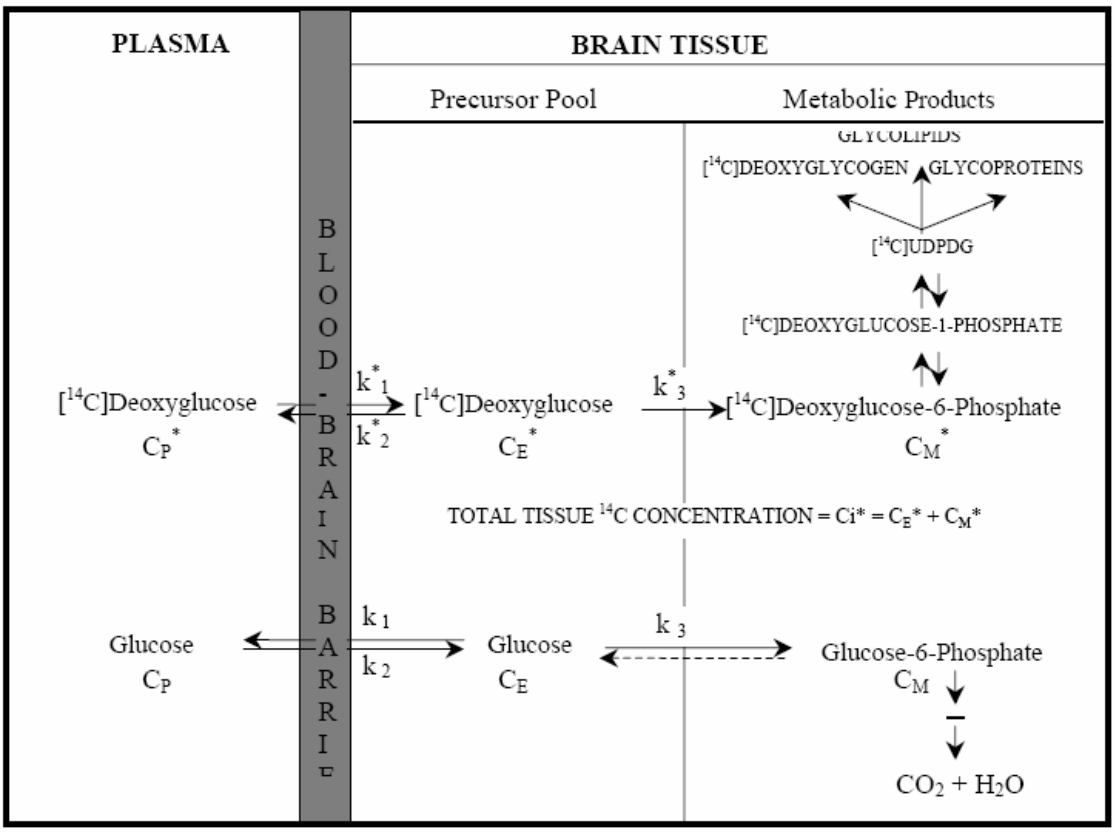

Figure 3.2: Theoretical basis of the radioactive deoxyglucose method for measurement of local cerebral glucose utilisation (Sokoloff et al. 1977). Diagrammatic representation of the theoretical model. C_i^* represents the total tissue ^{14}C concentration in a single homogeneous area of the brain. C_p^* and C_p represent the concentrations of [^{14}C]deoxyglucose and glucose in the arterial plasma, respectively; C_E^* and C_E represent their respective concentrations in the tissue pools that serve as substrates for hexokinase. C_M^* represents the concentration of [^{14}C] deoxyglucose-6-phosphate in the tissue. The constants k_1^*, k_2^*, and k_3^* represent the rate constants for carrier-mediated transport of [^{14}C] deoxyglucose from plasma to tissue, for carrier-mediated transport back from tissue to plasma, and for phosphorylation by hexokinase, respectively; the constants k_1, k_2, and k_3 are the equivalent rate constants for glucose. [^{14}C]deoxyglucose and glucose share and compete for the same carrier that transports both of them between plasma and tissue as well as for the hexokinase, which phosphorylates them to their respective hexose-6-phosphates. The dashed arrow represents the possibility of glucose-6-phosphate hydrolysis by glucose-6-phosphatase activity, if any.

These relations can be described mathematically by an operational equation, provided that: (a) glucose metabolism is in a steady-state throughout the experimental period, i.e. independent of plasma glucose, (b) homogeneous tissue compartment within the concentrations of glucose and 2DG are uniform and exchange directly with the plasma, and (c) 2DG concentrations are low compared to their glucose counterparts, i.e. tracer kinetics apply.
This operational equation defines the rate of glucose utilization (R) per unit mass of tissue i, (R_i) (Fig.3.3). It is a general statement of the standard relationship by which rates of enzyme-catalysed reactions are determined from measurements made with radioactive tracers. The numerator represents the amount of radioactive product formed in any given interval of time; it is equal to C_i^*, the combined concentrations of 2DG and 2DG-6-P in the tissue at time T (measured by quantitative autoradiography), minus a term that represents the free (non-metabolised) 2DG still remaining in the tissue at time T. This way, the rate of chemical transformation of the labeled 2DG can easily be measured. However this rate does not equal the rate of glucose phosphorylation. To derive the rate of the total reaction of a chemical substance from measurement of the reaction rate of its labeled species only, it is necessary to know the integrated specific activity (i.e. the ratio of labeled to total molecules) in the precursor pool. For this reason, the precursor pool specific activity is measured indirectly from measurements in the blood supplied to the tissue. The specific activity in the arterial blood or plasma can be directly measured and the precursor specific activity can be calculated by correcting for the lag in the equilibration of the precursor pool in the tissue with that of the plasma. Additionally, the labeled species often exhibit a kinetic difference from the natural compound, the so-called isotope effect. This isotope effect can be evaluated and corrected for. The denominator represents the integrated specific activity (the ratio of labeled to total molecules) in the precursor pool as measured in plasma, corrected for the lag in the equilibration of the tissue precursor pool with the plasma, times a factor (lumped constant) that corrects for kinetic differences between the labeled and natural compound (isotope effect).
The operational equation of the method specifies the variables to be measured in order to determine Ri, the local rate of glucose consumption in the brain. The following variables are measured in each experiment: (a) the entire history of the arterial plasma [^{14}C]- DG concentration, C_p^*, from zero time to the time of sacrifice T, (b) the steady state arterial plasma glucose level C_p, over the same interval and (c) the local concentration of ^{14}C in the tissue at the time of killing C_i^*(T).
The rate constants k_1^*, k_2^* and k_3^* and the lumped constant λ V_m^* K_m/ Φ V_m K_m^* are not measured in each experiment. The values for these constants are species specific and have been determined separately in other groups of animals [rat (Sokoloff et al. 1977), monkey (Kennedy et al. 1978)].
At this point we should stress that it is important to keep the experimental period at 45 min. This limitation is compelled by the possible phosphatase activity beyond this time point. It is known that glucose-6-phosphatase activity in the brain is very low and does not influence the deoxyglucose method. The [^{14}C]DG-6-P is formed in the cytosol, and the phosphatase is on the inner surface of the cisterns of the endoplasmic reticulum. In order the phosphatase to act on the [^{14}C]DG-6-P, it has to be transported from the cytosol across the endoplasmic reticular membrane by a specific carrier. However, this is a highly slow process because the carrier for G-6-P and DG-6-P is essentially absent in the brain (Fishman and Karnovsky 1986). The substrate then has access to the enzyme only by slow diffusion through the membrane. If one extends the experimental period beyond 45 min then correction must be made for the effects of phosphatase by including a k_4^* rate constant for the phosphatase activity (Sokoloff 1982).

$$R_{i=}\frac{\overbrace{\underbrace{C_i^*(T)}_{\text{Total 14C in tissue at time T}} - \underbrace{k_1^* e^{-(k_2^*+K_3^*)T}\int_o^T C_p^* e^{(k_2^*+k_3^*)t}\,dt}_{\text{14C in precursor remaining in tissue at time T}}}^{\text{Labeled product formed in interval of time 0 to T}}}{\underbrace{\left[\frac{\lambda \cdot V_m^* \cdot k_m}{\Phi \cdot V_m \cdot k_m^*}\right]}_{\text{Isotope effect correction factor}}\underbrace{\left[\underbrace{\int_o^T \left(\frac{C_p^*}{C_p}\right)dt}_{\text{Integrated plasma specific activity}} \underbrace{-e^{-(k_2^*+K_3^*)T}\int_o^T \left(\frac{C_p^*}{C_p}\right) e^{(k_2^*+k_3^*)t}\,dt}_{\text{Correction for lag in tissue equilibration with plasma}}\right]}_{\text{Integrated precursor specific activity in tissue}}}$$

Figure 3.3: Operational equation of the radioactive deoxyglucose method. T, time of termination of the experimental period; λ, ratio of the distribution space of deoxyglucose in the tissue of that of glucose; Φ, the fraction of glucose that once phosphorylated, continues down to glycolytic pathway; k_m^*, V_m^*, k_m, V_m, Michaelis-Menten kinetic constants of hexokinase for deoxyglucose and glucose, respectively. Other symbols as in Fig.3.2.

[^{14}C]-deoxyglucose experiment

The experiments were performed on conscious behaving animals. The day of the 2DG experiment, each animal was subjected to femoral vein and artery catheterisation under general anesthesia (ketamine hydrochloride, 20 mg/kg, i.m.). The catheters were plugged at one end and were filled with dilute heparin solution (1000U/ml). Both catheters were 45 cm long, to minimise extensive flushing of dead space during the sampling period. After catheterisation the animals were allowed to recover from anesthesia for 4-5 hours. Upon recovery the experimental session began.

Five min after each monkey started performing its task, the experimental period was initiated with the infusion of a single pulse of 2DG through the venous catheter over a period of 30s. A dose of 100 μCi/kg of animal weight of 2DG (specific activity 55 mCi/ml, ARC, St. Louis, MO, USA) was employed. Because the 2DG was supplied in an ethanol solution, it was evaporated to dryness and then re-dissolved in 1ml of saline. To monitor the course of the plasma and 2DG concentrations, arterial blood samples were collected in heparinized tubes during predetermined time intervals: 0 s (start of infusion), 15 s, 30 s, 45 s, 1 min, 2 min, 3 min, 5 min, 7.5 min, 10 min, 15 min, 25 min, 35 min and 45 min. Care was taken to clear the dead space of the arterial catheter prior to the collection of each sample. The samples were immediately centrifuged in a high speed Beckman centrifuge and kept on ice for analyses. After the collection of the last sample, the animal was sacrificed by an i.v. infusion of 50mg sodium thiopental (10 mg/ml) in 5ml saline followed by a saturated solution of KCl for cardiac arrest. Plasma glucose levels, blood pressure, hematocrit and blood gases ranged within normal values in all monkeys and remained constant throughout all [^{14}C]-DG experiments.

Analysis of arterial plasma 2DG and glucose concentrations

The concentration of deoxyglucose was calculated by its ^{14}C content in the plasma. Twenty μl of each plasma sample and 3 ml of scintillation liquid (Insta-Gel, Packard co., Illinois, USA) were placed in a counting vial and assayed in a liquid scintillation counter (Beckmann Coulerton Inc., Foullerton, CA, USA). The efficiency (E) of the counting measurement was estimated by internal standardisation (calibrated [^{14}C]-toluene), and the obtained counts per minute (cpm) were transformed into disintegrations per minute (dpm) according to the equation dpm=cpm/E. The plasma glucose concentration was assayed in a dry glucose analyser (Spotchem, Menarini, Italy) to establish the required steady state for plasma glucose levels.

Tissue processing

Immediately after the end of the experiment, the cerebral hemispheres, the cerebellum and the spinal cord were removed, photographed, frozen by immersion in isopentane at -50°C, covered in embedding medium (M1, Lipshaw Manufacturing, Co) to prevent dryness and stored at -80°C until sectioned. About 1300 serial horizontal sections of 20 μm thickness were cut in the horizontal plane for each hemisphere of each monkey, containing the visual areas of interest, using a cryostat at -20°C. The sections were collected on glass coverslips and dried on a hot plate at 60°C. Subsequently, the coverslips were glued on a cardboard, and were exposed to X-ray film (EMC1, Kodak) for a period of 3-14 days together with a set of precalibrated ^{14}C standards (Amersham plc, Little Chalfont, Buckinghamshire, UK). The autoradiographic films were developed in a Kodak X-OMAT 1000 automatic processor. One section every 500 μm was stained with thionine for identification of cytoarchitectonic borders.

Analysis of autoradiographs

Quantitative densitometric analysis of autoradiographs was performed with a computerised image processing system (MCID, Imaging Research, Ontario, Canada), which allowed integration of the local cerebral glucose utilisation (LCGU) values (in μmol/100g/min) within each area of interest, based on the original operational equation of the method (Sokoloff et al. 1977) and the appropriate kinetic constants for the monkey (Kennedy et al. 1978).

Two-dimensional reconstructions

Two-dimensional reconstructions (2D-maps) of the spatio-intensive pattern of metabolic activity (LCGU values in μmol/100 g/min), within the rostrocaudal and the dorsoventral extent of the occipital opercular striate visual cortex between the Cas and the Ls, and of the extrastriate visual cortex within the Ls and the IOs, were generated for each hemisphere from 20 μm thick horizontal sections (dorsoventral sampling resolution of 20 μm), as previously described (Dalezios et al. 1996; Savaki et al. 1997). The full extent of the visual areas of interest (V1, V2, V3, V3A, and V4) was analysed in about 1300 serial horizontal sections.

For each horizontal section, a data array was obtained by sampling the LCGU values along a rostrocaudal line parallel to the surface of the cortex, including all cortical layers. According to this procedure, the distribution of activity in the rostrocaudal extent in each section was determined by measuring LCGU values pixel by pixel, with 50 μm/pixel anteroposterior sampling spatial resolution in the visual cortex. All data arrays were aligned at a specific anatomical point, the V1/V2 border, near the posterior crown of Ls in dorsal sections or near the posterior crown of IOs in more ventral sections. Data arrays of 5 adjacent horizontal sections (in the dorsoventral dimension of the brain) were averaged and plotted to produce one line in the 2D maps. Accordingly, each 2D reconstructed map is made of 263 lines (1315 sections divided by 5 sections per line). Thus, the dorsoventral sampling resolution of our study equals 20 μm, whereas the dorsoventral plotting resolution of our 2D-maps equals 100 μm.

Normalisation of the measured LCGU values was based on the averaged unaffected gray matter value pooled across all monkeys (Bakola et al. 2007). Accordingly, LCGU values were multiplied with a factor that was separately determined for each hemisphere. This factor was equal to the

ratio of the mean LCGU value found in the unaffected occipito-temporal cortex of the hemisphere in question over the mean LCGU value obtained from the same area after pooling all hemispheres from all monkeys. Very similar normalisation factors were found when LCGU values from other unaffected cortical areas (such as the hind limb and body representations of the primary motor and somatosensory cortices in the central sulcus) were used instead (Raos et al. 2007). Because the ipsilateral to contralateral LCGU values of all the visual cortical areas of interest did not differ for more than 7%, which is the maximum inter-hemispheric difference in normal monkeys (Kennedy et al. 1978), we averaged all hemispheres of all monkeys in each group for the final statistical comparisons. Side to side percent differences within each monkey for the Gl, Cm and Gd groups were calculated as $\%Dif = [(Contra - Ipsi)/Ipsi] \times 100$, where Contra represents the LCGU average value in each cortical area of interest of the hemisphere contralateral to the moving forelimb, and Ipsi represents the respective ipsilateral LCGU value (or as $\%Dif = [(Left - Right)/Right] \times 100$ for the O and Cm monkeys, which observed the same reaching-to-grasp and reaching movements from the experimenter, whose arm was entering the monkey's visual field from its right side). Percent LCGU differences between experimental and control subjects were calculated as follows: $(Experimental - Control)/Control \times 100$. The statistical significance of differences in LCGU values for Contra to Ipsi (Table 4.1) and experimental to control comparisons (Table 4.2, bold values) was determined by the Student's unpaired t-test (Raos et al. 2007; Evangeliou et al. 2009; Savaki et al. 2010). Only differences exceeding 10% were considered for statistical analysis given that homologous areas of the two hemispheres of a normal resting monkey can differ by up to 7% (Savaki et al. 1993).

Geometrical normalisation and activity plots

To allow for direct comparison of the cortical regions of activation, due to the inter- and intra-hemispheric macroscopic-anatomical variability, the individual functional (^{14}C-DG/LCGU) maps were further processed to match a reference map. The general procedure of the geometrical normalisation of the LCGU maps, based on surface landmarks, was previously described (Evangeliou et al. 2009; Savaki et al. 2010). In specific, in each horizontal section, we measured the distances between the medialmost point of the posterior crown of the Cas (point 1, Fig.3.4b-d) and the point of alignment, i.e. the border between areas V1 and V2 close to the posterior crown of the Ls in the dorsal sections (point 2, Fig.3.4b,c) or the posterior crown of the IOs in the ventralmost sections (point 2, Fig.3.4d). Also, for the dorsal sections in which the Ls appears, we measured the distances between V1/V2 border (point 2) and its fundus (point 3, Fig.3.4b,c), its fundus and the medialmost point of the posterior bank of the parieto-occipital sulcus (point 4, Fig.3.4b) for the dorsalmost sections, and its fundus and its anterior crown (point 5, Fig.3.4c) in the subsequent ventral sections. In the latter sections, we also measured the distance between the anterior crown of the Ls (point 5) and the posterior crown of the superior temporal sulcus (point 6, Fig.3.4c). Finally, for the ventralmost sections where the IOs is apparent, we measured the distances between its posterior crown (point 2, Fig.3.4d) and its fundus (point 7, Fig.3.4d), and also between its fundus and its anterior crown (point 8, Fig.3.4d).

The average of each one of these measures was separately estimated from all 24 hemispheres (of the 12 monkeys used in our study) to produce a reference map of surface landmarks (Fig.3.4e). Subsequently, each individual cortical map with its own landmarks was linearly transformed

(Moschovakis et al. 2004) with the help of custom-designed routines in the Matlab environment (Mathworks) to match the reference map. The geometrically normalised maps were combined (a) to obtain average LCGU maps out of control or experimental hemispheres and (b) to subtract control from experimental averaged maps. In specific, to generate average maps (glucograms), the LCGU value found in a certain pixel in one of the geometrically normalised maps was added to the value found in the pixel occupying the same position in one or more other similar maps, and the result was divided by the number of maps used. Similarly, to generate a difference map, the LCGU value found in a certain pixel of a geometrically normalised map of a control hemisphere was subtracted from the value found in the pixel occupying the same position in a similar map obtained from an experimental hemisphere. With this procedure, although the total surface of an area may change when it is geometrically normalised, the intensity and the spatial distribution of LCGU effects are preserved within it because these effects are proportionally shrunk or expanded within its borders. To create geometrically normalised anatomical maps matching our metabolic ones we used the combined MRI and histology monkey atlas of Saleem and Logothetis (Saleem and Logothetis 2007). The horizontal sections of this atlas, including (a) the labelled surface landmarks and (b) the anatomical borders between visual cortical areas, were processed the same way as our autoradiographic sections, in order to match the same reference map. Thus, the so generated 2D-reconstruction (Fig.3.4f) contains the anatomical borders of the visual areas of interest, within a reconstructed map of surface landmarks matching our metabolic reference map (Fig.3.4e). Consequently, superimposition of the two kinds of maps (metabolic and anatomical ones) allows for the macroscopic localization of the ^{14}C-DG activations in our study.

Histology

One section every 500 μm was stained with thionine for the identification of cytoarchitectonic borders. In the literature, identification of areal borders for the visual areas V1, V2, V3, V3A, and V4 is based on the examination of myelin-stained material and/or CO staining. However, the thickness of our sections (20 μm) and the use of fresh-frozen, non-perfused tissue did not allow for the employment of these techniques.

However, we were able to cytoarchitectonically identify certain visual areas in the thionine-stained sections, based on characteristics described in other visual studies (von Bonin 1942; Rockland and Pandya 1981; Zilles and Clarke 1997; Luppino et al. 2005). Specifically, the primary visual cortical area V1 was easily distinguished from area V2, due to its well developed and differentiated lamina granularis interna (layer IV). The third (III) layer of area V2 contained larger pyramidal cells as compared with those in area V3. The fourth (IV) layer was more distinct and dense in area V2 as compared with that in area V3. Finally, the sixth layer (VI) in area V2 was sharply set off from the white matter, in contrast to that of area V3 which blended smoothly with the white matter. Reassuring is the fact that the surface of area V2 outlined by the cytoarchitectonically identified borders (between V1/V2 and between V2/V3) overlaps with the area characterised by stripes in our reconstructed maps of metabolic activity. Nevertheless, the cytoarchitectonic borders between areas V3, V3A and V4 were not as clear, and thus based on surface brain landmarks according to the atlas of Saleem and Logothetis (Saleem and Logothetis 2007).

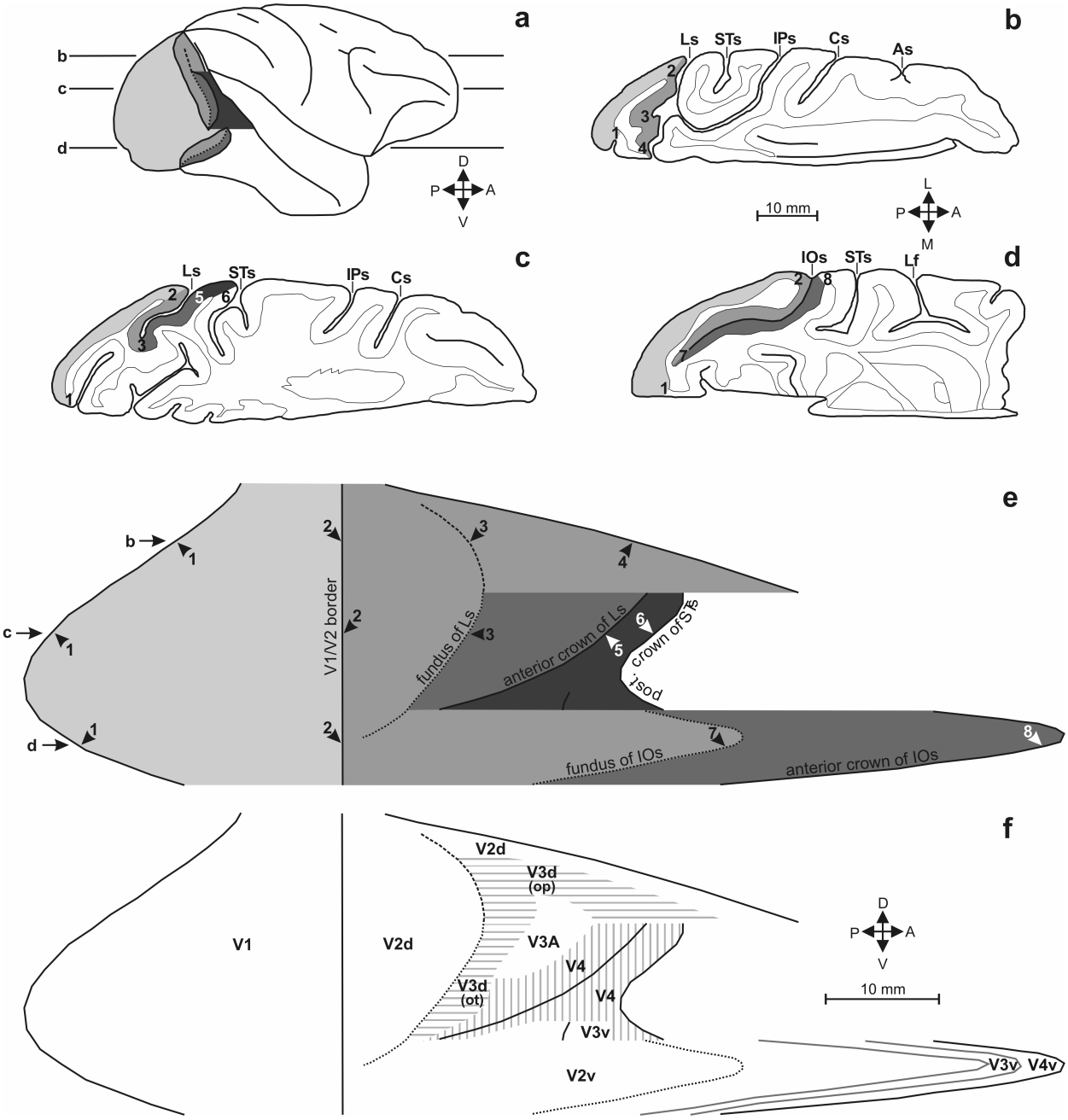

Figure 3.4: Two-dimensional reconstruction of metabolic and anatomical maps of the occipital cortex. ***a***, Lateral view of a monkey brain with the Ls and the IOs unfolded. Shaded areas indicate the reconstructed cortex in panel e. Horizontal lines b-d correspond to the three different dorsoventral levels of brain sectioning which are represented in the following 3 panels (b-d). ***b-d***, Schematic representations of horizontal sections at the dorsoventral levels indicated in panel a by corresponding letters (b-d). ***e***, Schematic illustration of the geometrically normalised reconstructed cortical field, i.e. the opercular primary visual cortex between calcarine and lunate sulci, and the extrastriate visual cortices within the Ls and the IOs. Black lines correspond to surface landmarks as labelled. Arrows b-d indicate the dorsoventral levels of the sections in the corresponding panels. Numbered lines 1-8 correspond to numbered tick-marks in panels b-d. ***f***, Schematic illustration of the same cortical field as that of panel e, reconstructed from corresponding horizontal sections of the combined MRI and histology atlas of the rhesus monkey (Saleem and Logothetis 2007), which contains the anatomical borders of the visual areas of interest in addition to the surface landmarks. A, Anterior; As, arcuate sulcus; Cs, central sulcus; D, dorsal; IOs, inferior occipital sulcus; IPs, intraparietal sulcus; Lf, lateral fissure; Ls, lunate sulcus; op and ot, occipito-parietal and occipito-temporal segments of area V3d, respectively; P, posterior; pc, posterior crown; STs, superior temporal sulcus; V, ventral.

CHAPTER 4

Results

In the present study we used the ^{14}C-DG quantitative method to map the distribution of metabolic activity of the occipital opercular primary visual cortex between the Cas and the Ls, and of the extrastriate visual cortex within the Ls and the IOs, in macaque monkeys during three behavioural tasks: (a) grasping execution in the light, (b) a grasping execution in the dark and (c) observation of the same grasping movements executed by the experimenter. In order to reveal the cortical areas involved in these tasks, three control monkeys were used, as it was previously described. The report of activated areas will follow our commentary on the oculomotor behaviour and behavioural performance of the monkeys.

Fig.4.1 illustrates in 3D-histograms the dwell time of the line of sight as a function of eye position averaged over the monkeys belonging to each one of the groups. Because approximately 85% of the radiolabelled glucose is taken up by cells during the critical first ten minutes of the ^{14}C-DG experiment (Sokoloff et al. 1977), this figure includes data from only this period. It presents the distribution of the end points of eye movements made by the two monkeys reaching-to-grasp in light (Fig.4.1 Gl), the three monkeys observing reaching-to-grasp movements of the experimenter (Fig.4.1 O), the two motion-control monkeys (Fig.4.1 Cm), the two monkeys reaching-to-grasp in the dark (Fig.4.1 Gd), the two dark-control monkeys (Fig.4.1 Cd), and the fixation-control monkey (Fig.4.1 Cf).

As required, all the monkeys performing their tasks in the light spent most of the critical time fixating within the window of the behavioural apparatus (Fig.4.1 Gl, O, Cm, Cf). This time ranged between 6 and 7 min. For the rest of the time, the animals did not display any systematic oculomotor behaviour that could account for false-positive effects in oculomotor related areas. In other words the line of sight of all the experimental monkeys was at random positions throughout the entire oculomotor space. The same is true of the Gd monkeys, except that in this case the distribution is shallow and more spread out because they were fixating in the absence of a visible target (Fig.4.1 Gd). As expected, the Cd monkeys display a roughly even distribution in much of the oculomotor space (Fig.4.1 Cd). Finally, the control fixation monkey (Cf) fixated the visual target for 75% of the time during the critical 10 first minutes of the 2DG experiment (Fig.4.1 Cf).

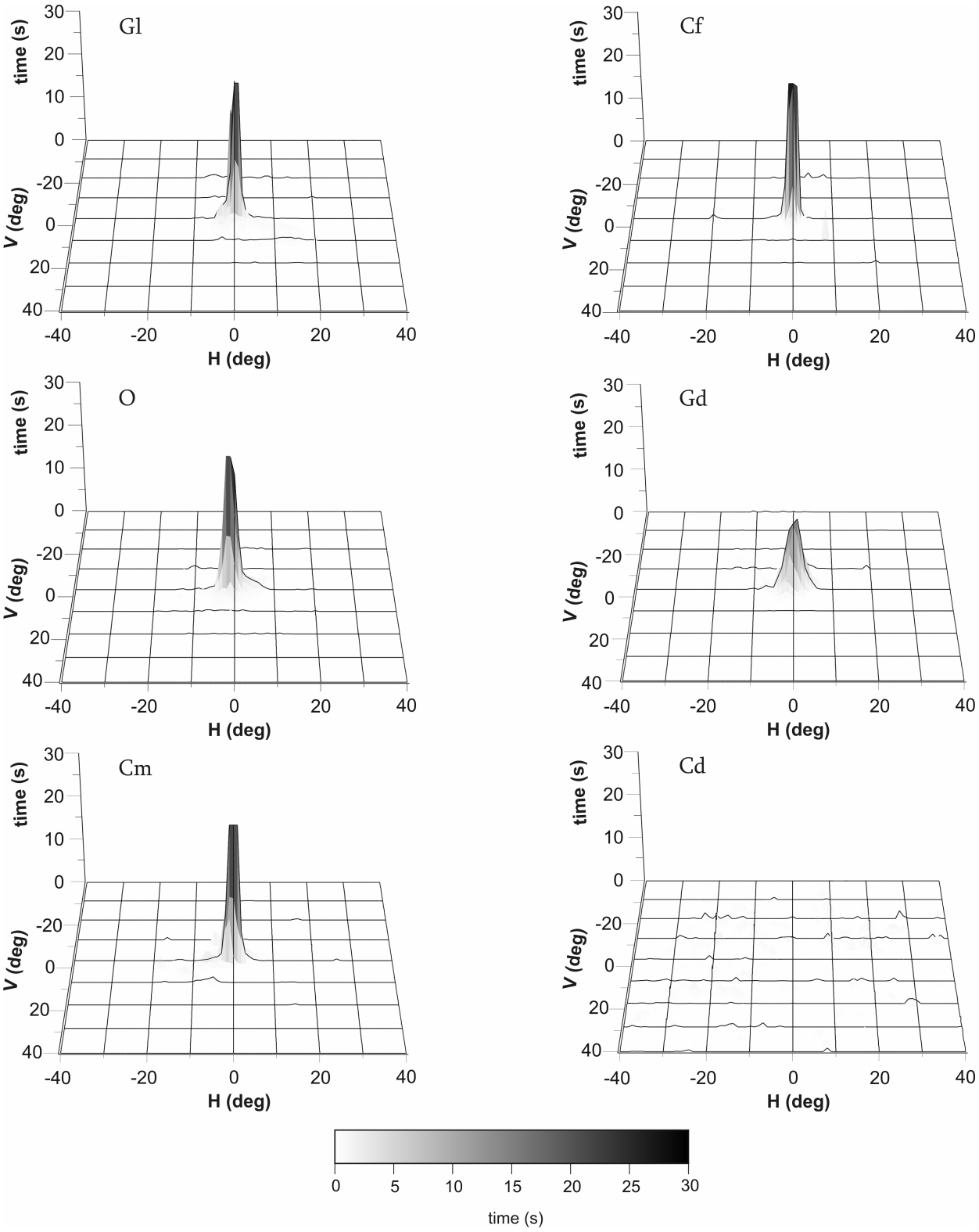

Figure 4.1: Three-dimensional histograms of the dwell time of the line of sight as a function of eye position. ***Gl***, averaged oculomotor behaviour from the two monkeys reaching-to-grasp in light. ***O***, averaged oculomotor behaviour from the three grasping-observation monkeys. ***Cm***, averaged behaviour from the two motion-control monkeys. ***Cf***, oculomotor behaviour from the fixation-control monkey. ***Gd***, averaged oculomotor behaviour from the two monkeys reaching-to-grasp in the dark. ***Cd***, averaged behaviour from the two dark-control monkeys. Horizontal axis (H; x) and vertical axis (V; y) in degrees, z-axis in seconds. Grayscale bar indicates time in seconds.

Cortical area	**n**	**CmRight** (LCGU±SD)	**CmLeft** (LCGU±SD)	**CmL/CmR** (%)
V1-OO	263	60 ± 2	61 ± 2	2
V1-OO (central)	172	59 ± 1	60 ± 3	2
V1-OO (peripheral)	263	60 ± 2	61 ± 2	2
V2d-Ls (central)	155	51 ± 2	52 ± 3	2
V2d-Ls (peripheral)	196	53 ± 3	54 ± 2	2
V2v-IOs	67	51 ± 2	52 ± 1	2
V3d-ot (central)	81	56 ± 5	54 ± 2	-4
V3d-op (peripheral)	62	54 ± 2	56 ± 1	4
V3v-IOs	67	55 ± 3	53 ± 1	-4
V3A	89	52 ± 3	53 ± 3	2
V4-Ls	81	52 ± 2	52 ± 2	0
V4-IOs	67	54 ± 3	52 ± 3	4

Table 4.1: **Average LCGU values from the two motion control (Cm) monkeys in the left and right hemispheres separately**. ***n***, number of sets of 5 adjacent horizontal sections used to obtain the mean LCGU values (in μmol/100 g/min) for each region. ***CmRight***, average LCGU values from the 2 right hemispheres of the 2 motion control monkeys. ***CmLeft***, average LCGU values from the 2 left hemispheres of the 2 motion control monkeys. ***SD***, standard deviation of the mean. ***CmL/CmR***, percent LCGU difference between CmLeft and CmRight.

In order to control for possible rate-related effects, the mean rate of movements was set to be similar for all behavioural tasks used. During the critical ten first minutes of the ^{14}C-DG experiment, the Gl monkeys executed an average of 10 grasping movements per min and fixated within the window of the behavioural apparatus (8 x 8 deg) for an average of 7 min. The O and the Cm monkeys observed an average of 12 grasping or reaching movements per min respectively and fixated for 7 min too. The Gd monkeys executed an average of 11 grasping movements per min and kept their gaze straight ahead within the window of the behavioural apparatus (10 x 10 deg) for an average of 7 min during the critical ten first minutes of the 14C-DG experiment.

As explained in the methods section, the lack of inter-hemispheric differences allowed us to average both hemispheres of each monkey to obtain the 2D map of the metabolic activation. At this point, we would like to comment on the side-to-side differences regarding the Cm monkey. Since the arm of the experimenter was entering the monkey's visual field from its right side, one could expect that the visual areas of the left hemisphere would be more activated. Yet, we found no statistically significant interhemispheric differences in any of the early visual areas of the Cm monkeys, as demonstrated in Table 4.1. This table displays the LCGU values separately for the right and left hemispheres of the two Cm monkeys, and the left to right difference. Left to right LCGU values were compared for statistical significance by the Student's unpaired t-test. Apparently, the interhemispheric difference did not exceed 4% for any of the visual areas studied, which is far below the percentage (7%) that LCGU values of homologous areas may differ in the two hemispheres of a normal resting monkey (Savaki et al. 1993).

To reveal the visual areas that are specifically activated for the grasping-in-the-light task, we compared the autoradiographs of the Gl and Cm groups. Accordingly, in order to obtain the 2D map of the metabolic activation pattern induced by the execution of grasping movements in the light, the

reconstructed maps of the individual hemispheres (Fig.4.2) were averaged across all members of the Gl group. These glucograms were used for measurement of the LCGU values in the striate area V1 and extrastriate cortical areas V2-V4 based on the borders of Fig.3.4f, and subsequently for their statistical comparisons and the estimation of the percent differences from the corresponding values of the Cm monkey (Table 4.2). Thus, the quantitative 2D map of the spatio-intensive distribution of metabolic activity (in μmol/100g/min of glucose consumption) within the reconstructed occipital operculum, the Ls and the IOs of the monkeys generating reaching-to-grasp movements in the light (Gl) is illustrated in Fig.4.3a. The Gl-map is the average LCGU map (glucogram) from the 4 hemispheres of 2 monkeys. The corresponding two-dimensional reconstructions of the spatio-intensive pattern of metabolic activity of the individual hemispheres of the animals that executed grasping-in-the-light (Gl) are illustrated in Fig.4.2. Similarly, the Cm-map is the average from 4 hemispheres of 2 monkeys (Fig.4.3b). The surface landmarks (black lines) and the cytoarchitectonic borders (white lines) are also included (Fig.4.3a, b)(see methods section). To reveal the regions that are significantly activated for grasping in the light, i.e. to illustrate the percent LCGU differences between the experimental Gl monkeys and the Cm, we generated images using the formula $(Gl - Cm)/Cm \times 100$. The Cm monkeys were used to take into account the effects of (a) the biological motion of the purposeless (non-goal-directed) reaching arm, and (b) the visual stimulation by the 3D object. When the averaged map of the Gl monkeys is compared with the averaged map of the Cm monkeys (Fig.4.3c), increased metabolic activity is evident in extrastriate areas V3d, V3A and V4 (Table 4.2, Gl/Cm, bold values), with the two segments of area V3d, the occipito-parietal reflecting peripheral vision and the occipito-temporal reflecting central vision (Baizer et al. 1991) being equally activated.

To reveal the regions which are significantly affected during observation of grasping movements, we statistically compared the LCGU values in the striate V1 and extrastriate visual areas V2-V4 of the O-map with the corresponding values of the average Cm-map. The two-dimensional reconstructions (2D-maps) of the spatio-intensive pattern of metabolic activity of the six individual hemispheres of the three O monkeys are illustrated in Fig.4.4, whereas the geometrically normalized 2D-map of the spatial distribution of metabolic activity for the *observation* task is the average glucogram of these hemispheres across all members of the group (Fig.4.5a).

To reveal the regions which are specifically affected during observation of grasping movements, we statistically compared the 2D metabolic O-map (Fig.4.5a) with the corresponding Cm-map (Fig.4.5b), using the formula $(O - Cm)/Cm \times 100$. The generated image (Fig.4.5c) illustrates that during the observation of grasping profound activations are displayed in areas V3d, and V3A. V1 in the representation of the central vision is also significantly activated, however this effect is of lower magnitude than that observed in V3. In contrast to the activation observed in the Gl monkeys, the dorsal part of area V4 was not activated in monkeys performing grasping observation. Additionally, the region of the representation of central vision in V3d exhibited enhanced metabolic activity as compared with the region of the representation of peripheral vision. The corresponding quantitative data (percent differences) are displayed in Table 4.2 (O/Cm, bold values). To better illustrate the similarities and the differences in the activation pattern of the Gl and O monkeys, their maps of net activations and the corresponding subtraction Gl-O are displayed in Figure 4.6. In comparison with the motion-control monkeys, V1 and V2 cortical regions of both the central and peripheral visual representations in the occipital operculum, as well as V3v and V4 regions within the inferior

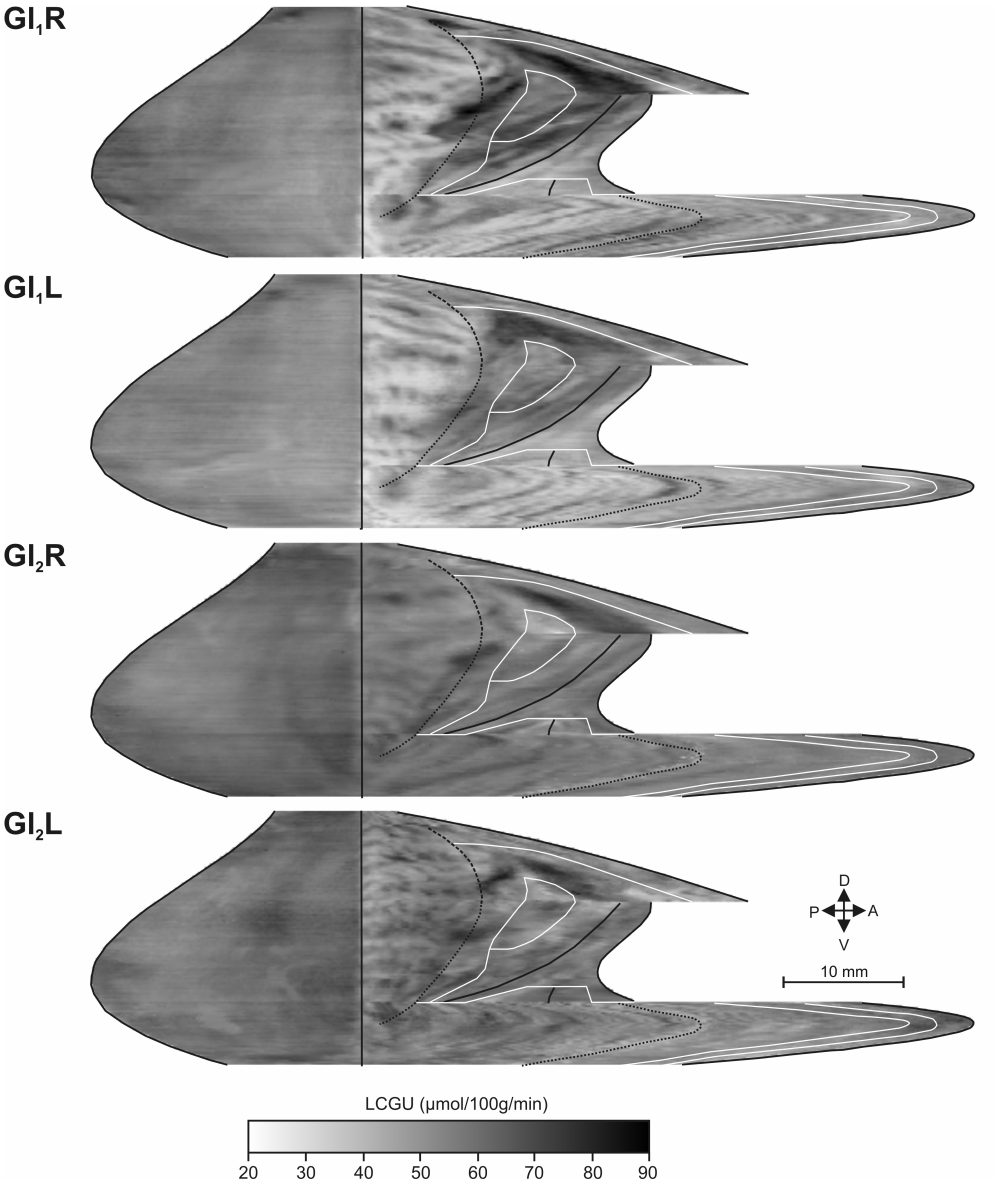

Figure 4.2: 2D spatial reconstruction of the LCGU values (μmol/100g/min) of the metabolic activity in the occipital cortex of the four hemispheres of the two monkeys reaching-to-grasp in the light (Gl). $\boldsymbol{Gl_1R}$ and $\boldsymbol{Gl_1L}$, quantitative 2D-maps of metabolic activity of the right and left hemisphere of the first Gl monkey respectively. $\boldsymbol{Gl_2R}$ and $\boldsymbol{Gl_2L}$, quantitative 2D-maps of metabolic activity of the right and left hemisphere of the second Gl monkey respectively.

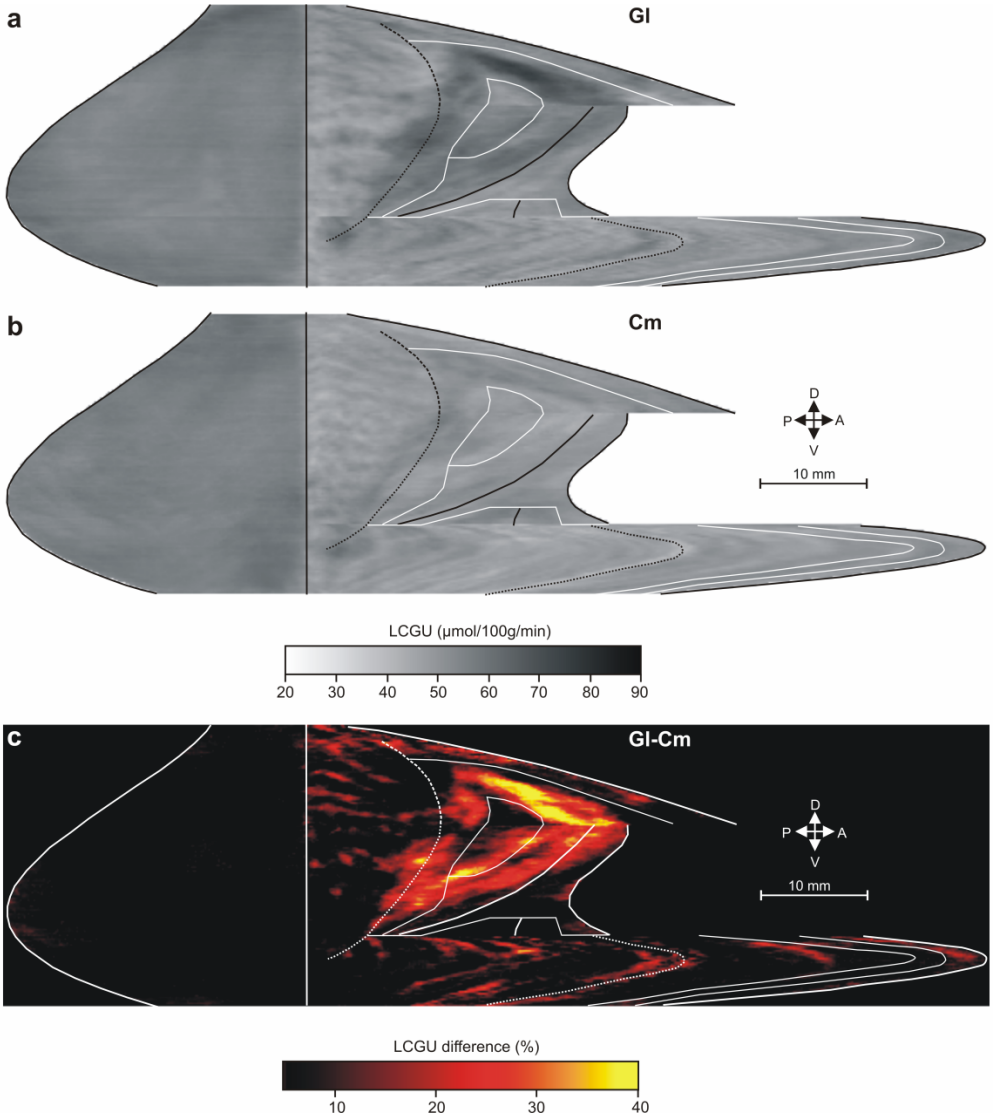

Figure 4.3: Quantitative 2D-maps of metabolic activity in the occipital cortex of the grasping light monkeys and percent LCGU difference from the motion control. ***a***, averaged map from the four hemispheres of the two monkeys reaching-to-grasp in the light (Gl). ***b***, averaged map from the four hemispheres of the two motion-control monkeys (Cm). ***c***, map of *net activations* induced by reaching-to-grasp in the light, averaged from the four hemispheres of the two Gl monkeys, as compared with the four hemispheres of the two Cm monkeys. In panels ***a*** and ***b***, black lines correspond to surface landmarks and white lines to anatomical borders of cortical areas, as illustrated and labeled in Fig.3.4. In panel ***c***, both the surface landmarks and the anatomical borders are represented in white lines. Grayscale bar indicates LCGU values in micromoles per 100 g per minute. Colour bar indicates percentage LCGU differences from the Cm.

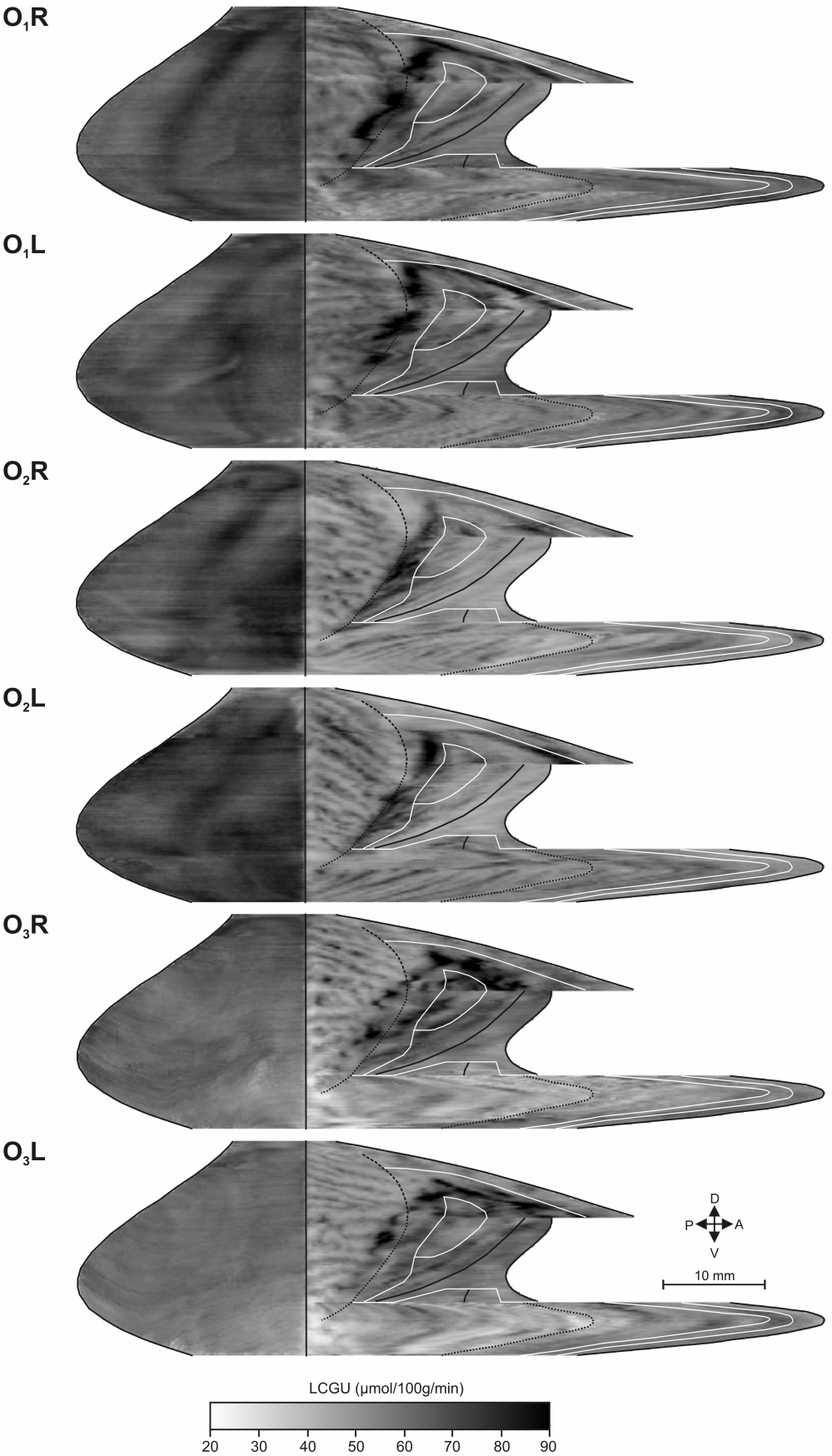

Figure 4.4: 2D spatial reconstruction of the metabolic activity in the occipital cortex of the six hemispheres of the three observation monkeys (O). $\boldsymbol{O_1R}$ and $\boldsymbol{O_1L}$, quantitative 2D-maps of metabolic activity in the right and left hemisphere of the first O monkey, respectively. $\boldsymbol{O_2R}$ and $\boldsymbol{O_2L}$, quantitative 2D-maps of metabolic activity in the right and left hemisphere of the second O monkey, respectively. $\boldsymbol{O_3R}$ and $\boldsymbol{O_3L}$, quantitative 2D-maps of metabolic activity in the right and left hemisphere of the third O monkey, respectively. Black lines correspond to surface landmarks and white lines to anatomical borders of cortical areas, as illustrated and labelled in Fig.3.4. Grayscale bar indicates LCGU values in micromoles per 100 g per minute.

occipital sulcus were not affected either by action-execution in the light or by action-observation. The lack of any effect within areas V1 and V2 indicates that the motion control group provided us with the means to correct for object-vision and arm-motion. Of interest is that in both groups, area V3d displays the highest activations when compared with the other extrastriate areas and the primary visual area. It should be reminded that when we subtract the Cm from the Gl and O groups, we actually subtract all visual information related to (a) the purposeless (non-goal directed) movement of the forelimb and (b) the visual stimulation by the presentation of the object. Thus the remaining *"net-activation"* specifically represents the visual information which is required by the motor system to guide the forelimb to reach accurately and grasp properly. Accordingly, areas V3d and V3A activated for both Gl and O groups after subtraction of the Cm should encode visual information useful for motor control. The absence of any activation in the ventral regions of V3 and V4 is explained by the fact that our behavioural tasks involved activities in the lower rather than in the upper visual field of the monkeys.

To reveal the effects induced by reaching-to-grasp in the dark, we averaged the individual geometrically normalized glucograms of the four hemispheres of the Gd group (Fig.4.7). The averaged Gd map (Fig.4.8a) was then compared with the metabolic map obtained from averaging the four hemispheres of the two control-in-the-dark monkeys (Cd-map) (Fig.4.8b). The Cd monkeys were presented with auditory stimuli similar to the acoustic cues presented to the Gd monkeys. Reward was delivered at random intervals to prevent association of the auditory stimuli with the reward expectancy. It is important to remind that the lack of inter-hemispheric differences allowed us to average both hemispheres of each monkey. To pictorially represent the LCGU differences between the Gd and the Cd groups of monkeys, we generated an image using the formula $(Gd - Cd)/Cd \times 100$ (Fig.4.8c). This image illustrates the increased metabolic activity (*net-activation*) in the areas which appear significantly affected in Table 4.2 (Gd/Cd, bold values). These activations include areas V1, V2, V3A, and V3v. Moreover, it is of great interest that the occipito-parietal segment of area V3d, representing peripheral vision, displayed a pronounced activation for action-generation in the dark in contrast to its occipito-temporal division reflecting central vision which remained inactive. At this point it should be mentioned that, although the activation of specific areas in our study reflects their explicit involvement in the generation and the observation of a reaching-to-grasp action, the overlapping activations for execution in the light or in the dark and for observation do not necessarily indicate involvement of the same cell populations in all conditions.

In order to subtract the effect due to unspecific arousal, and spot-fixation, we used as a reference the fixating control (Cf) monkey which was rewarded for maintaining its gaze fixed on a central illuminated spot, instead of the Cm. The 2D spatial distribution of the metabolic activity for the Cf monkey is illustrated 2DG in Fig.4.9a, and was generated by averaging the two geometrically normalized quantitative glucograms of the left and right hemispheres of that monkey. To pictorially represent the *net-effect of fixation*, we generated an image of LCGU differences between the Cf and the Cd monkeys, using the formula $(Cf - Cd)/Cd \times 100$ (Fig.4.9b). The early visual cortical regions which are illustrated in this figure to be involved in fixation (central vision) are in close agreement with those of a previous meticulous fMRI study (Brewer et al. 2002). Indeed, Fig.4.9b illustrates (a) increased metabolic activity within the foveal representation of the visual field (central 1.5deg, corresponding to the used target of fixation) which covers about 10 mm of cortex in the striate area

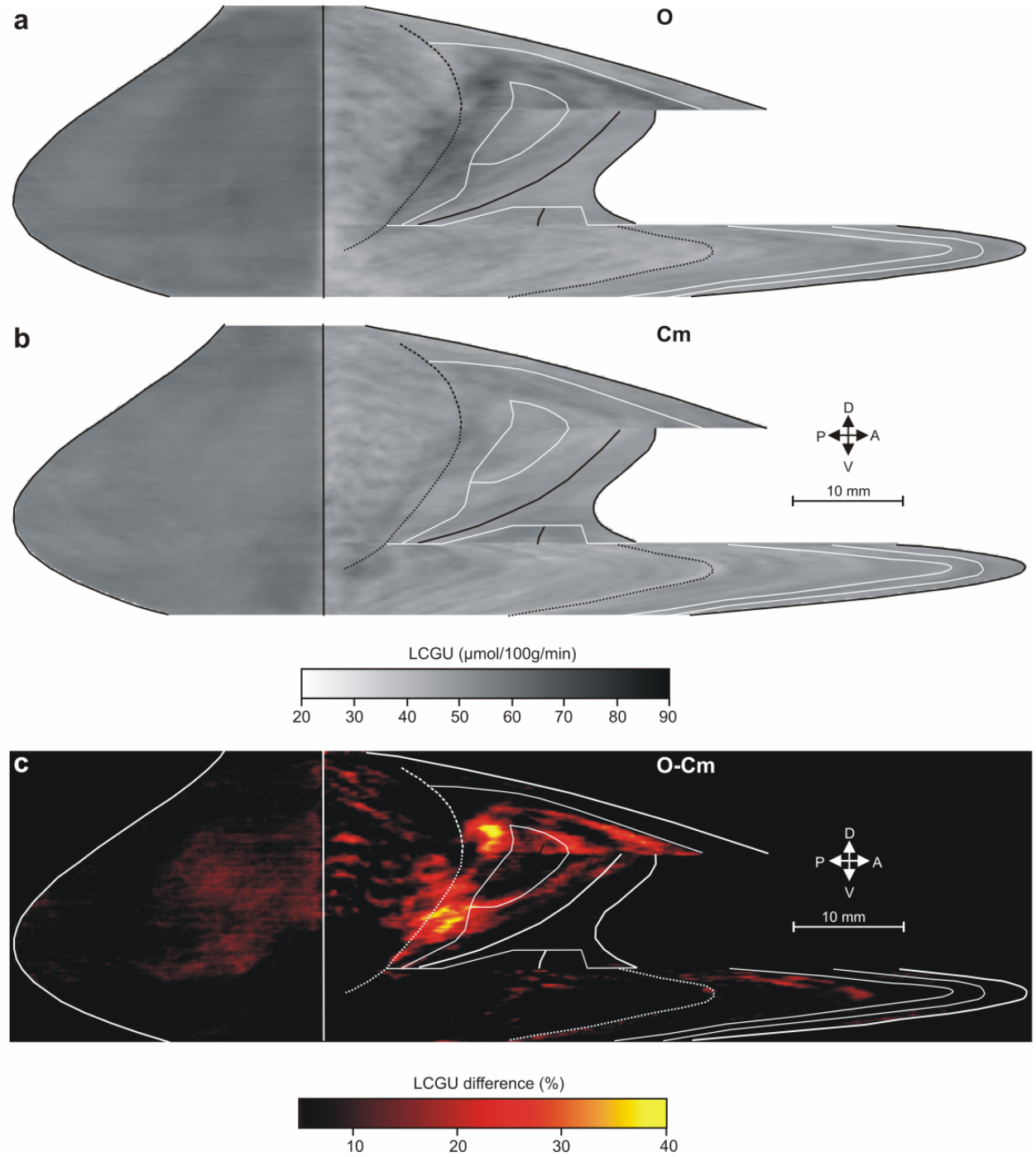

Figure 4.5: Quantitative 2D-maps of metabolic activity in the occipital cortex of the observation monkeys and percent LCGU difference from the motion control. ***a***, averaged map from the six hemispheres of the three monkeys observing another subject performing the same reaching-to-grasp movements (O). ***b***, averaged map from the four hemispheres of the two motion-control monkeys (Cm). ***c***, map of *net activations* induced by grasping observation, averaged from the six hemispheres of the three O monkeys as compared with the four hemispheres of the two Cm monkeys. In panels ***a*** and ***b***, black lines correspond to surface landmarks and white lines to anatomical borders of cortical areas, as illustrated and labelled in Fig.3.4. In panel ***c***, both the surface landmarks and the anatomical borders are represented in white lines. Grayscale bar indicates LCGU values in micromoles per 100 g per minute. Colour bar indicates percentage LCGU differences from the Cm.

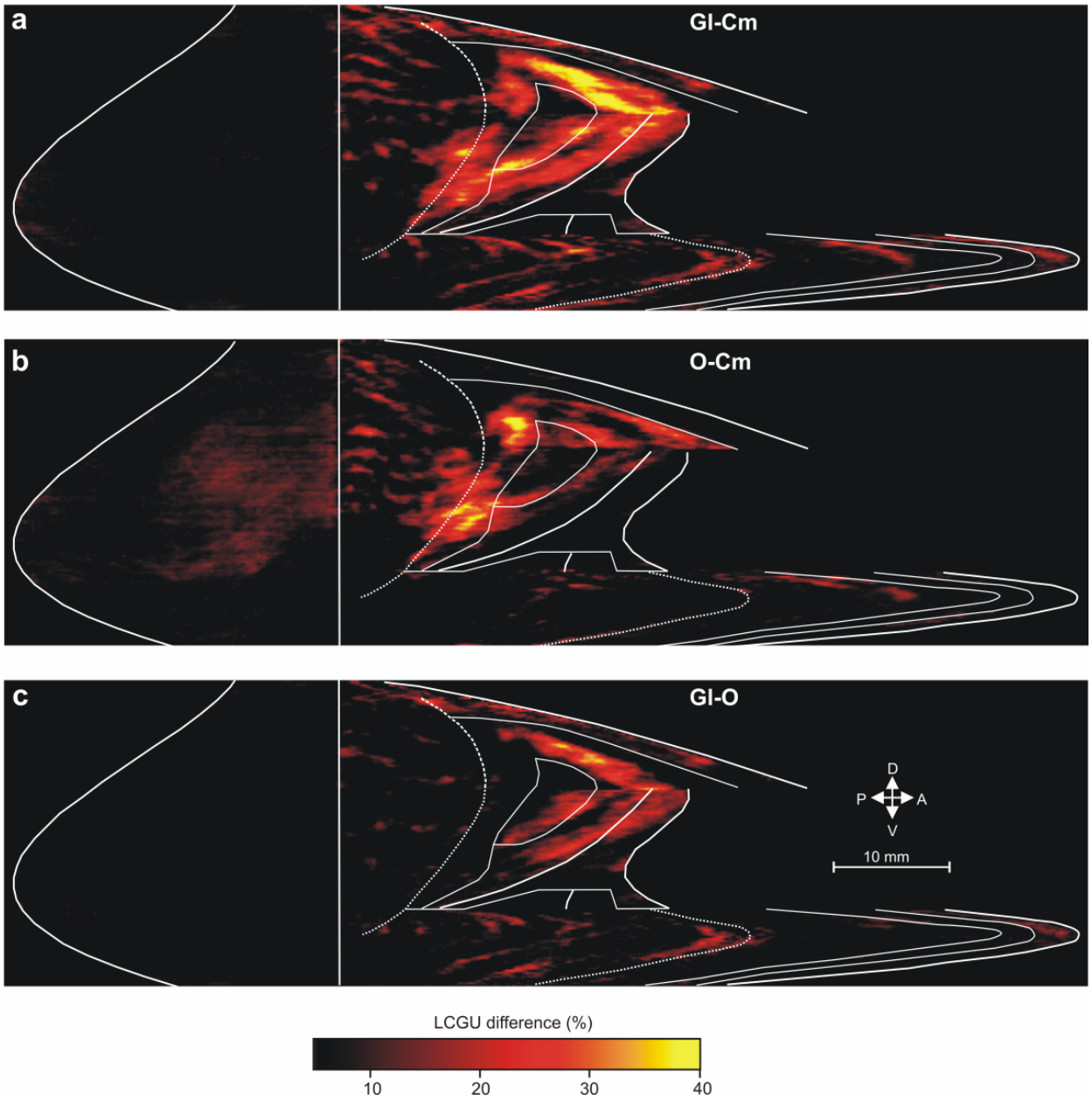

Figure 4.6: Differential activations induced by the Gl and O tasks. ***a***, map of *net activations* induced by reaching-to-grasp in the light, averaged from the four hemispheres of the two Gl monkeys as compared with the four hemispheres of the two Cm monkeys. ***b***, map of *net activations* induced by grasping-observation, averaged from the six hemispheres of the three O monkeys as compared with the four hemispheres of the two Cm monkeys. ***c***, subtraction of the average quantitative Gl map from that of the average O map illustrates the cortical regions differentially activated for the grasping-in-light monkeys. White lines correspond to surface landmarks and anatomical borders labeled in Fig.3.1. Colour bar indicates percentage LCGU differences from the Cm and O.

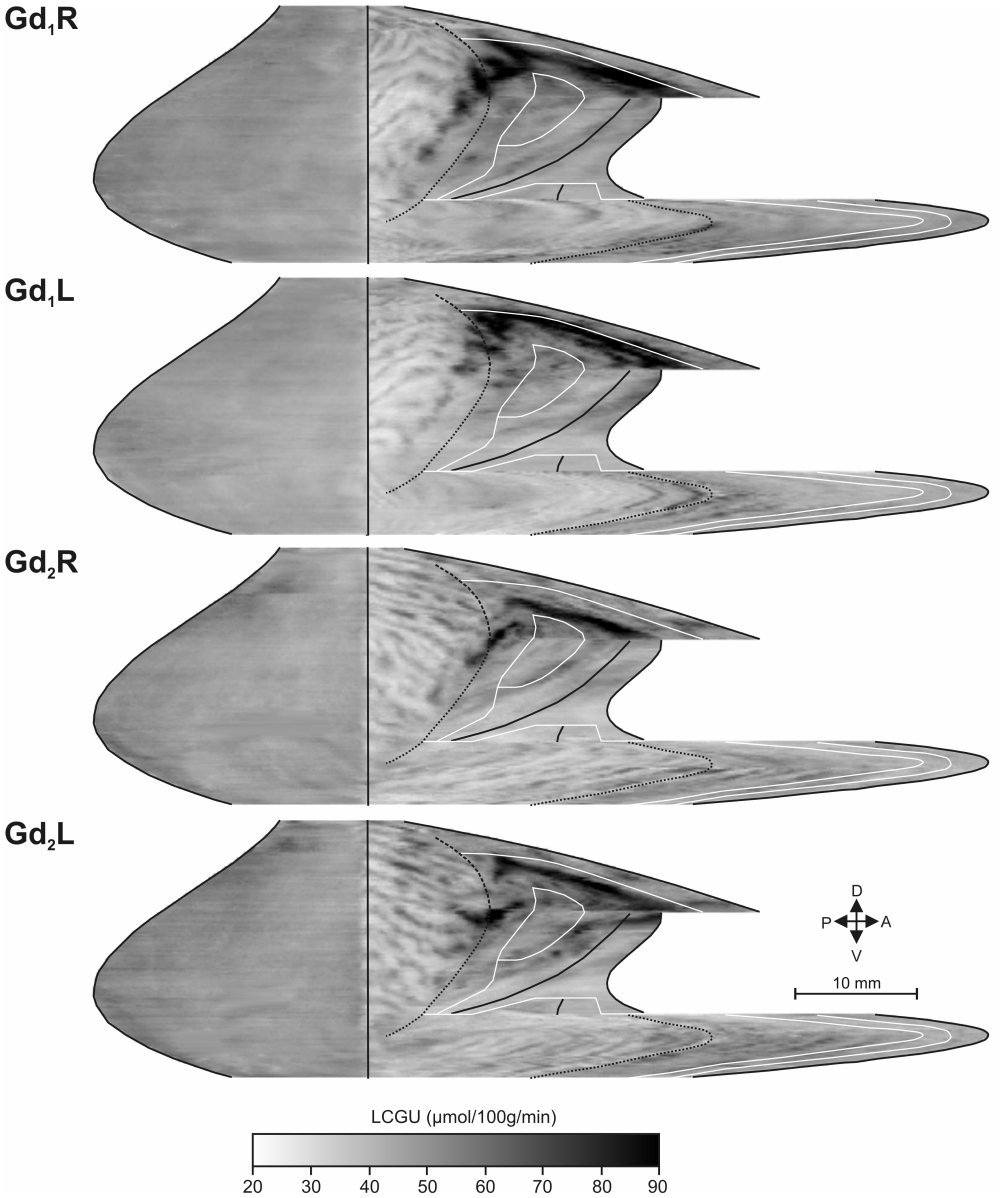

Figure 4.7: 2D spatial reconstruction of the LCGU values (μmol/100g/min) in the occipital cortex of the four hemispheres of the two grasping-in-the-dark monkeys (Gd). $\boldsymbol{Gd_1R}$ and $\boldsymbol{Gd_1L}$,quantitative 2D-maps of metabolic activity of the right and left hemisphere of the first Gd monkey respectively. $\boldsymbol{Gd_2R}$ and $\boldsymbol{Gd_2L}$, quantitative 2D-maps of metabolic activity of the right and left hemisphere of the second Gd monkey respectively.Black lines correspond to surface landmarks and white lines to anatomical borders of cortical areas, as illustrated and labeled in Fig.3.4. Grayscale bar indicates LCGU values in micromoles per 100 g per minute.

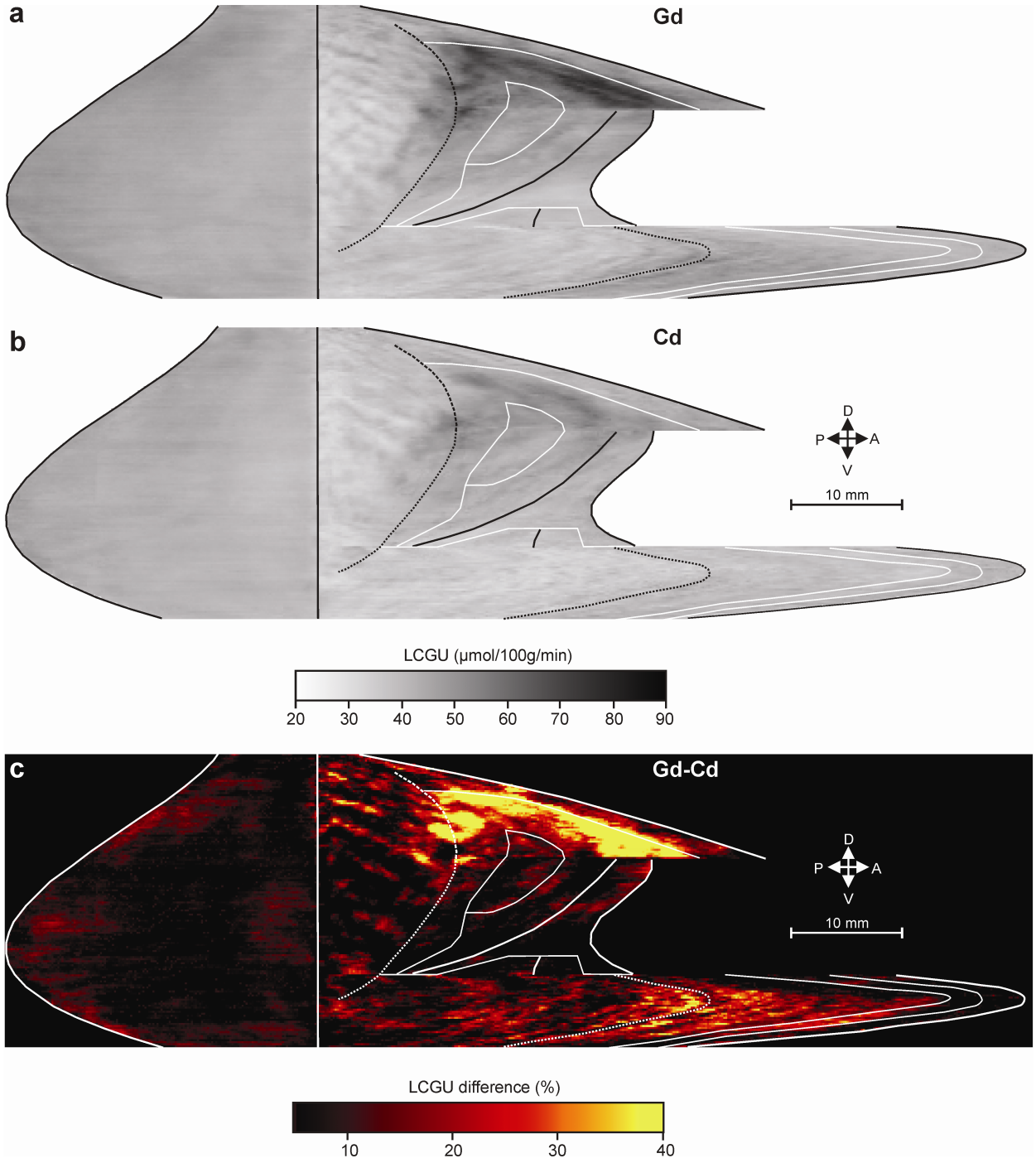

Figure 4.8: Quantitative maps of activity in the occipital cortex of blindfolded monkeys. ***a***, averaged map from the four hemispheres of the two monkeys reaching-to-grasp in the dark (Gd). ***b***, averaged map from the four hemispheres of the two control monkeys in the dark (Cd). Black lines correspond to surface landmarks and white lines to anatomical borders of cortical areas, as illustrated in Fig.3.4. Grayscale bar indicates LCGU values in micromoles per 100 g per minute. ***c***, map of *net activations* induced by reaching-to-grasp in the dark, averaged from the four hemispheres of the two Gd monkeys as compared with the four hemispheres of the two Cd monkeys. White lines correspond to surface landmarks and anatomical borders labeled in Fig.4.1. Colour bar indicates percent LCGU differences from the Cd.

V1 and about 7 mm in the extrastriate area V2, and (b) a continuous zone of activation occupying areas V2, V3 and V4 which corresponds to their central vision, which is adjacent to the V1 foveal activation. The percent LCGU differences between Gl and Cf and O and Cf were calculated by the formulas $(Gl - Cf)/Cf \times 100$ and $(O - Cf)/Cf \times 100$, respectively. Consequently, the activations observed in this case are different. When we used the Cf as control case, the striate area V1 of the occipital operculum as well as the extrastriate area V2 of the Ls and the IOs were found to be activated in both Gl and O groups as compared with the Cf, in addition to area V3 which was also activated as compared with the Cm (Table 4.1, Gl/Cf and O/Cf, bold values). Moreover, to illustrate the *net activations* induced by object-presentation and arm-motion, the percent LCGU differences between the motion control (Cm) and the fixation control (Cf) were calculated by the formula $(Cm - Cf)/Cf \times 100$ (Fig.4.9c).
The image of Fig.4.9b is nearly complementary to that of Fig.4.9c, verifying the zone of foveal vision in areas V1, V2, V3 and V4 of the occipital cortex (Brewer et al. 2002). Moreover, the fact that the Cm group displays activations in extrafoveal regions of areas V1, V2 and V3 (Fig.4.9c) explains the reason why more visual areas are activated when the Gl and the O groups are compared with the Cf (Table 4.2, Gl/Cf, O/Cf) than to the Cm (Table 4.2, Gl/Cm, O/Cm). In fact, when the Gl is compared with the Cf similar activations are found with those observed when the Gd is compared with the Cd.

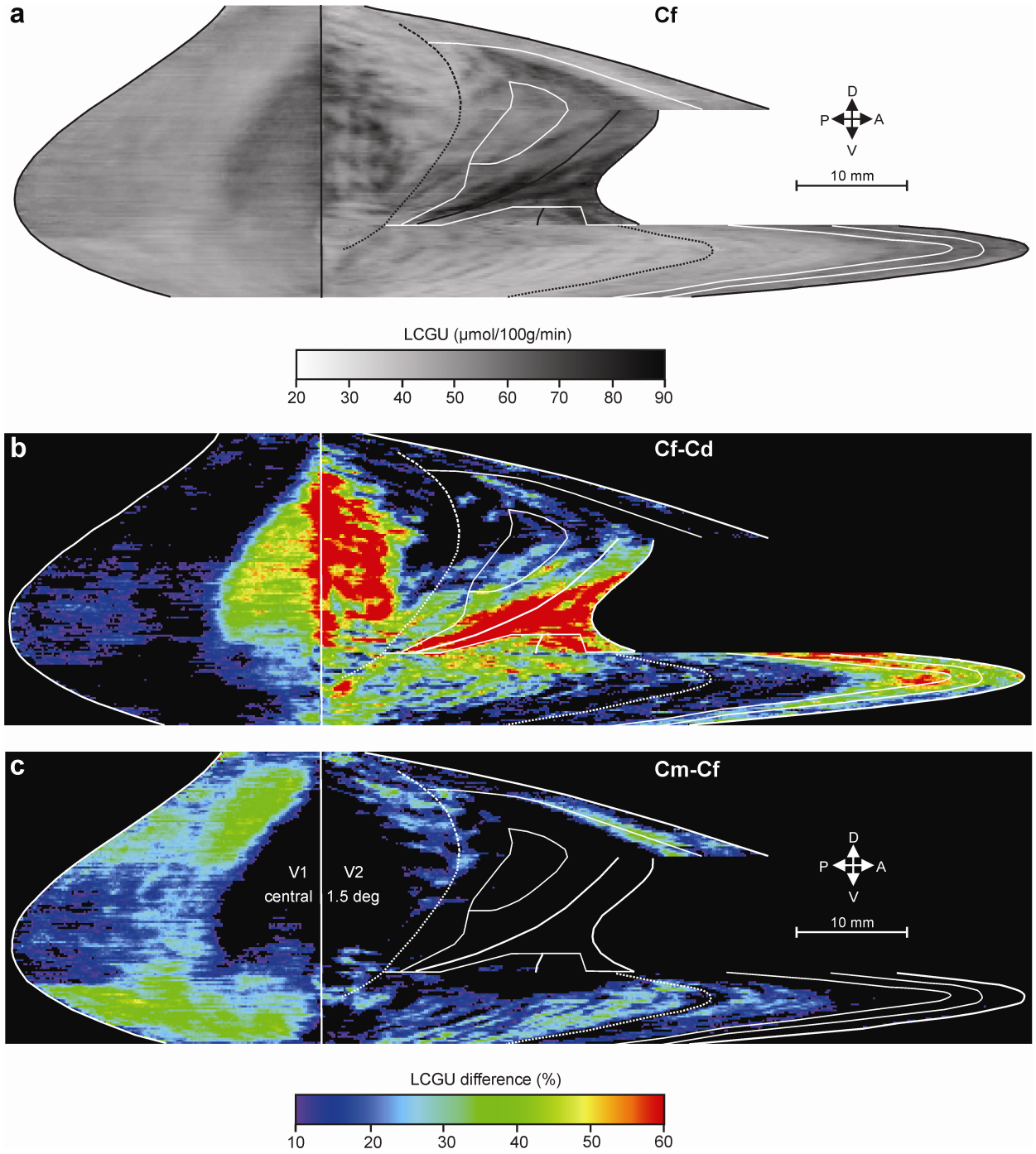

Figure 4.9: Effects of fixation and biological motion. ***a***, averaged map of metabolic activity from the two hemispheres of the fixation-control (Cf) monkey. ***b***, map of *net activation* induced by fixation, averaged from the two hemispheres of the Cf monkey as compared with the averaged four hemispheres of the two Cd monkeys. ***c***, map of *net activations* induced by object-presentation and arm-motion, averaged from the four hemispheres of the two Cm monkeys as compared with the Cf averaged map. Foveal representation (central 1.5 deg of the visual field) is marked within areas V1 and V2. In panel ***a***, black lines correspond to surface landmarks and white lines to anatomical borders of cortical areas, as illustrated and labeled in Fig.3.4. In panels ***b*** and ***c***, both the surface landmarks and the anatomical borders are represented in white lines. Grayscale bar indicates LCGU values in micromoles per 100 g per minute. Colour bar indicates percent LCGU differences.

Cortical area	**n**	**Cf** (LCGU±SD)	**Cm** (LCGU±SD)	**Gl** (LCGU±SD)	**Gl/Cm** (%)	**Gl/Cf** (%)	**O** (LCGU±SD)	**O/Cm** (%)	**O/Cf** (%)	**Cd** (LCGU±SD)	**Gd** (LCGU±SD)	**Gd/Cd** (%)
V1-OO	263	51±2	61±1	61±2	0	**20**	64±2	5	**25**	44±1	48±1	**9**
V1-OO (central)	172	59±4	60±2	60±1	0	2	65±2	**8**	**10**	42±1	44±1	5
V1-OO (peripheral)	263	50±2	61±1	61±2	0	**22**	64±2	5	**28**	45±2	49±1	**9**
V2d-Ls (central)	155	60±3	52±2	53±2	2	-12	53±2	2	-12	37±1	38±2	3
V2d-Ls (peripheral)	196	48±4	54±2	57±3	6	**19**	54±3	0	**13**	40±5	50±4	**25**
V2v-IOs	67	47±2	52±1	54±1	4	**15**	51±1	-2	**9**	39±1	43±2	**10**
V3d-ot (central)	81	57±4	55±3	65±2	**18**	**14**	65±2	**18**	**14**	48±3	51±6	6
V3d-op (peripheral)	62	54±3	55±1	65±4	**18**	**20**	61±4	**11**	**13**	52±3	68±3	**31**
V3v-IOs	67	58±4	54±2	56±1	4	-3	54±1	0	-7	42±2	46±3	**10**
V3A	89	56±3	53±2	61±4	**15**	**9**	59±4	**11**	5	49±3	55±7	**12**
V4-Ls	81	65±6	52±2	60±2	**15**	-8	54±1	4	-17	46±2	48±4	4
V4-IOs	67	57±4	53±2	56±3	6	0	54±2	2	-5	43±2	45±2	5

Table 4.2: Metabolic effects in occipital cortical areas of the monkey brain. Values represent the mean normalized glucose utilization(LCGU) in μmol/100g/min (± standard deviation). ***n***, number of sets of 5 adjacent horizontal sections used to obtain the mean LCGU values (in μmol/100g/min) for each region. ***Cf***, average LCGU values from the 2 hemispheres of the fixation-control monkey. ***Cm***, average LCGU values from the 4 hemispheres of the 2 motion-control monkeys. ***Gl***, average LCGU values from 4 hemispheres of 2 grasping-in-light monkeys. ***O***, average LCGU values from 6 hemispheres of 3 grasping-observation monkeys. ***Cd*** and ***Gd***, average LCGU values from 4 hemispheres of 2 control-in-dark and 2 grasping-in-dark monkeys, respectively. ***SD***, standard deviation of the mean. ***Gl/Cm***, ***O/Cm***, percent differences between Gl or O and Cm, respectively. ***Gl/Cf***, ***O/Cf***, percent differences between Gl or O and Cf, respectively. ***Gd/Cd***, percent differences between Gd and Cd. **Values in bold** indicate statistically significant differences by the Student's unpaired t-test at the level of $p < 0.001$. IOs, inferior occipital sulcus; Ls, lunate sulcus; OO, Occipital Operculum; op, occipito-parietal; ot, occipito-temporal.

To quantitatively define the location and extent of the V3 and V4 parts activated for the three experimental tasks, average LCGU values (in μmol/100g/min) and their 95% confidence intervals were plotted every 100 μm along the dorsoventral extent in the different subdivisions of areas V3d and V4 inthe anterior bank of the Ls (Fig.4.10). Each plot represents % LCGU differences between experimental groups and their corresponding controls, i.e. between the Gl or O and the Cm, and between the Gd and the Cd. Specifically, the plot of LCGU differences traces a path that traverses (a) the V3d cortex from its ventralmost posterior occipito-temporal point (0 mm) to its dorsalmost-posterior occipito-parietal point (12.5 mm) and then to its dorsalmost-anterior occipito-parietal point (35.4 mm), and (b) the V4 occipito-temporal cortex from its dorsal to its ventralmost point (49.2 mm), as indicated in the diagrammatic representation of the reconstructed map above the plots. The length of this path in the diagrammatic representation corresponds to the length of the abscissa in the graph. The spatial resolution of the demonstrated effects is 100 μm. The Gl monkeys (red line) demonstrate a peak of activity in the ventral occipito-temporal part of area V3d representing central vision (which extends between 0 and 10 mm) and another peak in its dorsal occipito-parietal segment representing peripheral vision (which extends between 10 and 35 mm), while area V4 is steadily activated throughout its extent. The O monkeys (green line) display also two peaks of activity, one in the occipito-temporal and another one in the occipito-parietal segment of V3d, and no activation in area V4. Finally, the Gd monkeys (blue line) demonstrate pronounced activity only in the occipito-parietal segment of area V3d.

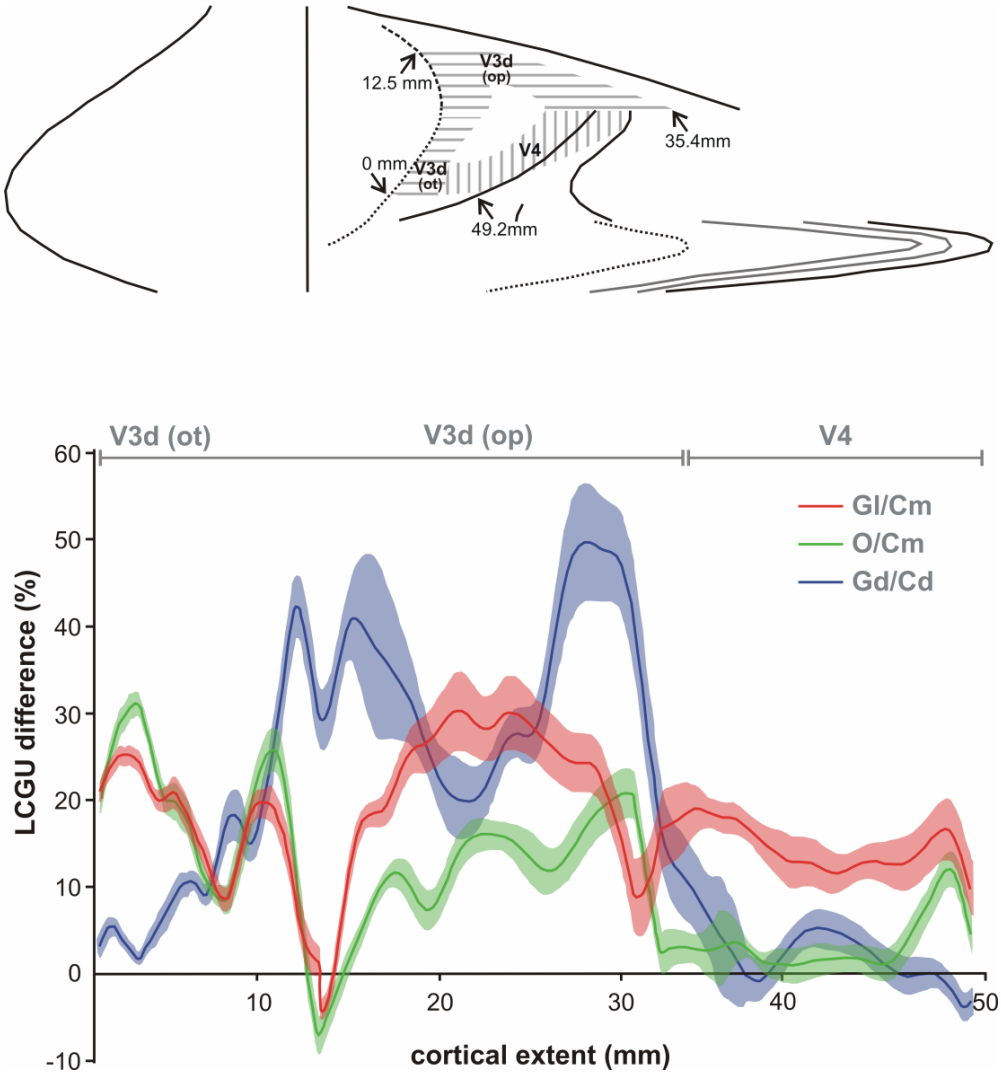

Figure 4.10: Plots of percent LCGU differences along areas V3d and V4. The striped region in the schematic representation of the reconstructed cortex above the plots, traces the path of measurement of the %LCGU differences in the reconstructed cortical fields. This path traverses the V3d cortex from the ventralmost (0 mm) to its dorsalmost extent (12.5 mm) and then from the caudalmost (12.5 mm) to its rostralmost coverage (35.4 mm), as well as area V4 dorsoventrally (between 35.4 and 49.2 mm). Coloured lines illustrate the %LCGU differences between control and experimental groups. The red line illustrates the %LCGU differences between the four Gl and the four Cm hemispheres. The green line demonstrates the differences between the six O and the four Cm hemispheres. The blue line illustrates the differences between the four Gd and the four Cd hemispheres. Red, green and blue shaded areas, around the corresponding lines, indicate 95% confidence intervals. Baseline (zero on the ordinate axis) corresponds to 0% LCGU difference from the corresponding control. The distances (mm) in the abscissa of the graph correspond to those marked in the schematic representation of the reconstructed cortex. op and ot, occipito-parietal and occipito-temporal segments of area V3d, representing peripheral and central vision, respectively.

CHAPTER 5

Discussion

We use mental imagery when we imagine ourselves executing an action or when we try to understand an observed action performed by someone else. It was previously demonstrated that the SI cortex is somatotopically activated when a monkey executes an action in the light and in the dark, as well as when the monkey observes another subject executing an action. This finding demonstrated that the action under observation recruits its motor and somatosensory representation in the observer's brain, in other words that the observer mentally (covertly) simulates the action in order to understand it (Gregoriou and Savaki 2003; Raos et al. 2004). In the present study we employed the quantitative 2DG autoradiographic method to examine whether the motor cognitive process of action-perception is based on memorized visual representations, in addition to the somatosensory ones. We present high-resolution quantitative functional and anatomical maps of primate brains (*Macaca mulatta*) during grasping-observation and during grasping-in-the-light and grasping-in-the-dark. Our results indicate that early visual cortices are involved in action representation. The present report undoubtedly assigns an important role to early visual cortices in the internal representation of a perceived action and in the execution of a motor act without visual guidance, which provides grounds for the contribution of early visual cortical areas in mental simulation of action.

Comparing the effects in the monkeys executing an action in the light and in monkeys observing the same action with the effects in the motion-control monkeys, which were exposed to the presentation of the object and the aimless arm motion, it is obvious that the central and peripheral visual representations of both V1 and V2 cortical regions in the occipital operculum, as well as V3v and V4 regions within the IOs were not affected. The lack of any effect within areas V1 and V2 indicates that the motion control group provided us with the means to correct for object-vision and arm-motion. The absence of any activation in the ventral regions of V3 and V4 is explained by the fact that our behavioural tasks involved activities in the lower rather than in the upper visual field of the monkeys (e.g. arm reaching to grasp). Additionally, there is evidence to suggest that the lower visual field is much more involved in the processing of visually guided movements. Danckert and Goodale (Danckert and Goodale 2001) using a visually guided pointing task revealed that the visuomotor system in the human brain shows a bias towards processing lower visual field

information. Other studies have also proposed that the lower visual field predominantly processes visual information regarding the peripersonal space whereas the upper visual field is mainly related to information from extrapersonal space. This difference in visual field representation may imply a different role in the processing of actions and object identification for the lower and the upper visual field respectively (Previc 1990; Previc 1998). It is suggested that this superior performance of the lower visual field for skilled visually guided actions can be attributed to the over-representation of this field into the visual/visuomotor areas of the dorsal visual stream, which support a functional bias toward the processing of action information. Indeed, several areas such as MT (Maunsell and Van Essen 1987) and V6 (Galletti et al. 1999) which are part of the dorsal stream exhibit an over-representation of the lower visual field. Yet, other studies partly support the advantage of the lower visual field in visuomotor processes. Binsted and Heath (Binsted and Heath 2005) extended the experiment of Danckert and Goodale to examine the putative differential role of the upper and lower visual fields. Their results overall did not confirm any effect of the visual field in the psychophysical kinematic measurements, although the endpoint accuracy of movements made in the lower visual field exhibited lower variable error as compared to the endpoint accuracy of movements made in the upper visual field.

The pronounced activation of areas V3d and V3A, which are part of the dorsal visual stream, for both execution in the light and observation, reflects the processing of stereoscopic depth information, useful for the analysis of forelimb-position, object-depth and 3D-form for the appropriate reaching-to-grasp. Therefore area V3 is processing visual information predominantly related to the requirements of the motor system to control the action. The activation of area V3 cannot be attributed to differences in oculomotor behaviour since the motion-control monkeys kept their eye position within the same window and for the same period of time as the experimental subjects in the light (Gl and O). It is important to emphasize that this motor-related visual information is processed not only during action-generation but also during action-observation. In the grasping-observation condition, V3 activation cannot be attributed to somatosensory feedback since no movement was executed. Consequently, our results suggest that cortical area V3 may be regarded as part of a network that is activated both for self-intended actions and for observed ones.

Specifically, based on our findings and in agreement with its known functional role, we suggest that area V3 may relay to the motor system, via the parieto-frontal visuo-motor stream, (a) visuospatial information required for the reaching component of the action, and (b) 3D-object-related information useful for the grasping constituent. Indeed, there are several reports supporting the above mentioned suggestion. First, it is known that V3 cells have strong binocular interactions (Zeki 1978a, 1978b) and are disparity-selective (Felleman and Van Essen 1987; Poggio et al. 1988; Adams and Zeki 2001) thus contributing to stereopsis, i.e. the perception of depth from small differences between the images in the two eyes. Moreover, area V3A (Van Essen and Zeki 1978) which receives projections from V3d (Felleman et al. 1997a), may construct an objective map of the visual field by combining visual and eye-position information (Galletti and Battaglini 1989), may play a role in cognitive functions, such as attention, anticipation and memory, by top-down influence (Nakamura and Colby 2000), and may play an important role in the visuomotor transformation from 3-D object vision to prehensile hand movements (Nakamura et al. 2001). In agreement with the above, areas V3d and V3A are considered to be involved in encoding 3D information, i.e. to either reconstruct the 3D shape of an object or to process global 3D layout (Tsao et al. 2003). Area

V3 is known to project to the posterior parietal areas (Felleman et al. 1997a) which are involved in visuomotor transformation for prehensile hand movements (Nakamura et al. 2001), and also to the parieto-occipital areas (Shipp et al. 1998) which are engaged in encoding the extrapersonal visual space (Galletti et al. 1995) and in sensory-motor integration of reaching arm movements (Galletti et al. 1997). Hence, the activation of area V3 for both execution and observation of the same action indicates the participation of this visual cortex in action-simulation, i.e. in the internal replication or re-enactment of a motor behaviour. As stated by Jeannerod, overt and covert actions represent a continuum, in the sense that every covert action has an overt constituent (Jeannerod 2006). Thus, an overlap of neural networks supporting the execution and the simulation of the same action is not surprising. Hence, the neural mechanism for spatial vision can be viewed as a bottom-up process subserved by feedforward projections between successive pairs of areas within the dorsal visual pathway. Given that the components of this neural substrate are reciprocally connected, feedback projections from higher-order processing stations back to lower-order ones can mediate top-down aspects of visual processing, such as the supply of a visuospatial frame for the covert completion of internally rehearsed actions, with the top-down mechanism presumably generated by a forward model (Wolpert and Ghahramani 2000). The forward models can estimate the forthcoming state of a process without the need to wait for the feedback information following its realization. It has been proposed that both actual and imagined movements involve predictions of the sensory consequences of the action (Blakemore and Sirigu 2003). In the actual execution, the predicted sensory consequences are compared to the actual sensory feedback, whereas in the absence of overt action e.g. during mental imagery, an internal representation of the body's state is preserved or stored in the corresponding brain areas (Wolpert et al. 1998; Blakemore and Sirigu 2003). Thus, forward models can be considered as an appropriate mechanism to account for the mental representation of an action. They can explain the nature of a mental representational mechanism that implements the same input and output as the perceptual-execution mechanism, since they can estimate the outcome of an action without executing it and without waiting for the reafference copy. Therefore they are in accord with the model of the internal representation of a motor action for planning an action or covertly simulating an observed action.

The monkeys which were reaching-to-grasp in complete darkness displayed pronounced activations in the parts of peripheral visual field representation of areas' V2 and V3 and small but significant activation in area V1. The activation of early visual cortices, especially for action-in-the-dark, may evoke reasonable questions. How the early visual cortical areas are activated in the lack of any visual input (in complete darkness)? Abundant literature underpins that the mechanisms that participate in the perception and the generation of an action involve the recruitment of visual and motor mental representations and that both visual and motor mental images share striking similarities with their overt counterparts. Higher level association, motor and visual areas constitute part of the neural networks that store information of combined spatial and representational features. These association areas are connected with early visual cortices, and most probably the appropriate information regarding the spatial properties of the goal directed movement (in the absence of visual guidance) is also represented in these early visual areas. Therefore the activation of these early visual cortices of our grasping-in-the-dark monkeys may reflect the top-down signals from the fronto-parietal dorsal stream areas, and their cross-talk with the early visual cortices, concerning memorized visual information about the movements. For example, the V3 complex may be receiving

an efferent feedback copy from the motor system priming the visual system to focus on elements useful for the successful completion of the action. Thus in the case of grasping in the dark, the neural mechanism for both object and spatial vision can be viewed as a "top-down" process subserved by the same pathway that supports grasping in the light. Projections from higher-order processing relay stations back to lower ones could mediate perceptual completion of the stimulus attributes, by recruiting an internal representation of the motor image. It has been proposed that the activation of somatosensory and motor areas for action-observation provides the internal representation of the action with its motor attributes (Raos et al. 2004, 2007). In a similar way, during action in the dark, the activated early visual areas may provide the mental image with its visual components. We suggest that this activation represents information about the spatial-location and the 3D-form of the object, required for motor control, i.e. for the estimation of the required reaching distance and the appropriate shaping of the hand for grasping in the dark. In our previous studies, the somatotopic activation of the primary somatosensory cortex during action-observation could support an introspective kinesthetic feeling of the movement by the observer in a first person perspective, i.e. mental simulation of the observed action along with its somatosesnsory consequences (Raos et al. 2004). In the present study, the activation of the early visual cortices during action-generation in complete darkness may support an introspective visual awareness of the invisible object to be reached and grasped within its unseen spatial surrounding, i.e. visual imagery during control of action. Therefore, imagery can partly substitute for visual input. Psychophysical experiments provide evidence which manifest that motor tasks are not influenced by the absence of vision. In an experiment using pointing movements, the researchers, by introducing a visual manipulation of the target (target visible/target occluded) observed that the accuracy in movements executed within the space of the lower field was not affected between the two conditions (Binsted and Heath 2005). Therefore, the recruitment of the occipito-parietal portion of V3d for the grasping-in-the dark monkeys could provide important information for the spatial components of the action.

Indeed activation of the primary visual cortex (area 17) and the adjacent visual areas (BA18, 19) for visual imagery, the faculty whereby we can re-visualize a visual item from memory, has been reported in numerous studies (Goldenberg et al. 1992; Kosslyn et al. 1993; Kosslyn et al. 1995; Kosslyn et al. 1996; Kosslyn et al. 1999a; Thompson et al. 2001; Lambert et al. 2002). Moreover, focal TMS over the occipital cortex interferes with the internal generation of mental visual images (Kosslyn et al. 1999). Activity in the primary visual cortex (calcarine sulcus and middle occipital gyrus) and in the extrastriate visual cortex was observed not only during visual imagery tasks but also during motor imagery tasks related to planning hand movements (de Lange et al. 2005). Selective activation of extrastriate visual areas (BA19) was reported during visuo-spatial imagery in early blind humans (Vanlierde et al. 2003). Moreover, cross-modal interaction between vision and touch, such as visual imagery during tactile perception, is supported by the activation of early visual cortices during Braille-reading in the blind (Sadato et al. 1996; Buchel et al. 1998), and is expected if the brain holds an inner inclusive representation of the body based on the integration of corresponding visual and somatosensory information (Haggard et al. 2007; Berlucchi and Aglioti 2010).

In contrast to area V3, area V4, which is a component of the ventral visual stream, was activated only for action-generation in the light, indicating that the attentive visual processing of detailed

colour- and form-related information about the object and the grasping hand is essential for the generation, but not for the observation/recognition of the action. The aspects of visual information processed in the dorsal stream are implicitly more relevant to motor control than static form or colour, which are predominantly processed in the vental pathway. Besides, it is well documented that the parietal and not the inferotemporal lesions produce visuomotor impairments (Hartje and Ettlinger 1973; Lamotte and Acuna 1978; Jeannerod 1986). Therefore, the activation of area V3 for directing actions-in-the-dark, for grasping invisible objects and for the formation of an internal representation of an observed action is compatible with its functional role as an area of the dorsal visual stream which is engaged in visuomotor transformations.

The fact that V1 is not activated for action-observation or that is marginally activated for action-execution in the dark may suggest that V1 activation is neither necessary nor sufficient for the implementation of mental simulation during observation of motor acts or during object-oriented actions without visual information. This assumption can be derived also from early studies on hemianopic patients caused by occipital lesions. It was shown that these patients retain capacities regarding spatial tasks, although they are impaired as far as basic visual attributes is concerned. For example, in one case when hemianopic patients were forced to make judgments about the location of a visual stimulus, without any experience of that stimulus, they produced accurate responses (Perenin and Jeannerod 1975). In another study, a patient with dense hemianopia of the right visual field, due to a lesion of the left occipital lobe, was tested for his capacities to process orientation and size of visual objects. He was requested to produce movements towards a visual slit oriented at different angles or a set of blocks of different sizes presented in his hemianopic field. These movements required some sort of motor transformation. It was shown that this patient was capable of executing these tasks successfully (Perenin and Rossetti 1996). Moreover, studies related to visuo-spatial imagery tasks in complete darkness and in blind subjects fail to activate the primary visual cortex (Mellet et al. 1996; Vanlierde et al. 2003). It should be mentioned however that many other studies have reported activation of area V1. For example, activity in the primary visual cortex (in the calcarine fissure) was observed in motor imagery tasks related to planning hand movements (de Lange et al. 2005) and during visual mental imagery (Le Bihan et al. 1993b; Kosslyn et al. 1995; Kosslyn and Thompson 2003). It was proposed that V1 activation depends on the spatial properties of the task. Imagery tasks which require high-resolution induce V1 activation, in contrast to spatial judgements tasks (Kosslyn et al. 2006a). Therefore, one could presume that during visual imagery V1 input contributes to a smaller extent to the function of the dorsal visual pathway, which is mainly involved in spatial perception and visuomotor transformation.

Recently, several studies examining memory-guided movements (by introducing brief delays between the stimulus presentation and the action onset) have proposed that in the absence of visual information delayed performances of motor behaviour might not be controlled by the dorsal neural circuit. These reports proposed that action and perception are carried out by the two independent visual systems (dorsal and ventral), but they also suggested that memory guided actions are based on perceptual mechanisms rather than on visuomotor coordinates. They suggested that the visuomotor mechanisms of the dorsal visual stream operate only for an on-line control of the movements when an action towards a visible target is required. They claimed that the control of actions when target vision is occluded, and hence the action is guided by memory retrieved information, is achieved by the perceptual mechanisms. Accordingly, memory-guided movements

are planned based on the relational metrics of the ventral visual stream where stored information regarding the target is used for a relatively accurate off line control of the action (Goodale et al. 1994; Hu et al. 1999; Lemay and Proteau 2002; Heath and Westwood 2003; Westwood et al. 2003; Goodale et al. 2004).

Indications which challenged the contribution of dorsal and the ventral stream in memory-guided movements, and impugned the nature of the information they convey, came from the effects of various visual illusions on action. Such experiments included size-contrast, orientation, and pictorial illusions and many modified versions of them. The explanations proposed to account for the susceptibility of memory-guided motor actions to visual illusions were as numerous as the corresponding experiments. On the grounds of the common illusory effect on perceptual and grasping tasks it was proposed that the dorsal visual pathway forms a target representation which is influenced by ventral inputs through the interconnections of the two functional streams (Pavani et al. 1999). Other researchers have interpreted similar results on the basis of relative and absolute perception. They argued that actions require absolute judgements and as such are relatively unaffected by context-illusions. Subsequently, they suggested that the demands of the task dictate if the motor or the perceptual representations will be influenced by illusions (Vishton et al. 1999). Another group has suggested the planning/motor model. According to it, actions at their initial stages are planned on a context-dependent representation that is subject to optical illusions, and at later stages on a context-independent representation which is relatively unaffected by illusions (Glover and Dixon 2001a; Glover and Dixon 2001b; Glover 2002). Westwood and Goodale studying perception, visually-guided and memory-guided grasping movements in conjunction with visual illusions, found that in the memorized condition both perception and action were affected by the illusion. Hence they restated their proposal that memorized actions are mediated by the ventral visual stream whereas the dorsal one mediates on-line visuomotor control (Hu and Goodale 2000; Westwood et al. 2000a; Westwood et al. 2000b; Westwood et al. 2001; Westwood and Goodale 2003).

However, other psychophysical studies indicate the participation of the dorsal visual stream in the motor control of memory-guided reaching and grasping. In a classic experiment, Bridgeman et al. (1981) asked subjects to point manually to a fixed target surrounded by a moving frame. At movement onset, the target was extinguished not allowing visual feedback. Despite that the fixed target appeared to drift in the opposite direction with respect to that of the frame, subjects pointed accurately to the true target location (Bridgeman et al. 1981). This study illustrates that execution and perception are mediated by the dorsal and the ventral visual stream respectively and that the stored target representation is based on the visuomotor coordinates of the dorsal system. Strong support for a dorsal involvement also comes from combined studies on visual illusions and grasping tasks. Ample results have demonstrated that visual illusions do not affect or insignificantly affect object-directed actions, while they influence on object perception. Aglioti et al. conducted a renowned experiment using the Titchener illusion and later Haffenden and Goodale demonstrated the same result expanding Aglioti's experiment in grasping movements without visual information of the hand and the stimulus. In this experiment, there was no opportunity for subjects to use visual feedback from their hand or the target to adjust their grip aperture in flight. It was observed that the maximum grip aperture continued to correspond to the physical rather than the perceived size of the object, suggesting that this real-world metrical calibration could not have been based

on adjustments made during the execution of the grasp. Instead, subjects must have programmed the aperture of their grasp on the basis of their initial glimpse of the target disk, presumably in relation to its real size (Aglioti et al. 1995; Haffenden and Goodale 1998). Later, the second group assayed the effect of pictorial illusions on grip size by examining meticulously the influence of flankers' position and direction relatively to the target on grip scale. They found that the distance of the flankers from the target did not affect grip scale, and that the horizontal orientation induced difference to the grip task. The authors suggested that these influences come from 'non-perceptual' sources, i.e. the surrounding annuli are perceived as potential obstacles which force the motor system to adjust the grip accordingly (Haffenden and Goodale 2000; Haffenden et al. 2001). In another experiment, two illusions which presumably interfere in different stages of the visual process were used. The "simultaneous tilt illusion (STI)" interfering early in vision should affect both the dorsal and the ventral stream, and the "rod-and-frame illusion (RFI)" interfering in later stages of the perceptual-ventral stream should influence perception rather than action. The results of this study confirmed the abovementioned hypothesis. The STI influenced the memory-guided motor task, indicating that the dorsal stream participates in the visuomotor representation of the motor act. On the other hand, the susceptibility only of the ventral stream to the RFI manifest its involvement in the perceptual mechanisms (Dyde and Milner 2002; Milner and Dyde 2003). Moreover, recent studies examined the memory-guided grasping and found no evidence for a shift in the motor control mechanism from the dorsal to the ventral stream (Franz et al. 2009; Hesse and Franz 2009). Finally, participation of the dorsal visual stream in the execution of memorized delayed movements has been indicated by TMS (Cohen et al. 2009) and fMRI (Singhal et al. 2006; Fiehler et al. 2008; Himmelbach et al. 2009) studies.

Our finding that the occipito-parietal V3d segment, which is part of the dorsal visual stream, is activated for action in the dark, is compatible with the results of the latter psychophysical, inactivation and imaging studies. At this point we wish to emphasize that all the above cited studies concern brief target-recall delays (up to 18 s), whereas in our case the monkeys grasping in the dark did not see the object to be grasped for months before the ^{14}C-DG experiment. Therefore, our study demonstrates that the motor system can use stored visual information for the control of memory-guided actions not only for short delays between visual occlusion and movement onset but also for much longer periods of time. Furthermore, our results illustrate that visual representation of the memory-guided action is stored in early components of the dorsal visual stream.

Besides, activation of the dorsal visual pathway related to visuospatial imagery was observed also in early blind (EB) subjects. In a PET study regarding estimation of the symmetry of a pattern mentally projected into a matrix, the parietal and extrastriate occipital regions were activated in EB subjects. Similar activation foci were also present in the control group. These results indicate that the dorsal visual pathway is activated in a resembling/equivalent way in the absence and in the presence of vision, and it is efficiently functional in EB (Vanlierde et al. 2003). Moreover, several studies provide consistent evidence that parietal areas are activated in motor relevant tasks, such as imagined grasping movements (Decety et al. 1994; Grafton et al. 1996) and action observation (Grafton et al. 1996; Buccino et al. 2001). Therefore, these observations support our reasoning that V3 activation is due to the visuo-spatial imagery, supported by the dorsal visual stream, which is recruited during action-execution in the dark.

The differential activation of the occipito-parietal segment of area V3d which represents peripheral vision and projects to the dorsal visual stream, and the occipito-temporal segment which represents central vision and projects to the ventral visual stream (Baizer et al. 1991), in our experimental groups, is compatible with previous reports. There is evidence in the literature (Levine et al. 1985; Farah et al. 1988a) of a dissociation between object discrimination and spatial localization in imagery tasks. These results suggest that mental imagery of object features involves mainly the ventral, occipito-temporal stream of visual processing, whereas spatial or movement-related imagery involves primarily the dorsal, occipito-parietal stream (Mishkin et al. 1983; Milner and Goodale 1995). Accordingly, the occipito-parietal segment of area V3d activated for reaching-to-grasp in the dark in our study, suggests a major involvement of visuospatial movement-related imagery during action-generation in the dark. The activation of both the occipito-temporal and occipito-parietal segments of area V3d for action-generation in the light and for action-observation supports the assumption that visual perception and mental simulation of action, respectively, involve both object-feature and visuospatial related components (Kosslyn and Thompson 2003). Moreover, the activation of the occipito-parietal portion of V3d which was stronger for grasping in the dark than in the light is reminiscent of the stronger somatosensory activation for reaching in the dark in previous studies (Savaki et al. 1993; Gregoriou and Savaki 2003). It appears that, both the somatosensory and visual consequences of an action are more heavily represented when the action is executed in the absence of visual guidance.

Another point worth discussing is the argument that activation of an area during visual imagery does not necessarily prove that this area is critical to imagery, or even participates in it (Moscovitch et al. 1994). The activation may reflect concomitant cognitive activities or shifts of attention which do not contribute to the generation of mental visual images. It has been proposed that attentional components in visual imagery tasks enhance the activity in early visual areas, and it was hypothesized that imagery is implemented by the interaction of memory-retrieval with focal-attention mechanisms (Sakai and Miyashita 1994). Other researchers have also proposed that space-related imagery is a cognitive activity involving attentional and intentional aspects (Bartolomeo and Chokron 2002). Yet, experimental evidence underpins the differences between imagery and attention and highlights that these two processes do not induce the same effects. In a PET study, subjects were examined in an imagery and an attentional task. In the imagery task they were asked to visualize letters in a grid and decide whether an X mark would fall on the letter. In the attentional task they were asked to watch the grid and respond when the same X mark disappeared. It was shown that these two conditions induced different activations, with those elicited by the imagery task being more pronounced (Kosslyn et al. 1993). In another study, which investigated the neural correlates underlying imagery generated from short- and long-term memory, it was found that memory and attention resulted in differential effects during the generation and maintenance of mental images of faces (Ishai et al. 2002). Hence, in all probability, the cortical activations during action-in-the-dark and action-observation cannot be attributed to attentional influence.

Our suggestion that the activation of areas V3d and V3A reflects handling of visual features of action representations, is in agreement with the existence of a region in the lateral occipital cortex of humans which responds to images of the human body (Downing et al. 2001). This area, called the ”extrastriate body area (EBA)” is activated by the presentation of pictures showing body parts or even whole bodies. In fact, further fMRI studies revealed that EBA is not only activated by

stationary body images but it responds also to movements of one's own body. The important finding is that this activation is not exclusively due to the visual input of the moving body. EBA response persists even when the moving limb is occluded from view, when the subject is preparing to move, and during limb movements to visual targets when the eyes are shut, and during mental imagination of a goal-directed movement (Astafiev et al. 2004). The implication of EBA, not only in perceptual but also in motor-related processes, was confirmed by later studies too (Ishizu et al. 2009). Activation of the extrastriate visual cortex, part of which could be related to EBA, was observed in a combined task of observation of gait and imaginary walking (Iseki et al. 2008). This activity could be at least partly explained by the detection of biological motion, i.e visuomotor imagery from the first-person perspective for the virtual-walking condition and from the third-person perspective for the gait-observation condition. Hence, the activation of EBA can be attributed to internal signals generated during the motor action and to the internal representation of that action. EBA responsiveness not only to reafferent visual or proprioceptive signals, but also to endogenous signals that are part of the process of generating actions, have led scientists to implicate it in the process of self/other discrimination (Downing et al. 2001; Jeannerod 2004; Saxe et al. 2006). Moreover, several fMRI studies have demonstrated an extrastriate occipital area associated with motor imagery of walking (Bakker et al. 2008), visual and motor imagery tasks (de Lange et al. 2005), and the imagery pre-shot routine of expert golfers (Milton et al. 2007). EBA and other areas receiving such information may form a network that could be involved in the perception of one's own body, in distinguishing the self from others or in assigning the actions and intentions to the correct agent. Experiments have described other regions that contain neurons responsive to the perception of body parts, such as regions within the STs (Haxby et al. 2000; Kourtzi and Kanwisher 2000), which were implicated in the perception of biological motion (Hietanen and Perrett 1996; Grossman et al. 2000) or such as the lateral occipital complex (LOC) which responds robustly to images of familiar and unfamiliar objects, including human bodies (Grill-Spector et al. 2001; Kourtzi and Kanwisher 2001; Saxe et al. 2006). Neighbouring face- and body selective regions have also been found in humans. A body-selective area in the fusiform gyrus (fusiform body area FBA), anatomically distinct from EBA, is adjacent and partly overlaps with the face-selective fusiform area (FFA) (Kanwisher et al. 1997; Peelen and Downing 2005; Schwarzlose et al. 2005). This topography could indicate the existence of a distributed, bridge circuit of areas representing salient information for the identification of conspecifics and the perception of the self and the "body schema".

Accordingly, the marked activation of the occipital areas V3d and V3A in our study may correspond to the activation of EBA in the human occipitotemporal cortex which is associated, as described above, with functions similar to those ascribed to monkey V3 in our and others' studies. Our suggestion that the activation of areas V3d and V3A reflects handling of visual features of action representations is in agreement with the functional and anatomical data available for these areas (Van Essen and Zeki 1978; Felleman and Van Essen 1987; Poggio et al. 1988; Galletti and Battaglini 1989; Nakamura and Colby 2000; Adams and Zeki 2001; Nakamura et al. 2001; Tsao et al. 2003). Although the only direct projection of area V3 to the frontal cortex is that to FEF (Barbas and Mesulam 1981), V3 is an important link between early visual cortical areas and the parietal sensory-motor integration areas (Andersen et al. 1990; Baizer et al. 1991; Felleman and Van Essen 1991; Felleman et al. 1997a; Shipp et al. 1998). Similarly it has been suggested that EBA (a) potentially

receives efference signals from motor areas, and (b) may interact with the frontoparietal areas (Peelen and Downing 2007).

On the basis of the cellular properties, the functional organization and the inter-cortical connections, we suggest that the activation of areas V3d and V3A for action-generation in the light reflects the processing of stereoscopic depth information, useful for the analysis of forelimb-position, object-depth and 3D-form for the appropriate reaching-to-grasp. Because mental simulation of action, or motor imagery (Jeannerod 2001), has already been demonstrated during action-observation in monkeys (Raos et al. 2004), the activation of areas V3d and V3A for action-observation and for action-generation in the dark reflects the processing of visual information related to the mental simulation of the action. This information may be relayed via the parietal projections of areas V3d and V3A (Andersen et al. 1990; Baizer et al. 1991; Felleman and Van Essen 1991) which were found to be activated for grasping-observation (Evangeliou et al. 2009), to the premotor/motor cortices (Petrides and Pandya 1984; Matelli et al. 1998; Petrides and Pandya 1999) which were also found to be activated during observation of reaching-to-grasp (Raos et al. 2007). Thus, area V3 may process visuomotor information related to internally represented actions.

We should clarify that when we use the terms "mental representation" or "imagery" we do not wish to imply that a conscious process is in operation. This is particularly true of non human primates, in which the involvement of mental imagery is speculative as it cannot be assessed directly. Instead, we use it to refer to the retrieval of internal representations of the act which were memorized months before the experiment. However, it should be noted that even in humans several aspects of the covertly executed action and their relation to consciousness remain unknown. According to Jeannerod, even though a person can consciously generate a mental motor image, most of its generation is opaque to the subject and its constituents are revealed only through meticulous experimental measurements (Jeannerod 1994, 2006). Other researchers also agree that the implementation of mental imagery in humans can be assessed only indirectly. Annet presumes that although in mental imagery tasks the participants are explicitly asked to apply mental imagery, the degree to which they comply with the instructions and the actual use of imagery are always based on subjective judgements which by no means are infallible evaluations (Annett 1995).

At this point it is also important to mention that although visual imagery and perception share the supporting substrate and the underlying mechanisms, they are not identical processes. Evidence comes from observations concerning the dissociation between imagery and perception. Several cases of patients have been reported with profound visual object agnosia but well-preserved ability for imagery (Riddoch and Humphreys 1987; Behrmann et al. 1992; Jankowiak et al. 1992; Servos et al. 1993; Chatterjee and Southwood 1995; Goldenberg et al. 1995). These patients despite the severe object recognition deficit were able to carry out tasks typically used to assess mental imagery, such as detailed decisions on visual images, and to provide drawings of objects from memory despite their inability to recognize these objects. There are also reports of neuropsychological patients who have preserved perception but impaired imagery (Farah et al. 1988b). This segregation of functions is consistent with a functional imaging study, in which the subjects' brains were scanned using PET while they performed perceptual and imagery tasks. It was found that two thirds of the visual brain areas were activated during both imagery and perception, whereas two areas were activated only for the perception and five were more activated for imagery (Kosslyn et al. 1997). This result was replicated in another study by the same group, when subjects were asked to visualize and compare

low and high resolution stripes of different orientations, in perceptual and imagery tasks. It was shown that, although in both conditions subjects were prone to more errors when they evaluated the oblique stripes as compared with the vertical and horizontal ones, in the imagery condition they required more time to evaluate high-resolution patterns than to evaluate low resolution ones. This result indicates that imagery does not rely on all perceptual mechanisms (Kosslyn et al. 1999b). Moreover, we should keep in mind that despite the consensus on functional equivalence of imagery and perception, scientists have suggested different models for the implementation of mental imagery. In its simplest form, it was proposed that visual imagery can be thought of as running visual perception in reverse. Accordingly, during visual imagery the stored representation of an object is accessed and information is sent to the systems processing the object- and the spatial-properties to recruit detailed representations of the corresponding visual properties. This recruitment is identical to the priming that occurs during bottom-up process. However, in imagery the priming is so strong that the activation propagates backwards, and an image representation is formed in the visual buffer (Kosslyn et al. 2006b). Other researchers, especially triggered by the study of motor imagery, have proposed that the simulation does not relate to a conscious reactivation of previously executed actions stored in memory but to unspecific elements that comprise the stimulus. According to that interpretation, internal representations are dynamic procedures automatically assembled in response to the action requirements and the motor rules are embodied in the interconnections of the areas involved (Jeannerod 1997). Nonetheless, the crucial issue remains that the mass body of the experimental results indicate that processes underlying mental representations of movements within mentally represented visual space are similar to those underlying actual movements within physical space.

Overall we suggest that areas V3d and V3A, which are activated for action observation and action in the dark, may be specifically involved in the visuo-spatial processing associated with movement-related mental imagery. V3 may contribute to transport the hand to a desired location within extrapersonal space and to shape the hand with the purpose of manipulating objects. Both grasping-in-the-dark and action-observation imply visuomotor transformations, represented mostly in the dorsal visual stream. Our suggestion that the occipito-parietal segment of area V3d is specifically involved in mental imagery is in accordance with the following reports. First, the occipital visual cortex BA19 was found activated during imagined passive locomotion (Flanagin et al. 2009) and also in blindfolded volunteers reaching to remembered targets, reflecting its involvement in the creation of mental visual images of the target locations (Darling et al. 2007). Second, an extrastriate visual area near the parieto-occipital fissure was associated with the visual imagery implicated in tactile perception of unseen objects (Sathian and Zangaladze 2002). Therefore, we suggest that visual imagery may take place during reaching-to-grasp in the dark, recruiting stored visual representations to support the action-execution in blindfolded subjects. Accordingly, stored visual representations of the unseen forelimb in the environment for reaching and of the invisible 3D-object to be grasped are recalled for the accomplishment of an appropriate action in the absence of visual input. By analogy to the activation of motor, somatosensory and parietal areas during action-observation, which is required to provide the action representation with a sensory-motor format (Gregoriou and Savaki 2003; Raos et al. 2004, 2007; Evangeliou et al. 2009), the activation of visual areas is required to provide the motor action in the dark with a visual/visuospatial content.

Summarizing, until now the existing literature showed that mental imagery in action-observation and action-in-the-dark implied the recollection of information composed of sensory and kinaesthetic sequences (Raos et al. 2004, 2007; Evangeliou et al. 2009). The central advance of this study is the demonstration that the single neural substrate used "bottom-up" (sensory-driven) or "top-down" (mentally-driven) to represent physical or mental practice, respectively, extends beyond the parieto-frontal somatosensory-motor circuit described in the past (Raos et al. 2004, 2007; Evangeliou et al. 2009), to also include early occipital cortices which reflect the physical or mental visuospatial representations of the motor act. We provide evidence supporting that predominantly the extrastriate visual area V3 is engaged in visuomotor associations of internally represented actions, which may include the target of the action, the means to reach it and its consequences. These results indicate a novel coupling between visual and motor representations in the field of motor cognition.

References

Acuna C, Cudeiro J, Gonzalez F, Alonso JM, Perez R. 1990. Lateral-posterior and pulvinar reaching cells-comparison with parietal area 5a: a study in behaving Macaca nemestrina monkeys. Exp Brain Res. 82: 158-166.

Adams DL, Zeki S. 2001. Functional organization of macaque V3 for stereoscopic depth. J Neurophysiol. 86: 2195-2203.

Adams L, Guz A, Innes JA, Murphy K. 1987. The early circulatory and ventilatory response to voluntary and electrically induced exercise in man. J Physiol. 383: 19.

Aglioti S, DeSouza JFX, Goodale MA. 1995. Size-contrast illusions deceive the eye but not the hand. Curr Biol. 5: 679-685.

Allman JM, Kaas JH. 1971. Representation of the visual field in striate and adjoining cortex of the owl monkey (Aotus trivirgatus). Brain Res. 35: 89-106.

Allman JM, Kaas JH. 1974a. A crescent-shaped cortical visual area surrounding the middle temporal area (MT) in the owl monkey (Aotus trivirgatus). Brain Res. 81: 199-213.

Allman JM, Kaas JH. 1974b. The organization of the second visual area (VII) in the owl monkey: a second order transformation of the visual hemifield. Brain Res. 76: 247-265.

Allman JM, Kaas JH. 1975. The dorsomedial cortical visual area: a third tier area in the occipital lobe of the owl monkey (Aotus trivirgatus). Brain Res. 100: 473-487.

Andersen RA, Asanuma C, Essick G, Siegel RM. 1990. Corticocortical connections of anatomically and physiologically defined subdivisions within the inferior parietal lobule. J Comp Neurol. 296: 65-113.

Anderson JC, Martin KA. 2002. Connection from cortical area V2 to MT in macaque monkey. J Comp Neurol. 443: 56-70.

Anderson JC, Martin KA. 2005. Connection from cortical area V2 to V3A in macaque monkey. J Comp Neurol. 488: 320-330.

Annett J. 1995. Motor imagery: perception or action? Neuropsychologia. 33: 1395-1417.

Astafiev SV, Stanley CM, Shulman GL, Corbetta M. 2004. Extrastriate body area in human occipital cortex responds to the performance of motor actions. Nat Neurosci. 7: 542-548.

Avikainen S, Forss N, Hari R. 2002. Modulated activation of the human SI and SII cortices during observation of hand actions. Neuroimage. 15: 640-646.

Bachelard HS. 1971. Specificity and kinetic properties of monosaccharide uptake into guinea pig cerebral cortex in vitro. J Neurochem. 18: 213-222.

Baizer JS. 1982. Receptive field properties of V3 neurons in monkey. Invest Ophthalmol Vis Sci. 23: 87-95.

Baizer JS, Desimone R, Ungerleider LG. 1993. Comparison of subcortical connections of inferior temporal and posterior parietal cortex in monkeys. Vis Neurosci. 10: 59-72.

Baizer JS, Maguire WM. 1983. Double representation of lower visual quadrant in prelunate gyrus of rhesus monkey. Invest Ophthalmol Vis Sci. 24: 1436-1439.

Baizer JS, Robinson DL, Dow BM. 1977. Visual responses of area 18 neurons in awake, behaving monkey. J Neurophysiol. 40: 1024-1037.

Baizer JS, Ungerleider LG, Desimone R. 1991. Organization of visual inputs to the inferior temporal and posterior parietal cortex in macaques. J Neurosci. 11: 168-190.

Bakker M, De Lange FP, Helmich RC, Scheeringa R, Bloem BR, Toni I. 2008. Cerebral correlates of motor imagery of normal and precision gait. Neuroimage. 41: 998-1010.

Bakola S, Gregoriou GG, Moschovakis AK, Raos V, Savaki HE. 2007. Saccade-related information in the superior temporal motion complex: quantitative functional mapping in the monkey. J Neurosci. 27: 2224-2229.

Baleydier C, Mauguiere F. 1985. Anatomical evidence for medial pulvinar connections with the posterior cingulate cortex, the retrosplenial area, and the posterior parahippocampal gyrus in monkeys. J Comp Neurol. 232: 219-228.

Baleydier C, Morel A. 1992. Segregated thalamocortical pathways to inferior parietal and inferotemporal cortex in macaque monkey. Vis Neurosci. 8: 391-405.

Barbas H. 1988. Anatomic organization of basoventral and mediodorsal visual recipient prefrontal regions in the rhesus monkey. J Comp Neurol. 276: 313-342.

Barbas H, Henion TH, Dermon CR. 1991. Diverse thalamic projections to the prefrontal cortex in the rhesus monkey. J Comp Neurol. 313: 65-94.

Barbas H, Mesulam MM. 1981. Organization of afferent input to subdivisions of area 8 in the rhesus monkey. J Comp Neurol. 200: 407-431.

Barlow HB, Blakemore C, Pettigrew JD. 1967. The neural mechanism of binocular depth discrimination. J Physiol. 193: 327-342.

Bartolomeo P, Chokron S. 2002. Can we change our vantage point to explore imaginal neglect? Behav Brain Sci. 25: 184-185.

Behrmann M, Winocur G, Moscovitch M. 1992. Dissociation between mental imagery and object recognition in a brain-damaged patient. Nature. 359: 636-637.

Bender DB. 1981. Retinotopic organization of macaque pulvinar. J Neurophysiol. 46: 672-693.

Benevento LA, Davis B. 1977. Topographical projections of the prestriate cortex to the pulvinar nuclei in the macaque monkey: an autoradiographic study. Exp Brain Res. 30: 405-424.

Benevento LA, Rezak M. 1976. The cortical projections of the inferior pulvinar and adjacent lateral pulvinar in the rhesus monkey (Macaca mulatta): an autoradiographic study. Brain Res. 108: 1-24.

Berlucchi G. 1972. Anatomical and physiological aspects of visual functions of corpus callosum. Brain Res. 37: 371-392.

Berlucchi G, Aglioti SM. 2010. The body in the brain revisited. Exp Brain Res. 200: 25-35.

Bethell-Fox CE, Shepard RN. 1988. Mental rotation: Effects of stimulus complexity and familiarity. Journal of Experimental Psychology: Human Perception and Performance. 14: 12-23.

Bidder TG. 1968. Hexose translocation across the blood-brain interface: configurational aspects. J Neurochem. 15: 867-874.

Bilge M, Bingle A, Seneviratne KN, Whitteridge D. 1967. A map of the visual cortex in the cat. J Physiol. 191: 116-118.

Billings-Gagliardi S, Chan-Palay V, Palay SL. 1974. A review of lamination in area 17 of the visual cortex Macaca mulatta. J Neurocytol. 3: 619-629.

Binsted G, Heath M. 2005. No evidence of a lower visual field specialization for visuomotor control. Exp Brain Res. 162: 89-94.

Blakemore SJ, Sirigu A. 2003. Action prediction in the cerebellum and in the parietal lobe. Exp Brain Res. 153: 239-245.

Blasdel G, Campbell D. 2001. Functional retinotopy of monkey visual cortex. J Neurosci. 21: 8286-8301.

Blasdel GG. 1992a. Differential imaging of ocular dominance and orientation selectivity in monkey striate cortex. J Neurosci. 12: 3115-3138.

Blasdel GG. 1992b. Orientation selectivity, preference, and continuity in monkey striate cortex. J Neurosci. 12: 3139-3161.

Blasdel GG, Lund JS, Fitzpatrick D. 1985. Intrinsic connections of macaque striate cortex: axonal projections of cells outside lamina 4C. J Neurosci. 5: 3350-3369.

Blasdel GG, Salama G. 1986. Voltage-sensitive dyes reveal a modular organization in monkey striate cortex. Nature. 321: 579-585.

Blatt GJ, Andersen RA, Stoner GR. 1990. Visual receptive field organization and cortico-cortical connections of the lateral intraparietal area (area LIP) in the macaque. J Comp Neurol. 299: 421-445.

Born RT, Tootell RB. 1991. Spatial frequency tuning of single units in macaque supragranular striate cortex. Proc Natl Acad Sci USA. 88: 7066-7070.

Boussaoud D, Desimone R, Ungerleider LG. 1991. Visual topography of area TEO in the macaque. J Comp Neurol. 306: 554-575.

Boussaoud D, Desimone R, Ungerleider LG. 1992. Subcortical connections of visual areas MST and FST in macaques. Vis Neurosci. 9: 291-302.

Boussaoud D, Ungerleider LG, Desimone R. 1990. Pathways for motion analysis: cortical connections of the medial superior temporal and fundus of the superior temporal visual areas in the macaque. J Comp Neurol. 296: 462-495.

Bower GH. 1970. Imagery as a relational organizer in associative learning. Journal of Verbal Learning and Verbal Behavior. 9: 529-533.

Braddick OJ, O'Brien JM, Wattam-Bell J, Atkinson J, Hartley T, Turner R. 2001. Brain areas sensitive to coherent visual motion. Perception. 30: 61-72.

Brewer AA, Press WA, Logothetis NK, Wandell BA. 2002. Visual areas in macaque cortex measured using functional magnetic resonance imaging. J Neurosci. 22: 10416-10426.

Bridgeman B, Kirch M, Sperling A. 1981. Segregation of cognitive and motor aspects of visual function using induced motion. Percept Psychophys. 29: 336-342.

Brodmann K. 1905. Beiträge zur histologischen Lokalisation der Grosshirnrinde. Dritte Mitteilung: Die Rindenfelder der niederen Affen. . J Psychol Neurol Lpz. 4: 177-226.

Brodmann K. 1909. Vergleichende Lokalisationslehre den Grosshirminde. Barth, Leipzig.

Brouwer B, Zeeman WPC. 1925. Experimental anatomical investigation concerning the projection of the retina on the primary optic centers in apes. J Neurol Psychopath. 6: 1-10.

Buccino G, Binkofski F, Fink GR, Fadiga L, Fogassi L, Gallese V, Seitz RJ, Zilles K, Rizzolatti G, Freund HJ. 2001. Action observation activates premotor and parietal areas in a somatotopic manner: an fMRI study. Eur J Neurosci. 13: 400-404.

Buchel C, Price C, Frackowiak RS, Friston K. 1998. Different activation patterns in the visual cortex of late and congenitally blind subjects. Brain. 121: 409-419.

Bullier J, Kennedy H. 1983. Projection of the lateral geniculate nucleus onto cortical area V2 in the macaque monkey. Exp Brain Res. 53: 168-172.

Burkhalter A, Felleman DJ, Newsome WT, Van Essen DC. 1986. Anatomical and physiological asymmetries related to visual areas V3 and VP in macaque extrastriate cortex. Vision Res. 26: 63-80.

Burkhalter A, Van Essen DC. 1986. Processing of color, form and disparity information in visual areas VP and V2 of ventral extrastriate cortex in the macaque monkey. J Neurosci. 6: 2327-2351.

Burton H, Jones EG. 1976. The posterior thalamic region and its cortical projection in New World and Old World monkeys. J Comp Neurol. 168: 249-301.

Callaway EM. 1998. Local circuits in primary visual cortex of the macaque monkey. Annu Rev Neurosci. 21: 47-74.

Caplovitz GP, Tse PU. 2007. V3A processes contour curvature as a trackable feature for the perception of rotational motion. Cereb Cortex. 17: 1179-1189.

Cavada C, Goldman-Rakic PS. 1989. Posterior parietal cortex in rhesus monkey: I. Parcellation of areas based on distinctive limbic and sensory corticocortical connections. J Comp Neurol. 287: 393-421.

Cerritelli B, Maruff P, Wilson P, Currie J. 2000. The effect of an external load on the force and timing components of mentally represented actions. Behav Brain Res. 108: 91-96.

Charlot V, Tzourio N, Zilbovicius M, Mazoyer B, Denis M. 1992. Different mental imagery abilities result in different regional cerebral blood flow activation patterns during cognitive tasks. Neuropsychologia. 30: 565-580.

Chatterjee A, Southwood MH. 1995. Cortical blindness and visual imagery. Neurology. 45: 2189-2195.

Chen W, Kato T, Zhu XH, Ogawa S, Tank DW, Ugurbil K. 1998. Human primary visual cortex and lateral geniculate nucleus activation during visual imagery. Neuroreport. 9: 3669.

Choudhury BP, Whitteridge D, Wilson ME. 1965. The function of callosal connections of the visual cortex. Experimental Physiology. 50: 214-219.

Cisek P, Kalaska JF. 2004. Neural correlates of mental rehearsal in dorsal premotor cortex. Nature. 431: 993-996.

Clark VP, Courchesne E, Grafe M. 1992. In vivo myeloarchitectonic analysis of human striate and extrastriate cortex using magnetic resonance imaging. Cereb Cortex. 2: 417-424.

Clark WE. 1925. The visual cortex of primates. J Anat. 59: 350-357.

Clark WE. 1942. The cells of Meynert in the visual cortex of the monkey. J Anat. 76: 369-376.

Cohen NR, Cross ES, Tunik E, Grafton ST, Culham JC. 2009. Ventral and dorsal stream contributions to the online control of immediate and delayed grasping: a TMS approach. Neuropsychologia. 47: 1553-1562.

Colby CL, Gattass R, Olson CR, Gross CG. 1988. Topographical organization of cortical afferents to extrastriate visual area PO in the macaque: a dual tracer study. J Comp Neurol. 269: 392-413.

Conway BR, Tsao DY. 2006. Color architecture in alert macaque cortex revealed by fMRI. Cereb Cortex. 16: 1604-1613.

Cooper LA, Shepard RN. 1973. The time required to prepare for a rotated stimulus. Mem Cognit. 1: 246-250.

Cragg BG. 1969. The topography of the afferent projections in the circumstriate visual cortex of the monkey studied by the Nauta method. Vision Res. 9: 733-747.

Crair MC, Ruthazer ES, Gillespie DC, Stryker MP. 1997. Ocular dominance peaks at pinwheel center singularities of the orientation map in cat visual cortex. J Neurophysiol. 77: 3381-3385.

Crowley JC, Katz LC. 2000. Early development of ocular dominance columns. Science. 290: 1321-1324.

Cumming BG, Parker AJ. 1997. Responses of primary visual cortical neurons to binocular disparity without depth perception. Nature. 389: 280-283.

Cumming BG, Parker AJ. 1999. Binocular neurons in V1 of awake monkeys are selective for absolute, not relative, disparity. J Neurosci. 19: 5602.

Cumming J, Hall C. 2002. Deliberate imagery practice: the development of imagery skills in competitive athletes. J Sports Sci. 20: 137-145.

Cusick CG, Kaas JH. 1988. Cortical connections of area 18 and dorsolateral visual cortex in squirrel monkeys. Vis Neurosci. 1: 211-237.

Dalezios Y, Raos VC, Savaki HE. 1996. Metabolic activity pattern in the motor and somatosensory cortex of monkeys performing a visually guided reaching task with one forelimb. Neuroscience. 72: 325-333.

Danckert J, Goodale MA. 2001. Superior performance for visually guided pointing in the lower visual field. Exp Brain Res. 137: 303-308.

Daniel PM, Whitteridge D. 1961. The representation of the visual field on the cerebral cortex in monkeys. J Physiol. 159: 203-221.

Darling WG, Seitz RJ, Peltier S, Tellmann L, Butler AJ. 2007. Visual cortex activation in kinesthetic guidance of reaching. Exp Brain Res. 179: 607-619.

de Lange FP, Hagoort P, Toni I. 2005. Neural topography and content of movement representations. J Cogn Neurosci. 17: 97-112.

De Valois RL, Albrecht DG, Thorell LG. 1982a. Spatial frequency selectivity of cells in macaque visual cortex. Vision Res. 22: 545-559.

De Valois RL, Yund EW, Hepler N. 1982b. The orientation and direction selectivity of cells in macaque visual cortex. Vision Res. 22: 531-544.

Decety J. 1991. Motor information may be important for updating the cognitive processes involved in mental imagery of movement. European Bulletin of Cognitive Psychology. 4: 415-426.

Decety J, Grezes J, Costes N, Perani D, Jeannerod M, Procyk E, Grassi F, Fazio F. 1997. Brain activity during observation of actions. Influence of action content and subject's strategy. Brain. 120: 1763-1777.

Decety J, Jeannerod M. 1996. Mentally simulated movements in virtual reality: does Fitt's law hold in motor imagery? Behav Brain Res. 72: 127-134.

Decety J, Jeannerod M, Durozard D, Baverel G. 1993. Central activation of autonomic effectors during mental simulation of motor actions in man. J Physiol. 461: 549.

Decety J, Jeannerod M, Germain M, Pastene J. 1991. Vegetative response during imagined movement is proportional to mental effort. Behav Brain Res. 42: 1-5.

Decety J, Jeannerod M, Prablanc C. 1989. The timing of mentally represented actions. Behav Brain Res. 34: 35-42.

Decety J, Michel F. 1989. Comparative analysis of actual and mental movement times in two graphic tasks. Brain Cogn. 11: 87-97.

Decety J, Perani D, Jeannerod M, Bettinardi V, Tadary B, Woods R, Mazziotta JC, Fazio F. 1994. Mapping motor representations with positron emission tomography. Nature. 371: 600-602.

Decety J, Philippon B, Ingvar DH. 1988. rCBF landscapes during motor performance and motor ideation of a graphic gesture. Eur Arch Psychiatr Neurol Sci. 238: 33-38.

Decety J, Sjöholm H, Ryding E, Stenberg G, Ingvar DH. 1990. The cerebellum participates in mental activity: tomographic measurements of regional cerebral blood flow. Brain Res. 535: 313-317.

Deiber M-P, Ibañez V, Honda M, Sadato N, Raman R, Hallett M. 1998. Cerebral processes related to visuomotor imagery and generation of simple finger movements studied with Positron Emission Tomography. Neuroimage. 7: 73-85.

Derrington AM, Lennie P. 1984. Spatial and temporal contrast sensitivities of neurones in lateral geniculate nucleus of macaque. J Physiol. 357: 219-240.

Desimone R, Albright TD, Gross CG, Bruce C. 1984. Stimulus-selective properties of inferior temporal neurons in the macaque. J Neurosci. 4: 2051-2062.

Desimone R, Fleming J, Gross CG. 1980. Prestriate afferents to inferior temporal cortex: an HRP study. Brain Res. 184: 41-55.

Desimone R, Gross CG. 1979. Visual areas in the temporal cortex of the macaque. Brain Res. 178: 363-380.

Desimone R, Schein SJ. 1987. Visual properties of neurons in area V4 of the macaque: sensitivity to stimulus form. J Neurophysiol. 57: 835-868.

Desimone R, Schein SJ, Moran J, Ungerleider LG. 1985. Contour, color and shape analysis beyond the striate cortex. Vision Res. 25: 441-452.

Desimone R, Ungerleider LG. 1986. Multiple visual areas in the caudal superior temporal sulcus of the macaque. J Comp Neurol. 248: 164-189.

DeYoe EA, Van Essen DC. 1985. Segregation of efferent connections and receptive field properties in visual area V2 of the macaque. Nature. 317: 58-61.

DeYoe EA, Van Essen DC. 1988. Concurrent processing streams in monkey visual cortex. Trends Neurosci. 11: 219-226.

Distler C, Boussaoud D, Desimone R, Ungerleider LG. 1993. Cortical connections of inferior temporal area TEO in macaque monkeys. J Comp Neurol. 334: 125-150.

Dow BM, Gouras P. 1973. Color and spatial specificity of single units in Rhesus monkey foveal striate cortex. J Neurophysiol. 36: 79-100.

Dow BM, Snyder AZ, Vautin RG, Bauer R. 1981. Magnification factor and receptive field size in foveal striate cortex of the monkey. Exp Brain Res. 44: 213-228.

Dow BM, Vautin RG, Bauer R. 1985. The mapping of visual space onto foveal striate cortex in the macaque monkey. J Neurosci. 5: 890-902.

Downing PE, Jiang Y, Shuman M, Kanwisher N. 2001. A cortical area selective for visual processing of the human body. Science. 293: 2470-2473.

Dreher B, Fukada Y, Rodieck RW. 1976. Identification, classification and anatomical segregation of cells with X-like and Y-like properties in the lateral geniculate nucleus of old-world primates. J Physiol. 258: 433-452.

Driskell JE, Copper C, Moran A. 1994. Does mental practice enhance performance? J Appl Psychol. 79: 481-492.

Dyde RT, Milner AD. 2002. Two illusions of perceived orientation: One fools all of the people some of the time; the other fools all of the people all of the time. Exp Brain Res. 144: 518-527.

Edwards DP, Purpura KP, Kaplan E. 1995. Contrast sensitivity and spatial frequency response of primate cortical neurons in and around the cytochrome oxidase blobs. Vision Res. 35: 1501-1523.

Elliott D, Khan M. 2010. Vision and Goal-Directed Movement: Neurobehavioral Perspectives: Human Kinetics.

Ettlinger G. 1959. Visual discrimination following successive temporal ablations in monkeys. Brain. 82: 232-250.

Evangeliou MN, Raos V, Galletti C, Savaki HE. 2009. Functional imaging of the parietal cortex during action execution and observation. Cereb Cortex. 19: 624-639.

Farah MJ, Hammond ND, Katherine M, Calvanio R. 1988a. Visual and spatial mental imagery: Dissociable systems of representation. Cognit Psychol. 20: 439-462.

Farah MJ, Levine DN, Calvanio R. 1988b. A case study of mental imagery deficit. Brain Cogn. 8: 147-164.

Farias MF, Gattass R, Pinon MC, Ungerleider LG. 1997. Tangential distribution of cytochrome oxidase-rich blobs in the primary visual cortex of macaque monkeys. J Comp Neurol. 386: 217-228.

Felleman DJ, Burkhalter A, Van Essen DC. 1997a. Cortical connections of areas V3 and VP of macaque monkey extrastriate visual cortex. J Comp Neurol. 379: 21-47.

Felleman DJ, Van Essen DC. 1987. Receptive field properties of neurons in area V3 of macaque monkey extrastriate cortex. J Neurophysiol. 57: 889-920.

Felleman DJ, Van Essen DC. 1991. Distributed hierarchical processing in the primate cerebral cortex. Cereb Cortex. 1: 1-47.

Felleman DJ, Xiao Y, McClendon E. 1997b. Modular organization of occipito-temporal pathways: cortical connections between visual area 4 and visual area 2 and posterior inferotemporal ventral area in macaque monkeys. J Neurosci. 17: 3185-3200.

Fiamenghi GA. 1997. Intersubjectivity and infant-infant interaction: Imitation as a way of making contact. Annual Report, Research and Clinical Center for Child Development. 19: 15-21.

Fiehler K, Burke M, Engel A, Bien S, Rosler F. 2008. Kinesthetic working memory and action control within the dorsal stream. Cereb Cortex. 18: 243-253.

Filimon F, Nelson JD, Hagler DJ, Sereno MI. 2007. Human cortical representations for reaching: mirror neurons for execution, observation, and imagery. Neuroimage. 37: 1315-1328.

Fischer B, Boch R, Bach M. 1981. Stimulus versus eye movements: comparison of neural activity in the striate and prelunate visual cortex (A17 and A19) of trained rhesus monkey. Exp Brain Res. 43: 69-77.

Fishman RS, Karnovsky ML. 1986. Apparent absence of a translocase in the cerebral glucose-6-phosphatase system. J Neurochem. 46: 371-378.

Fitts PM. 1992. The information capacity of the human motor system in controlling the amplitude of movement. J Exp Psychol. 121: 262-269.

Fitzpatrick D, Lund JS, Blasdel GG. 1985. Intrinsic connections of macaque striate cortex: afferent and efferent connections of lamina 4C. J Neurosci. 5: 3329-3349.

Flanagin VL, Wutte M, Glasauer S, Jahn K. 2009. Driving dreams: cortical activations during imagined passive and active whole body movement. Ann NY Acad Sci. 1164: 372-375.

Fletcher PC, Frith CD, Baker SC, Shallice T, Frackowiak RSJ, Dolan RJ. 1995. The mind's eye-precuneus activation in memory-related imagery. Neuroimage. 2: 195-200.

Florence SL, Kaas JH. 1992. Ocular dominance columns in area 17 of Old World macaque and talapoin monkeys: Complete reconstructions and quantitative analyses. Vis Neurosci. 8: 449-462.

Foster KH, Gaska JP, Nagler M, Pollen DA. 1985. Spatial and temporal frequency selectivity of neurones in visual cortical areas V1 and V2 of the macaque monkey. J Physiol. 365: 331-363.

Franz VH, Hesse C, Kollath S. 2009. Visual illusions, delayed grasping, and memory: no shift from dorsal to ventral control. Neuropsychologia. 47: 1518-1531.

Fries W. 1981. The projection from the lateral geniculate nucleus to the prestriate cortex of the macaque monkey. Proc R Soc Lond B Biol Sci. 213: 73-86.

Fries W. 1990. Pontine projection from striate and prestriate visual cortex in the macaque monkey: An anterograde study. Vis Neurosci. 4: 205-216.

Fujita I, Tanaka K, Ito M, Cheng K. 1992. Columns for visual features of objects in monkey inferotemporal cortex. Nature. 360: 343-346.

Gallese V, Fadiga L, Fogassi L, Rizzolatti G. 1996. Action recognition in the premotor cortex. Brain. 119: 593-609.

Gallese V, Goldman A. 1998. Mirror neurons and the simulation theory of mind-reading. Trends Cogn Sci. 2: 493-501.

Galletti C, Battaglini PP. 1989. Gaze-dependent visual neurons in area V3A of monkey prestriate cortex. J Neurosci. 9: 1112-1125.

Galletti C, Battaglini PP, Aicardi G. 1988. 'Real-motion' cells in visual area V2 of behaving macaque monkeys. Exp Brain Res. 69: 279-288.

Galletti C, Battaglini PP, Fattori P. 1990. 'Real-motion' cells in area V3A of macaque visual cortex. Exp Brain Res. 82: 67-76.

Galletti C, Battaglini PP, Fattori P. 1995. Eye position influence on the parieto-occipital area PO (V6) of the macaque monkey. Eur J Neurosci. 7: 2486-2501.

Galletti C, Fattori P, Kutz DF, Battaglini PP. 1997. Arm movement-related neurons in the visual area V6A of the macaque superior parietal lobule. Eur J Neurosci. 9: 410-413.

Galletti C, Fattori P, Kutz DF, Gamberini M. 1999. Brain location and visual topography of cortical area V6A in the macaque monkey. Eur J Neurosci. 11: 575-582.

Galletti C, Squatrito S, Battaglini PP, Grazia Maioli M. 1984. 'Real-motion' cells in the primary visual cortex of macaque monkeys. Brain Res. 301: 95-110.

Gaska JP, Jacobson LD, Pollen DA. 1987. Response suppression by extending sine-wave gratings within the receptive fields of neurons in visual cortical area V3A of the macaque monkey. Vision Res. 27: 1687-1692.

Gaska JP, Jacobson LD, Pollen DA. 1988. Spatial and temporal frequency selectivity of neurons in visual cortical area V3A of the macaque monkey. Vision Res. 28: 1179-1191.

Gattass R, Gross CG, Sandell JH. 1981. Visual topography of V2 in the macaque. J Comp Neurol. 201: 519-539.

Gattass R, Sousa AP, Gross CG. 1988. Visuotopic organization and extent of V3 and V4 of the macaque. J Neurosci. 8: 1831-1845.

Gattass R, Sousa AP, Mishkin M, Ungerleider LG. 1997. Cortical projections of area V2 in the macaque. Cereb Cortex. 7: 110-129.

Gegenfurtner KR, Kiper DC, Fenstemaker SB. 1996. Processing of color, form, and motion in macaque area V2. Vis Neurosci. 13: 161-172.

Gegenfurtner KR, Kiper DC, Levitt JB. 1997. Functional properties of neurons in macaque area V3. J Neurophysiol. 77: 1906-1923.

Gerardin E, Sirigu A, Lehéricy S, Poline JB, Gaymard B, Marsault C, Agid Y, Le Bihan D. 2000. Partially overlapping neural networks for real and imagined hand movements. Cereb Cortex. 10: 1093-1104.

Girard P, Bullier J. 1989. Visual activity in area V2 during reversible inactivation of area 17 in the macaque monkey. J Neurophysiol. 62: 1287-1302.

Girard P, Salin PA, Bullier J. 1991. Visual activity in areas V3a and V3 during reversible inactivation of area V1 in the macaque monkey. J Neurophysiol. 66: 1493-1503.

Glover S. 2002. Visual illusions affect planning but not control. Trends Cogn Sci. 6: 288-292.

Glover S, Dixon P. 2001a. The role of vision in the on-line correction of illusion effects on action. Can J Exp Psychol. 55: 96-103.

Glover SR, Dixon P. 2001b. Dynamic illusion effects in a reaching task: Evidence for separate visual representations in the planning and control of reaching. Journal of Experimental Psychology: Human Perception and Performance. 27: 560-572.

Goldenberg G, Müllbacher W, Nowak A. 1995. Imagery without perception-a case study of anosognosia for cortical blindness. Neuropsychologia. 33: 1373-1382.

Goldenberg G, Steiner M, Podreka I, Deecke L. 1992. Regional cerebral blood flow patterns related to verification of low- and high-imagery sentences. Neuropsychologia. 30: 581-586.

Goodale MA. 1998. Visuomotor control: where does vision end and action begin? Curr Biol. 8: 489-491.

Goodale MA, Humphrey GK. 1998. The objects of action and perception. Cognition. 67: 181-207.

Goodale MA, Jakobson LS, Keillor JM. 1994. Differences in the visual control of pantomimed and natural grasping movements. Neuropsychologia. 32: 1159-1178.

Goodale MA, Milner AD. 1992. Separate visual pathways for perception and action. Trends Neurosci. 15: 20-25.

Goodale MA, Westwood DA, Milner AD. 2004. Two distinct modes of control for object-directed action. Prog Brain Res. 144: 131-144.

Gouras P, Kruger J. 1979. Responses of cells in foveal visual cortex of the monkey to pure color contrast. J Neurophysiol. 42: 850-860.

Grafton ST, Arbib MA, Fadiga L, Rizzolatti G. 1996. Localization of grasp representations in humans by positron emission tomography. 2. Observation compared with imagination. Exp Brain Res. 112: 103-111.

Gregg M, Hall C. 2006. The relationship of skill level and age to the use of imagery by golfers. Journal of Applied Sport Psychology. 18: 363 - 375.

Gregoriou GG, Savaki HE. 2003. When vision guides movement: a functional imaging study of the monkey brain. Neuroimage. 19: 959-967.

Grill-Spector K, Kourtzi Z, Kanwisher N. 2001. The lateral occipital complex and its role in object recognition. Vision Res. 41: 1409-1422.

Grosof DH, Shapley RM, Hawken MJ. 1993. Macaque V1 neurons can signal 'illusory' contours. Nature. 365: 550-552.

Grossman E, Donnelly M, Price R, Pickens D, Morgan V, Neighbor G, Blake R. 2000. Brain areas involved in perception of biological motion. J Cogn Neurosci. 12: 711-720.

Gutierrez C, Cusick CG. 1997. Area V1 in macaque monkeys projects to multiple histochemically defined subdivisions of the inferior pulvinar complex. Brain Res. 765: 349-356.

Hackett TA, Stepniewska I, Kaas JH. 1998. Thalamocortical connections of the parabelt auditory cortex in macaque monkeys. J Comp Neurol. 400: 271-286.

Haffenden AM, Goodale MA. 1998. The effect of pictorial illusion on prehension and perception. J Cogn Neurosci. 10: 122-136.

Haffenden AM, Goodale MA. 2000. Independent effects of pictorial displays on perception and action. Vision Res. 40: 1597-1607.

Haffenden AM, Schiff KC, Goodale MA. 2001. The dissociation between perception and action in the Ebbinghaus illusion: Nonillusory effects of pictorial cues on grasp. Curr Biol. 11: 177-181.

Haggard P, Christakou A, Serino A. 2007. Viewing the body modulates tactile receptive fields. Exp Brain Res. 180: 187-193.

Hallett M, Fieldman J, Cohen LG, Sadato N, Pascual-Leone A. 1994. Involvement of primary motor cortex in motor imagery and mental practice. Behav Brain Sci. 17: 210.

Hammond P. 1981. Simultaneous determination of directional tuning of complex cells in cat striate cortex for bar and for texture motion. Exp Brain Res. 41: 364-369.

Hammond P, MacKay DM. 1977. Differential responsiveness of simple and complex cells in cat striate cortex to visual texture. Exp Brain Res. 30: 275-296.

Hanakawa T, Immisch I, Toma K, Dimyan MA, Van Gelderen P, Hallett M. 2003. Functional properties of brain areas associated with motor execution and imagery. J Neurophysiol. 89: 989-1002.

Hari R, Forss N, Avikainen S, Kirveskari E, Salenius S, Rizzolatti G. 1998. Activation of human primary motor cortex during action observation: a neuromagnetic study. Proc Natl Acad Sci USA. 95: 15061.

Hartje W, Ettlinger G. 1973. Reaching in light and dark after unilateral posterior parietal ablations in the monkey. Cortex. 9: 346-354.

Haxby JV, Hoffman EA, Gobbini MI. 2000. The distributed human neural system for face perception. Trends Cogn Sci. 4: 223-233.

Heath M, Westwood DA. 2003. Can a visual representation support the online control of memory-dependent reaching? Evidence from a variable spatial mapping paradigm. Motor Control. 7: 346-361.

Hebb DO. 1968. Concerning imagery. Psychol Rev. 75: 466-477.

Hendrickson AE. 1985. Dots, stripes and columns in monkey visual cortex. Trends Neurosci. 8: 406-410.

Hendry SH, Reid RC. 2000. The koniocellular pathway in primate vision. Annu Rev Neurosci. 23: 127-153.

Hendry SH, Yoshioka T. 1994. A neurochemically distinct third channel in the macaque dorsal lateral geniculate nucleus. Science. 264: 575-577.

Hesse C, Franz VH. 2009. Memory mechanisms in grasping. Neuropsychologia. 47: 1532-1545.

Heywood CA, Cowey A. 1987. On the role of cortical area V4 in the discrimination of hue and pattern in macaque monkeys. J Neurosci. 7: 2601-2617.

Hicks TP, Lee BB, Vidyasagar TR. 1983. The responses of cells in macaque lateral geniculate nucleus to sinusoidal gratings. J Physiol. 337: 183-200.

Hietanen JK, Perrett DI. 1996. Motion sensitive cells in the macaque superior temporal polysensory area: response discrimination between self-generated and externally generated pattern motion. Behav Brain Res. 76: 155-167.

Himmelbach M, Nau M, Zundorf I, Erb M, Perenin MT, Karnath HO. 2009. Brain activation during immediate and delayed reaching in optic ataxia. Neuropsychologia. 47: 1508-1517.

Hinds OP, Polimeni JR, Blackwell ML, Wiggins CJ, Wiggins G, van der Kouwe AJW, Wald LL, Schwartz EL, Fischl B. 2005. Reconstruction and analysis of human V1 by imaging the stria of Gennari using MRI at 7T. (Abstract, presented at 35th Annual Meeting of the Society for Neuroscience. Abstract number 137.5.).

Hinds OP, Rajendran N, Polimeni JR, Augustinack JC, Wiggins G, Wald LL, Diana Rosas H, Potthast A, Schwartz EL, Fischl B. 2008. Accurate prediction of V1 location from cortical folds in a surface coordinate system. NeuroImage. 39: 1585-1599.

Horton JC. 1984. Cytochrome oxidase patches: a new cytoarchitectonic feature of monkey visual cortex. Philos Trans R Soc Lond B Biol Sci. 304: 199-253.

Horton JC, Hedley-Whyte ET. 1984. Mapping of cytochrome oxidase patches and ocular dominance columns in human visual cortex. Philos Trans R Soc Lond B Biol Sci. 304: 255-272.

Horton JC, Hubel DH. 1981. Regular patchy distribution of cytochrome oxidase staining in primary visual cortex of macaque monkey. Nature. 292: 762-764.

Hu Y, Eagleson R, Goodale MA. 1999. The effects of delay on the kinematics of grasping. Exp Brain Res. 126: 109-116.

Hu Y, Goodale MA. 2000. Grasping after a delay shifts size-scaling from absolute to relative metrics. J Cogn Neurosci. 12: 856-868.

Hubel DH, Livingstone MS. 1987. Segregation of form, color, and stereopsis in primate area 18. J Neurosci. 7: 3378-3415.

Hubel DH, Wiesel TN. 1962. Receptive fields, binocular interaction and functional architecture in the cat's visual cortex. J Physiol. 160: 106-154.

Hubel DH, Wiesel TN. 1965. Receptive fields and functional architecture in two nonstriate visual areas (18 and 19) of the cat. J Neurophysiol. 28: 229-289.

Hubel DH, Wiesel TN. 1968. Receptive fields and functional architecture of monkey striate cortex. J Physiol. 195: 215-243.

Hubel DH, Wiesel TN. 1970. Stereoscopic vision in macaque monkey. Cells sensitive to binocular depth in area 18 of the macaque monkey cortex. Nature. 225: 41-42.

Hubel DH, Wiesel TN. 1972. Laminar and columnar distribution of geniculo-cortical fibers in the macaque monkey. J Comp Neurol. 146: 421-450.

Hubel DH, Wiesel TN. 1974. Uniformity of monkey striate cortex: a parallel relationship between field size, scatter, and magnification factor. J Comp Neurol. 158: 295-305.

Hubel DH, Wiesel TN, Stryker MP. 1978. Anatomical demonstration of orientation columns in macaque monkey. J Comp Neurol. 177: 361-380.

Humphrey NK, Weiskrantz L. 1967. Vision in monkeys after removal of the striate cortex. Nature. 215: 595-597.

Huttenlocher J, Higgins ET, Clark HH. 1972. On reasoning, congruence, and other matters. Psychol Rev. 79: 420-427.

Iseki K, Hanakawa T, Shinozaki J, Nankaku M, Fukuyama H. 2008. Neural mechanisms involved in mental imagery and observation of gait. Neuroimage. 41: 1021-1031.

Ishai A, Haxby JV, Ungerleider LG. 2002. Visual imagery of famous faces: effects of memory and attention revealed by fMRI. Neuroimage. 17: 1729-1741.

Ishizu T, Noguchi A, Ito Y, Ayabe T, Kojima S. 2009. Motor activity and imagery modulate the body-selective region in the occipital-temporal area: a near-infrared spectroscopy study. Neurosci Lett. 465: 85-89.

Issa NP, Trachtenberg JT, Chapman B, Zahs KR, Stryker MP. 1999. The critical period for ocular dominance plasticity in the Ferret's visual cortex. J Neurosci. 19: 6965-6978.

Jankowiak J, Kinsbourne M, Shalev RS, Bachman DL. 1992. Preserved visual imagery and categorization in a case of associative visual agnosia. J Cogn Neurosci. 4: 119-131.

Jeannerod M. 1986. Mechanisms of visuomotor coordination: a study in normal and brain-damaged subjects. Neuropsychologia. 24: 41-78.

Jeannerod M. 1994. The representing brain: Neural correlates of motor intention and imagery. Behav Brain Sci. 17: 187-202.

Jeannerod M. 1995. Mental imagery in the motor context. Neuropsychologia. 33: 1419-1432.

Jeannerod M. 1997. The cognitive neuroscience of action. Oxford: Blackwell Publishers

Jeannerod M. 2001. Neural simulation of action: a unifying mechanism for motor cognition. Neuroimage. 14: 103-109.

Jeannerod M. 2004. Visual and action cues contribute to the self-other distinction. Nat Neurosci. 7: 422-423.

Jeannerod M. 2006. Motor cognition: What actions tell the self: Oxford University Press, USA.

Johnson SH. 2000. Thinking ahead: the case for motor imagery in prospective judgements of prehension. Cognition. 74: 33-70.

Kanwisher N, McDermott J, Chun MM. 1997. The fusiform face area: a module in human extrastriate cortex specialized for face perception. J Neurosci. 17: 4302-4311.

Kaplan E, Shapley RM. 1982. X and Y cells in the lateral geniculate nucleus of macaque monkeys. J Physiol. 330: 125-143.

Kayama Y, Riso RR, Bartlett JR, Doty RW. 1979. Luxotonic responses of units in macaque striate cortex. J Neurophysiol. 42: 1495-1517.

Kennedy C, Sakurada O, Shinohara M, Jehle J, Sokoloff L. 1978. Local cerebral glucose utilization in the normal conscious macaque monkey. Ann Neurol. 4: 293-301.

Kennedy H, Bullier J. 1985. A double-labeling investigation of the afferent connectivity to cortical areas V1 and V2 of the macaque monkey. J Neurosci. 5: 2815-2830.

Kiper DC, Fenstemaker SB, Gegenfurtner KR. 1997. Chromatic properties of neurons in macaque area V2. Vis Neurosci. 14: 1061-1072.

Kluver H. 1941. Visual functions after removal of the occipital lobes. J Psychol. 11: 23-45.

Kosslyn SM, Alpert NM, Thompson WL, Maljkovic V, Weise SB, Chabris CF, Hamilton SE, Rauch SL, Buonanno FS. 1993. Visual mental imagery activates topographically organized visual cortex: PET investigations. J Cogn Neurosci. 5: 263-287.

Kosslyn SM, Ball TM, Reiser BJ. 1978. Visual images preserve metric spatial information: evidence from studies of image scanning. J Exp Psychol Hum Percept Perform. 4: 47-60.

Kosslyn SM, Ganis G, Thompson WL. 2006a. Mental imagery and the human brain: In Q. Jing, M. R. Rosenzweig, G. d'Ydewalle, H. Zhang, H-C. Chen, & K. Zhang (Eds.), Progress in psychological science around the world, vol 1: Neural, cognitive and developmental issues. New York: Psychology Press (pp 195-209).

Kosslyn SM, Pascual-Leone A, Felician O, Camposano S, Keenan JP, Thompson WL, Ganis G, Sukel KE, Alpert NM. 1999a. The role of area 17 in visual imagery: convergent evidence from PET and rTMS. Science. 284: 167-170.

Kosslyn SM, Shin LM, Thompson WL, McNally RJ, Rauch SL, Pitman RK, Alpert NM. 1996. Neural effects of visualizing and perceiving aversive stimuli: a PET investigation. Neuroreport. 7: 1569-1576.

Kosslyn SM, Sukel KE, Bly BM. 1999b. Squinting with the mind's eye: effects of stimulus resolution on imaginal and perceptual comparisons. Memory & cognition. 27: 276.

Kosslyn SM, Thompson WL. 2003. When is early visual cortex activated during visual mental imagery? Psychol Bull. 129: 723-746.

Kosslyn SM, Thompson WL, Alpert NM. 1997. Neural systems shared by visual imagery and visual perception: a positron emission tomography study. Neuroimage. 6: 320-334.

Kosslyn SM, Thompson WL, Ganis G. 2006b. The case for mental imagery: Oxford University Press, USA.

Kosslyn SM, Thompson WL, Kim IJ, Alpert NM. 1995. Topographical representations of mental images in primary visual cortex. Nature. 378: 496-498.

Kourtzi Z, Kanwisher N. 2000. Activation in human MT/MST by static images with implied motion. J Cogn Neurosci. 12: 48-55.

Kourtzi Z, Kanwisher N. 2001. Representation of perceived object shape by the human lateral occipital complex. Science. 293: 1506-1509.

Krubitzer L, Kaas J. 1990. Convergence of processing channels in the extrastriate cortex of monkeys. Vis Neurosci. 5: 609-613.

Krubitzer LA, Kaas JH. 1993. The dorsomedial visual area of owl monkeys: connections, myeloarchitecture, and homologies in other primates. J Comp Neurol. 334: 497-528.

Kruger J, Gouras P. 1980. Spectral selectivity of cells and its dependence on slit length in monkey visual cortex. J Neurophysiol. 43: 1055-1069.

Kugiumutzakis G. 1998. Neonatal imitation in the intersubjective companion space. In Intersubjective Communication and Emotion in Early Ontogeny (ed. S. Braten). Cambridge: Cambridge University Press. .

Kuljis RO, Rakic P. 1990. Hypercolumns in primate visual cortex can develop in the absence of cues from photoreceptors. Proc Natl Acad Sci USA. 87: 5303-5306.

Lachica EA, Beck PD, Casagrande VA. 1992. Parallel pathways in macaque monkey striate cortex: anatomically defined columns in layer III. Proc Natl Acad Sci USA. 89: 3566-3570.

Lambert S, Sampaio E, Scheiber C, Mauss Y. 2002. Neural substrates of animal mental imagery: calcarine sulcus and dorsal pathway involvement-an fMRI study. Brain Res. 924: 176-183.

Lamme VA. 1995. The neurophysiology of figure-ground segregation in primary visual cortex. J Neurosci. 15: 1605-1615.

Lamotte RH, Acuna C. 1978. Defects in accuracy of reaching after removal of posterior parietal cortex in monkeys. Brain Res. 139: 309-326.

Le Bihan D, Turner R, Zeffiro TA, Cuenod CA, Jezzard P, Bonnerot V. 1993a. Activation of human primary visual cortex during visual recall: a magnetic resonance imaging study. Proc Natl Acad Sci USA. 90: 11802.

Le Bihan D, Turner R, Zeffiro TA, Cuenod CA, Jezzard P, Bonnerot V. 1993b. Activation of human primary visual cortex during visual recall: a magnetic resonance imaging study. Proc Natl Acad Sci USA. 90: 11802-11805.

Lemay M, Proteau L. 2002. Effects of target presentation time, recall delay, and aging on the accuracy of manual pointing to remembered targets. J Mot Behav. 34: 11-23.

LeVay S, Connolly M, Houde J, Van Essen DC. 1985. The complete pattern of ocular dominance stripes in the striate cortex and visual field of the macaque monkey. J Neurosci. 5: 486-501.

Leventhal AG, Rodieck RW, Dreher B. 1981. Retinal ganglion cell classes in the old world monkey: morphology and central projections. Science. 213: 1139-1142.

Levine DN, Warach J, Farah M. 1985. Two visual systems in mental imagery: dissociation of "what" and "where" in imagery disorders due to bilateral posterior cerebral lesions. Neurology. 35: 1010-1018.

Levitt JB, Kiper DC, Movshon JA. 1994a. Receptive fields and functional architecture of macaque V2. J Neurophysiol. 71: 2517-2542.

Levitt JB, Yoshioka T, Lund JS. 1994b. Intrinsic cortical connections in macaque visual area V2: evidence for interaction between different functional streams. J Comp Neurol. 342: 551-570.

Levitt JB, Yoshioka T, Lund JS. 1995. Connections between the pulvinar complex and cytochrome oxidase-defined compartments in visual area V2 of macaque monkey. Exp Brain Res. 104: 419-430.

Lin CS, Weller RE, Kaas JH. 1982. Cortical connections of striate cortex in the owl monkey. J Comp Neurol. 211: 165-176.

Liu J, Wandell BA. 2005. Specializations for chromatic and temporal signals in human visual cortex. J Neurosci. 25: 3459-3468.

Livingstone M, Hubel D. 1988. Segregation of form, color, movement, and depth: anatomy, physiology, and perception. Science. 240: 740-749.

Livingstone MS, Hubel DH. 1983. Specificity of cortico-cortical connections in monkey visual system. Nature. 304: 531-534.

Livingstone MS, Hubel DH. 1984. Anatomy and physiology of a color system in the primate visual cortex. J Neurosci. 4: 309-356.

Livingstone MS, Hubel DH. 1987. Connections between layer 4B of area 17 and the thick cytochrome oxidase stripes of area 18 in the squirrel monkey. J Neurosci. 7: 3371-3377.

Lotze M, Montoya P, Erb M, Hulsmann E, Flor H, Klose U, Birbaumer N, Grodd W. 1999. Activation of cortical and cerebellar motor areas during executed and imagined hand movements: an fMRI study. J Cogn Neurosci. 11: 491-501.

Lund JS. 1973. Organization of neurons in the visual cortex, area 17, of the monkey (Macaca mulatta). J Comp Neurol. 147: 455-496.

Lund JS, Boothe RG. 1975. Interlaminar connections and pyramidal neuron organisation in the visual cortex, area 17, of the macaque monkey. J Comp Neurol. 159: 305-334.

Lund JS, Hendrickson AE, Ogren MP, Tobin EA. 1981. Anatomical organization of primate visual cortex area VII. J Comp Neurol. 202: 19-45.

Lund JS, Lund RD, Hendrickson AE, Bunt AH, Fuchs AF. 1975. The origin of efferent pathways from the primary visual cortex, area 17, of the macaque monkey as shown by retrograde transport of horseradish peroxidase. J Comp Neurol. 164: 287-303.

Luppino G, Hamed SB, Gamberini M, Matelli M, Galletti C. 2005. Occipital (V6) and parietal (V6A) areas in the anterior wall of the parieto-occipital sulcus of the macaque: a cytoarchitectonic study. Eur J Neurosci. 21: 3056-3076.

Lyon DC, Kaas JH. 2001. Connectional and architectonic evidence for dorsal and ventral V3, and dorsomedial area in marmoset monkeys. J Neurosci. 21: 249-261.

Lyon DC, Kaas JH. 2002. Evidence for a modified V3 with dorsal and ventral halves in macaque monkeys. Neuron. 33: 453-461.

Maguire WM, Baizer JS. 1984. Visuotopic organization of the prelunate gyrus in rhesus monkey. J Neurosci. 4: 1690-1704.

Mahoney MJ, Avener M. 1977. Psychology of the elite athlete: An exploratory study. Cognit Ther Res. 1: 135-141.

Marcus DS, Van Essen DC. 2002. Scene segmentation and attention in primate cortical areas V1 and V2. J Neurophysiol. 88: 2648-2658.

Marr D. 1982. Vision: A Computational Investigation into the Human Representation and Processing of Visual Information: Henry Holt and Co., Inc.

Martin KAC. 1992. Parallel pathways converge. Curr Biol. 2: 555-557.

Matelli M, Govoni P, Galletti C, Kutz DF, Luppino G. 1998. Superior area 6 afferents from the superior parietal lobule in the macaque monkey. J Comp Neurol. 402: 327-352.

Maunsell JH, van Essen DC. 1983. The connections of the middle temporal visual area (MT) and their relationship to a cortical hierarchy in the macaque monkey. J Neurosci. 3: 2563-2586.

Maunsell JH, Van Essen DC. 1987. Topographic organization of the middle temporal visual area in the macaque monkey: representational biases and the relationship to callosal connections and myeloarchitectonic boundaries. J Comp Neurol. 266: 535-555.

McKeefry DJ, Burton MP, Morland AB. 2010. The contribution of human cortical area V3A to the perception of chromatic motion: a transcranial magnetic stimulation study. Eur J Neurosci. 31: 575-584.

Mellet E, Tzourio-Mazoyer N, Bricogne S, Mazoyer B, Kosslyn SM, Denis M. 2000. Functional anatomy of high-resolution visual mental imagery. J Cogn Neurosci. 12: 98-109.

Mellet E, Tzourio N, Crivello F, Joliot M, Denis M, Mazoyer B. 1996. Functional anatomy of spatial mental imagery generated from verbal instructions. J Neurosci. 16: 6504-6512.

Mellet E, Tzourio N, Denis M, Mazoyer B. 1995. A positron emission tomography study of visual and mental spatial exploration. J Cogn Neurosci. 7: 433-445.

Merigan WH, Maunsell JH. 1993. How parallel are the primate visual pathways? Annu Rev Neurosci. 16: 369-402.

Merigan WH, Nealey TA, Maunsell JH. 1993. Visual effects of lesions of cortical area V2 in macaques. J Neurosci. 13: 3180-3191.

Michael CR. 1981. Columnar organization of color cells in monkey's striate cortex. J Neurophysiol. 46: 587-604.

Milner AD, Goodale MA. 1995. The Visual Brain in Action. New York: Oxford University Press.

Milner D, Dyde R. 2003. Why do some perceptual illusions affect visually guided action, when others don't? Trends Cogn Sci. 7: 10-11.

Milton J, Solodkin A, Hlustik P, Small SL. 2007. The mind of expert motor performance is cool and focused. Neuroimage. 35: 804-813.

Mishkin M, Ungerleider LG, Macko KA. 1983. Object vision and spatial vision: Two cortical pathways. Trends Neurosci. 6: 414-417.

Mizuno N, Uchida K, Nomura S, Nakamura Y, Sugimoto T, Uemura-Sumi M. 1981. Extrageniculate projections to the visual cortex in the macaque monkey: an HRP study. Brain Res. 212: 454-459.

Moschovakis AK, Gregoriou GG, Ugolini G, Doldan M, Graf W, Guldin W, Hadjidimitrakis K, Savaki HE. 2004. Oculomotor areas of the primate frontal lobes: A transneuronal transfer of rabies virus and [14C]-2-Deoxyglucose functional imaging study. J Neurosci. 24: 5726-5740.

Moscovitch M, Behrmann M, Winocur G. 1994. Do PETS have long or short ears? Mental imagery and neuroimaging. Trends Neurosci. 17: 292-294.

Mountcastle VB. 1957. Modality and topographic properties of single neurons of cat's somatic sensory cortex. J Neurophysiol. 20: 408-434.

Mountcastle VB. 1997. The columnar organization of the neocortex. Brain. 120: 701-722.

Moutoussis K, Keliris G, Kourtzi Z, Logothetis N. 2005. A binocular rivalry study of motion perception in the human brain. Vision Res. 45: 2231-2243.

Moutoussis K, Zeki S. 2002. Responses of spectrally selective cells in macaque area V2 to wavelengths and colors. J Neurophysiol. 87: 2104-2112.

Nagy E, Molnar P. 2004. Homo imitans or homo provocans? Human imprinting model of neonatal imitation. Infant Behav Dev. 27: 54-63.

Nakamura H, Gattass R, Desimone R, Ungerleider LG. 1993. The modular organization of projections from areas V1 and V2 to areas V4 and TEO in macaques. J Neurosci. 13: 3681-3691.

Nakamura H, Kuroda T, Wakita M, Kusunoki M, Kato A, Mikami A, Sakata H, Itoh K. 2001. From three-dimensional space vision to prehensile hand movements: the lateral intraparietal area links the area V3A and the anterior intraparietal area in macaques. J Neurosci. 21: 8174-8187.

Nakamura K, Colby CL. 2000. Visual, saccade-related, and cognitive activation of single neurons in monkey extrastriate area V3A. J Neurophysiol. 84: 677-692.

Nealey TA, Maunsell JH. 1994. Magnocellular and parvocellular contributions to the responses of neurons in macaque striate cortex. J Neurosci. 14: 2069-2079.

Nelson T, Kaufman EE, Sokoloff L. 1984. 2-Deoxyglucose incorporation into rat brain glycogen during measurement of local cerebral glucose utilization by the 2-deoxyglucose method. J Neurochem. 43: 949-956.

Newsome WT, Allman JM. 1980. Interhemispheric connections of visual cortex in the owl monkey, Aotus trivirgatus, and the bushbaby, Galago senegalensis. J Comp Neurol. 194: 209-233.

Newsome WT, Maunsell JH, Van Essen DC. 1986. Ventral posterior visual area of the macaque: visual topography and areal boundaries. J Comp Neurol. 252: 139-153.

Newsome WT, Wurtz RH, Dursteler MR, Mikami A. 1985. Deficits in visual motion processing following ibotenic acid lesions of the middle temporal visual area of the macaque monkey. J Neurosci. 5: 825-840.

O'Kusky J, Colonnier M. 1982. A laminar analysis of the number of neurons, glia, and synapses in the adult cortex (area 17) of adult macaque monkeys. J Comp Neurol. 210: 278-290.

Obermayer K, Blasdel GG. 1993. Geometry of orientation and ocular dominance columns in monkey striate cortex. J Neurosci. 13: 4114-4129.

Ogren MP, Hendrickson AE. 1977. The distribution of pulvinar terminals in visual areas 17 and 18 of the monkey. Brain Res. 137: 343-350.

Olavarria JF, Van Essen DC. 1997. The global pattern of cytochrome oxidase stripes in visual area V2 of the macaque monkey. Cereb Cortex. 7: 395-404.

Orban GA, Fize D, Peuskens H, Denys K, Nelissen K, Sunaert S, Todd J, Vanduffel W. 2003. Similarities and differences in motion processing between the human and macaque brain: evidence from fMRI. Neuropsychologia. 41: 1757-1768.

Orban GA, Kennedy H, Bullier J. 1986. Velocity sensitivity and direction selectivity of neurons in areas V1 and V2 of the monkey: influence of eccentricity. J Neurophysiol. 56: 462-480.

Orban GA, Van Calenbergh F, De Bruyn B, Maes H. 1985. Velocity discrimination in central and peripheral visual field. J Opt Soc Am A. 2: 1836-1847.

Paccalin C, Jeannerod M. 2000. Changes in breathing during observation of effortful actions. Brain Res. 862: 194-200.

Paivio A. 1975. Imagery and long-term memory. Studies in Long Term Memory. 57-85.

Palmer LA, Rosenquist AC, Tusa RJ. 1978. The retinotopic organization of lateral suprasylvian visual areas in the cat. J Comp Neurol. 177: 237-256.

Papaxanthis C, Pozzo T, Kasprinski R, Berthoz A. 2003. Comparison of actual and imagined execution of whole-body movements after a long exposure to microgravity. Neurosci Lett. 339: 41-44.

Papaxanthis C, Pozzo T, Skoura X, Schieppati M. 2002a. Does order and timing in performance of imagined and actual movements affect the motor imagery process? The duration of walking and writing task. Behav Brain Res. 134: 209-215.

Papaxanthis C, Schieppati M, Gentili R, Pozzo T. 2002b. Imagined and actual arm movements have similar durations when performed under different conditions of direction and mass. Exp Brain Res. 143: 447-452.

Parsons LM. 1994. Temporal and kinematic properties of motor behavior reflected in mentally simulated action. Journal of Experimental Psychology: Human Perception and Performance. 20: 709-730.

Pavani F, Boscagli I, Benvenuti F, Rabuffetti M, Farne A. 1999. Are perception and action affected differently by the Titchener circles illusion? Exp Brain Res. 127: 95-101.

Peelen MV, Downing PE. 2005. Selectivity for the human body in the fusiform gyrus. J Neurophysiol. 93: 603-608.

Peelen MV, Downing PE. 2007. The neural basis of visual body perception. Nat Rev Neurosci. 8: 636-648.

Perenin MT, Jeannerod M. 1975. Residual vision in cortically blind hemiphields. Neuropsychologia. 13: 1-7.

Perenin MT, Rossetti Y. 1996. Grasping without form discrimination in a hemianopic field. Neuroreport. 7: 793-797.

Perkel DJ, Bullier J, Kennedy H. 1986. Topography of the afferent connectivity of area 17 in the macaque monkey: a double-labelling study. J Comp Neurol. 253: 374-402.

Perry VH, Oehler R, Cowey A. 1984. Retinal ganglion cells that project to the dorsal lateral geniculate nucleus in the macaque monkey. Neuroscience. 12: 1101-1123.

Peterhans E, von der Heydt R. 1989. Mechanisms of contour perception in monkey visual cortex. II. Contours bridging gaps. J Neurosci. 9: 1749-1763.

Peterhans E, von der Heydt R. 1993. Functional organization of area V2 in the alert macaque. Eur J Neurosci. 5: 509-524.

Petersen SE, Baker JF, Allman JM. 1980. Dimensional selectivity of neurons in the dorsolateral visual area of the owl monkey. Brain Res. 197: 507-511.

Petersen SE, Robinson DL, Keys W. 1985. Pulvinar nuclei of the behaving rhesus monkey: visual responses and their modulation. J Neurophysiol. 54: 867-886.

Petrides M, Pandya DN. 1984. Projections to the frontal cortex from the posterior parietal region in the rhesus monkey. J Comp Neurol. 228: 105-116.

Petrides M, Pandya DN. 1999. Dorsolateral prefrontal cortex: comparative cytoarchitectonic analysis in the human and the macaque brain and corticocortical connection patterns. Eur J Neurosci. 11: 1011-1036.

Pinon MC, Gattass R, Sousa AP. 1998. Area V4 in Cebus monkey: extent and visuotopic organization. Cereb Cortex. 8: 685-701.

Poggio GF, Doty RW, Jr., Talbot WH. 1977. Foveal striate cortex of behaving monkey: single-neuron responses to square-wave gratings during fixation of gaze. J Neurophysiol. 40: 1369-1391.

Poggio GF, Fischer B. 1977. Binocular interaction and depth sensitivity in striate and prestriate cortex of behaving rhesus monkey. J Neurophysiol. 40: 1392-1405.

Poggio GF, Gonzalez F, Krause F. 1988. Stereoscopic mechanisms in monkey visual cortex: binocular correlation and disparity selectivity. J Neurosci. 8: 4531-4550.

Poggio GF, Talbot WH. 1981. Mechanisms of static and dynamic stereopsis in foveal cortex of the rhesus monkey. J Physiol. 315: 469-492.

Pohl W. 1973. Dissociation of spatial discrimination deficits following frontal and parietal lesions in monkeys. J Comp Physiol Psychol. 82: 227-239.

Porro CA, Cettolo V, Francescato MP, Baraldi P. 2000. Ipsilateral involvement of primary motor cortex during motor imagery. Eur J Neurosci. 12: 3059-3063.

Porro CA, Francescato MP, Cettolo V, Diamond ME, Baraldi P, Zuiani C, Bazzocchi M, di Prampero PE. 1996. Primary motor and sensory cortex activation during motor

performance and motor imagery: a functional magnetic resonance imaging study. J Neurosci. 16: 7688-7698.

Previc FH. 1990. Functional specialization in the lower and upper visual fields in humans: Its ecological origins and neurophysiological implications. Behav Brain Sci. 13: 519-575.

Previc FH. 1998. The neuropsychology of 3-D space. Psychol Bull. 124: 123-164.

Purves D, LaMantia AS. 1990. Numbers of "blobs" in the primary visual cortex of neonatal and adult monkeys. Proc Natl Acad Sci USA. 87: 5764-5767.

Pylyshyn Z. 2003. Return of the mental image: are there really pictures in the brain? Trends Cogn Sci. 7: 113-118.

Pylyshyn ZW. 1973. What the mind's eye tells the mind's brain: A critique of mental imagery. Psychol Bull. 80: 1-24.

Pylyshyn ZW. 2002. Mental imagery: in search of a theory. Behav Brain Sci. 25: 157-182; discussion 182-237.

Rao SM, Binder JR, Bandettini PA, Hammeke TA, Yetkin FZ, Jesmanowicz A, Lisk LM, Morris GL, Mueller WM, Estkowski LD. 1993. Functional magnetic resonance imaging of complex human movements. Neurology. 43: 2311-2318.

Raos V, Evangeliou MN, Savaki HE. 2004. Observation of action: grasping with the mind's hand. Neuroimage. 23: 193-201.

Raos V, Evangeliou MN, Savaki HE. 2007. Mental simulation of action in the service of action perception. J Neurosci. 27: 12675-12683.

Riddoch MJ, Humphreys GW. 1987. A case of integrative visual agnosia Brain. 110: 1431-1462.

Rizzolatti G, Fadiga L, Gallese V, Fogassi L. 1996. Premotor cortex and the recognition of motor actions. Brain Res Cogn Brain Res. 3: 131-141.

Rockland KS. 1985. A reticular pattern of intrinsic connections in primate area V2 (area 18). J Comp Neurol. 235: 467-478.

Rockland KS, Pandya DN. 1979. Laminar origins and terminations of cortical connections of the occipital lobe in the rhesus monkey. Brain Res. 179: 3-20.

Rockland KS, Pandya DN. 1981. Cortical connections of the occipital lobe in the rhesus monkey: interconnections between areas 17, 18, 19 and the superior temporal sulcus. Brain Res. 212: 249-270.

Rodman HR, Gross CG, Albright TD. 1989. Afferent basis of visual response properties in area MT of the macaque. I. Effects of striate cortex removal. J Neurosci. 9: 2033-2050.

Roe AW, Ts'o DY. 1995. Visual topography in primate V2: multiple representation across functional stripes. J Neurosci. 15: 3689-3715.

Roe AW, Ts'o DY. 1999. Specificity of color connectivity between primate V1 and V2. J Neurophysiol. 82: 2719-2730.

Roland PE, Eriksson L, Stone-Elander S, Widen L. 1987. Does mental activity change the oxidative metabolism of the brain? J Neurosci. 7: 2373-2389.

Roland PE, Gulyas B. 1994. Visual imagery and visual representation. Trends Neurosci. 17: 281-287.

Romanski LM, Giguere M, Bates JF, Goldman-Rakic PS. 1997. Topographic organization of medial pulvinar connections with the prefrontal cortex in the rhesus monkey. J Comp Neurol. 379: 313-332.

Rosa MG, Pinon MC, Gattass R, Sousa AP. 2000. "Third tier" ventral extrastriate cortex in the New World monkey, Cebus apella. Exp Brain Res. 132: 287-305.

Rosenbaum DA, Loukopoulos LD, Meulenbroek RGJ, Vaughan J, Engelbrecht SE. 1995. Planning reaches by evaluating stored postures. Psychol Rev. 102: 28-66.

Roth M, Decety J, Raybaudi M, Massarelli R, Delon-Martin C, Segebarth C, Morand S, Gemignani A, Décorps M, Jeannerod M. 1996. Possible involvement of primary motor cortex in mentally simulated movement: a functional magnetic resonance imaging study. Neuroreport. 7: 1280.

Roy AC, Paulignan Y, Farne A, Jouffrais C, Boussaoud D. 2000. Hand kinematics during reaching and grasping in the macaque monkey. Behav Brain Res. 117: 75-82.

Ryding E, Decety J, Sjöholm H, Stenberg G, Ingvar DH. 1993. Motor imagery activates the cerebellum regionally. A SPECT rCBF study with 99mTc-HMPAO. Brain Res Cogn Brain Res. 1: 94-99.

Sabbah P, Simond G, Levrier O, Habib M, Trabaud V, Murayama N, Mazoyer BM, Briant JF, Raybaud C, Salamon G. 1995. Functional magnetic resonance imaging at 1.5 T during sensorimotor and cognitive task. European Neurology. 35: 131-136.

Sadato N, Pascual-Leone A, Grafman J, Ibanez V, Deiber MP, Dold G, Hallett M. 1996. Activation of the primary visual cortex by Braille reading in blind subjects. Nature. 380: 526-528.

Sakai K, Miyashita Y. 1994. Visual imagery: an interaction between memory retrieval and focal attention. Trends Neurosci. 17: 287-289.

Sakata H, Taira M, Kusunoki M, Murata A, Tanaka Y. 1997. The TINS Lecture. The parietal association cortex in depth perception and visual control of hand action. Trends Neurosci. 20: 350-357.

Saleem K, Logothetis N. 2007. A combined MRI and histology atlas of the rhesus monkey brain in stereotaxic coordinates. London, UK: Academic Press.

Sathian K, Zangaladze A. 2002. Feeling with the mind's eye: contribution of visual cortex to tactile perception. Behav Brain Res. 135: 127-132.

Savaki HE, Gregoriou GG, Bakola S, Raos V, Moschovakis AK. 2010. The place code of saccade metrics in the lateral bank of the intraparietal sulcus. J Neurosci. 30: 1118-1127.

Savaki HE, Kennedy C, Sokoloff L, Mishkin M. 1993. Visually guided reaching with the forelimb contralateral to a "blind" hemisphere: a metabolic mapping study in monkeys. J Neurosci. 13: 2772-2789.

Savaki HE, Raos VC, Dalezios Y. 1997. Spatial cortical patterns of metabolic activity in monkeys performing a visually guided reaching task with one forelimb. Neuroscience. 76: 1007-1034.

Saxe R, Jamal N, Powell L. 2006. My body or yours? The effect of visual perspective on cortical body representations. Cereb Cortex. 16: 178-182.

Schein SJ, Desimone R. 1990. Spectral properties of V4 neurons in the macaque. J Neurosci. 10: 3369-3389.

Schein SJ, Marrocco RT, de Monasterio FM. 1982. Is there a high concentration of color-selective cells in area V4 of monkey visual cortex? J Neurophysiol. 47: 193-213.

Schiller PH, Finlay BL, Volman SF. 1976. Quantitative studies of single-cell properties in monkey striate cortex. III. Spatial frequency. J Neurophysiol. 39: 1334-1351.

Schiller PH, Malpeli JG. 1978. Functional specificity of lateral geniculate nucleus laminae of the rhesus monkey. J Neurophysiol. 41: 788-797.

Schmid MC, Panagiotaropoulos T, Augath MA, Logothetis NK, Smirnakis SM. 2009. Visually driven activation in macaque areas V2 and V3 without input from the primary visual cortex. PLoS One. 4: e5527.

Schwarzlose RF, Baker CI, Kanwisher N. 2005. Separate face and body selectivity on the fusiform gyrus. J Neurosci. 25: 11055-11059.

Segal SJ, Fusella V. 1970. Influence of imaged pictures and sounds on detection of visual and auditory signals. J Exp Psychol. 83: 458-464.

Selemon LD, Goldman-Rakic PS. 1988. Common cortical and subcortical targets of the dorsolateral prefrontal and posterior parietal cortices in the rhesus monkey: evidence for a distributed neural network subserving spatially guided behavior. J Neurosci. 8: 4049-4068.

Seltzer B, Pandya DN. 1978. Afferent cortical connections and architectonics of the superior temporal sulcus and surrounding cortex in the rhesus monkey. Brain Res. 149: 1-24.

Servos P, Goodale MA, Humphrey GK. 1993. The drawing of objects by a visual form agnosic: contribution of surface properties and memorial representations. Neuropsychologia. 31: 251-259.

Sharma N, Pomeroy VM, Baron JC. 2006. Motor imagery: a backdoor to the motor system after stroke? Stroke. 37: 1941-1952.

Shepard RN, Metzler J. 1971. Mental rotation of three-dimensional objects. Science. 171: 701-703.

Sherman SM, Wilson JR, Kaas JH, Webb SV. 1976. X- and Y-Cells in the Dorsal Lateral Geniculate Nucleus of the Owl Monkey (Aotus trivirgatus). Science. 192: 475-477.

Shipp S. 1995. Visual processing. The odd couple. Curr Biol. 5: 116-119.

Shipp S. 2002. Fundamentals of association cortex. In Cortical areas: unity and diversity (ed A Schuez & R Miller), pp 387- 422 London: Taylor & Francis.

Shipp S. 2006. Parallel Visual Pathways. ACNR. 6: 21-23.

Shipp S, Blanton M, Zeki S. 1998. A visuo-somatomotor pathway through superior parietal cortex in the macaque monkey: cortical connections of areas V6 and V6A. Eur J Neurosci. 10: 3171-3193.

Shipp S, Watson JD, Frackowiak RS, Zeki S. 1995. Retinotopic maps in human prestriate visual cortex: the demarcation of areas V2 and V3. Neuroimage. 2: 125-132.

Shipp S, Zeki S. 1985. Segregation of pathways leading from area V2 to areas V4 and V5 of macaque monkey visual cortex. Nature. 315: 322-325.

Shipp S, Zeki S. 1989a. The organization of connections between areas V5 and V1 in macaque monkey visual cortex. Eur J Neurosci. 1: 309-332.

Shipp S, Zeki S. 1989b. The organization of connections between areas V5 and V2 in macaque monkey visual cortex. Eur J Neurosci. 1: 333-354.

Shipp S, Zeki S. 2002a. The functional organization of area V2. I. Specialization across stripes and layers. Vis Neurosci 19: 187-210.

Shipp S, Zeki S. 2002b. The functional organization of area V2. II. The impact of stripes on visual topography. Vis Neurosci. 19: 211-231.

Silverman MS, Grosof DH, De Valois RL, Elfar SD. 1989. Spatial-frequency organization in primate striate cortex. Proc Natl Acad Sci USA. 86: 711-715.

Sincich LC, Horton JC. 2002a. Divided by cytochrome oxidase: a map of the projections from V1 to V2 in macaques. Science. 295: 1734-1737.

Sincich LC, Horton JC. 2002b. Pale cytochrome oxidase stripes in V2 receive the richest projection from macaque striate cortex. J Comp Neurol. 447: 18-33.

Sincich LC, Horton JC. 2005. Input to V2 Thin Stripes Arises from V1 Cytochrome Oxidase Patches. J Neurosci. 25: 10087-10093.

Sincich LC, Park KF, Wohlgemuth MJ, Horton JC. 2004. Bypassing V1: a direct geniculate input to area MT. Nat Neurosci. 7: 1123-1128.

Singhal A, Kaufman L, Valyear K, Culham JC. 2006. fMRI reactivation of the human lateral occipital complex during delayed actions to remembered objects. Vis Cogn. 14: 122-125.

Sirigu A, Duhamel JR, Cohen L, Pillon B, Dubois B, Agid Y. 1996. The mental representation of hand movements after parietal cortex damage. Science. 273: 1564-1568.

Sokoloff L. 1982. The radioactive deoxyglucose method. Theory, procedure, and applications for the measurement of local glucose utilization in the central nervous system. Advances in neurochemistry. 4: 1-82.

Sokoloff L, Reivich M, Kennedy C, Des Rosiers MH, Patlak CS, Pettigrew KD, Sakurada O, Shinohara M. 1977. The [14C]deoxyglucose method for the measurement of local cerebral glucose utilization: theory, procedure, and normal values in the conscious and anesthetized albino rat. J Neurochem. 28: 897-916.

Sols A, Crane RK. 1954. Substrate specificity of brain hexokinase. J Biol Chem. 210: 581-595.

Spatz WB. 1977. Topographically organized reciprocal connections between areas 17 and MT (visual area of superior temporal sulcus) in the marmoset Callithrix jacchus. Exp Brain Res. 27: 559-572.

Spatz WB, Tigges J, Tigges M. 1970. Subcortical projections, cortical associations, and some intrinsic interlaminar connections of the striate cortex in the squirrel monkey (Saimiri). J Comp Neurol. 140: 155-174.

Steele GE, Weller RE, Cusick CG. 1991. Cortical connections of the caudal subdivision of the dorsolateral area (V4) in monkeys. J Comp Neurol. 306: 495-520.

Stephan KM, Fink GR, Passingham RE, Silbersweig D, Ceballos-Baumann AO, Frith CD, Frackowiak RS. 1995. Functional anatomy of the mental representation of upper extremity movements in healthy subjects. J Neurophysiol. 73: 373-386.

Stepniewska I, Kaas JH. 1996. Topographic patterns of V2 cortical connections in macaque monkeys. J Comp Neurol. 371: 129-152.

Stevens JA, Stoykov ME. 2003. Using motor imagery in the rehabilitation of hemiparesis. Arch Phys Med Rehabil. 84: 1090-1092.

Stone J, Fukuda Y. 1974. Properties of cat retinal ganglion cells: a comparison of W-cells with X- and Y-cells. J Neurophysiol. 37: 722-748.

Suzuki W, Saleem KS, Tanaka K. 2000. Divergent backward projections from the anterior part of the inferotemporal cortex (area TE) in the macaque. J Comp Neurol. 422: 206-228.

Tanaka K. 1996. Inferotemporal cortex and object vision. Annu Rev Neurosci. 19: 109-139.

Tanaka K, Saito H, Fukada Y, Moriya M. 1991. Coding visual images of objects in the inferotemporal cortex of the macaque monkey. J Neurophysiol. 66: 170-189.

Thomas OM, Cumming BG, Parker AJ. 2002. A specialization for relative disparity in V2. Nat Neurosci. 5: 472-478.

Thompson WL, Kosslyn SM, Sukel KE, Alpert NM. 2001. Mental imagery of high-and low-resolution gratings activates area 17. Neuroimage. 14: 454-464.

Thorell LG, De Valois RL, Albrecht DG. 1984. Spatial mapping of monkey V1 cells with pure color and luminance stimuli. Vision Res. 24: 751-769.

Tigges J, Spatz WB, Tigges M. 1974. Efferent cortico-cortical fiber connections of area 18 in the squirrel monkey (Saimiri). J Comp Neurol. 158: 219-235.

Tkach D, Reimer J, Hatsopoulos NG. 2007. Congruent activity during action and action observation in motor cortex. J Neurosci. 27: 13241-13250.

Tlauka M, McKenna FP. 1998. Mental imagery yields stimulus-response compatibility. Acta Psychologica. 98: 67-79.

Tootell RB, Hamilton SL. 1989. Functional anatomy of the second visual area (V2) in the macaque. J Neurosci. 9: 2620-2644.

Tootell RB, Hamilton SL, Switkes E. 1988a. Functional anatomy of macaque striate cortex. IV. Contrast and magno-parvo streams. J Neurosci. 8: 1594-1609.

Tootell RB, Mendola JD, Hadjikhani NK, Ledden PJ, Liu AK, Reppas JB, Sereno MI, Dale AM. 1997. Functional analysis of V3A and related areas in human visual cortex. J Neurosci. 17: 7060-7078.

Tootell RB, Silverman MS, De Valois RL, Jacobs GH. 1983. Functional organization of the second cortical visual area in primates. Science. 220: 737-739.

Tootell RB, Silverman MS, Hamilton SL, De Valois RL, Switkes E. 1988b. Functional anatomy of macaque striate cortex. III. Color. J Neurosci. 8: 1569-1593.

Tootell RB, Silverman MS, Hamilton SL, Switkes E, De Valois RL. 1988c. Functional anatomy of macaque striate cortex. V. Spatial frequency. J Neurosci. 8: 1610-1624.

Tootell RB, Silverman MS, Switkes E, De Valois RL. 1982. Deoxyglucose analysis of retinotopic organization in primate striate cortex. Science. 218: 902-904.

Tootell RB, Switkes E, Silverman MS, Hamilton SL. 1988d. Functional anatomy of macaque striate cortex. II. Retinotopic organization. J Neurosci. 8: 1531-1568.

Ts'o DY, Frostig RD, Lieke EE, Grinvald A. 1990. Functional organization of primate visual cortex revealed by high resolution optical imaging. Science. 249: 417-420.

Ts'o DY, Gilbert CD. 1988. The organization of chromatic and spatial interactions in the primate striate cortex. J Neurosci. 8: 1712-1727.

Ts'o DY, Roe AW, Gilbert CD. 2001. A hierarchy of the functional organization for color, form and disparity in primate visual area V2. Vision Res. 41: 1333-1349.

Tsao DY, Vanduffel W, Sasaki Y, Fize D, Knutsen TA, Mandeville JB, Wald LL, Dale AM, Rosen BR, Van Essen DC, Livingstone MS, Orban GA, Tootell RB. 2003. Stereopsis activates V3A and caudal intraparietal areas in macaques and humans. Neuron. 39: 555-568.

Ungerleider LG, Desimone R. 1986a. Cortical connections of visual area MT in the macaque. J Comp Neurol. 248: 190-222.

Ungerleider LG, Desimone R. 1986b. Projections to the superior temporal sulcus from the central and peripheral field representations of V1 and V2. J Comp Neurol. 248: 147-163.

Ungerleider LG, Desimone R, Galkin TW, Mishkin M. 1984. Subcortical projections of area MT in the macaque. J Comp Neurol. 223: 368-386.

Ungerleider LG, Galkin TW, Desimone R, Gattass R. 2008. Cortical connections of area V4 in the macaque. Cereb Cortex. 18: 477-499.

Ungerleider LG, Galkin TW, Mishkin M. 1983. Visuotopic organization of projections from striate cortex to inferior and lateral pulvinar in rhesus monkey. J Comp Neurol. 217: 137-157.

Ungerleider LG, Haxby JV. 1994. 'What' and 'where' in the human brain. Curr Opin Neurobiol. 4: 157-165.

Ungerleider LG, Mishkin M. 1982. Two cortical visual systems. in *Analysis of Visual Behavior*, Ingle, DJ, Goodale, MA, amd Mansfield, RJ, Eds, MIT Press, Cambridge, MA,. 549.

Valverde F. 1978. The organization of area 18 in the monkey. A Golgi study. Anat Embryol (Berl). 154: 305-334.

Van Essen DC, Maunsell JH. 1983. Hierarchical organization and functional streams in the visual cortex. Trends Neurosci. 6: 370-375.

Van Essen DC, Newsome WT, Bixby JL. 1982. The pattern of interhemispheric connections and its relationship to extrastriate visual areas in the macaque monkey. J Neurosci. 2: 265-283.

Van Essen DC, Newsome WT, Maunsell JH. 1984. The visual field representation in striate cortex of the macaque monkey: asymmetries, anisotropies, and individual variability. Vision Res. 24: 429-448.

Van Essen DC, Newsome WT, Maunsell JH, Bixby JL. 1986. The projections from striate cortex (V1) to areas V2 and V3 in the macaque monkey: asymmetries, areal boundaries, and patchy connections. J Comp Neurol. 244: 451-480.

Van Essen DC, Zeki SM. 1978. The topographic organization of rhesus monkey prestriate cortex. J Physiol. 277: 193-226.

Vanduffel W, Fize D, Mandeville JB, Nelissen K, Van Hecke P, Rosen BR, Tootell RB, Orban GA. 2001. Visual motion processing investigated using contrast agent-enhanced fMRI in awake behaving monkeys. Neuron. 32: 565-577.

Vanduffel W, Tootell RB, Schoups AA, Orban GA. 2002. The organization of orientation selectivity throughout macaque visual cortex. Cereb Cortex. 12: 647-662.

Vanlierde A, De Volder AG, Wanet-Defalque MC, Veraart C. 2003. Occipito-parietal cortex activation during visuo-spatial imagery in early blind humans. Neuroimage. 19: 698-709.

Vishton PM, Rea JG, Cutting JE, Nuñez LN. 1999. Comparing effects of the horizontal-vertical illusion on grip scaling and judgement: Relative versus absolute, not perception versus action. Journal of Experimental Psychology: Human Perception and Performance. 25: 1659-1672.

vogt Weisenhorn DM, Illing RB, Spatz WB. 1995. Morphology and connections of neurons in area 17 projecting to the extrastriate areas MT and 19DM and to the superior colliculus in the monkey Callithrix jacchus. J Comp Neurol. 362: 233-255.

von Bonin G. 1942. The striate area of primates. J Comp Neurol. 77: 405-429.

von Bonin G, Bailey P. 1947. The Neocortex of Macaca Mulatta. University of Illinois Press, Urbana.

von der Heydt R, Peterhans E. 1989. Mechanisms of contour perception in monkey visual cortex. I. Lines of pattern discontinuity. J Neurosci. 9: 1731-1748.

von der Heydt R, Peterhans E, Baumgartner G. 1984. Illusory contours and cortical neuron responses. Science. 224: 1260-1262.

von Economo C. 1929. The Cytoarchitectonics of the Human Cerebral Cortex. Humphrey Milford; Oxford University Press, London.

Wagor E, Lin CS, Kaas JH. 1975. Some cortical projections of the dorsomedial visual area (DM) of association cortex in the owl monkey, Aotus trivirgatus. J Comp Neurol. 163: 227-250.

Walsh V, Carden D, Butler SR, Kulikowski JJ. 1993. The effects of V4 lesions on the visual abilities of macaques: hue discrimination and colour constancy. Behav Brain Res. 53: 51-62.

Walsh V, Kulikowski JJ, Butler SR, Carden D. 1992. The effects of lesions of area V4 on the visual abilities of macaques: colour categorization. Behav Brain Res. 52: 81-89.

Webster MJ, Bachevalier J, Ungerleider LG. 1994. Connections of inferior temporal areas TEO and TE with parietal and frontal cortex in macaque monkeys. Cereb Cortex. 4: 470-483.

Weller RE, Kaas JH. 1983. Retinotopic patterns of connections of area 17 with visual areas V-II and MT in macaque monkeys. J Comp Neurol. 220: 253-279.

Weller RE, Kaas JH. 1985. Cortical projections of the dorsolateral visual area in owl monkeys: the prestriate relay to inferior temporal cortex. J Comp Neurol. 234: 35-59.

Weller RE, Kaas JH. 1987. Subdivisions and connections of inferior temporal cortex in owl monkeys. J Comp Neurol. 256: 137-172.

Westwood DA, Chapman CD, Roy EA. 2000a. Pantomimed actions may be controlled by the ventral visual stream. Exp Brain Res. 130: 545-548.

Westwood DA, Goodale MA. 2003. Perceptual illusion and the real-time control of action. Spat Vis. 16: 243-254.

Westwood DA, Heath M, Roy EA. 2000b. The effect of a pictorial illusion on closed-loop and open-loop prehension. Exp Brain Res. 134: 456-463.

Westwood DA, Heath M, Roy EA. 2003. No evidence for accurate visuomotor memory: Systematic and variable error in memory-guided reaching. J Mot Behav. 35: 127-133.

Westwood DA, McEachern T, Roy EA. 2001. Delayed grasping of a Müller-Lyer figure. Exp Brain Res. 141: 166-173.

Wiesel TN, Hubel DH. 1966. Spatial and chromatic interactions in the lateral geniculate body of the rhesus monkey. J Neurophysiol. 29: 1115-1156.

Wiesel TN, Hubel DH, Lam DM. 1974. Autoradiographic demonstration of ocular-dominance columns in the monkey striate cortex by means of transneuronal transport. Brain Res. 79: 273-279.

Wild HM, Butler SR, Carden D, Kulikowski JJ. 1985. Primate cortical area V4 important for colour constancy but not wavelength discrimination. Nature. 313: 133-135.

Wolpert DM, Ghahramani Z. 2000. Computational principles of movement neuroscience. Nat Neurosci. 3 Suppl: 1212-1217.

Wolpert DM, Goodbody SJ, Husain M. 1998. Maintaining internal representations: the role of the human superior parietal lobe. Nat Neurosci. 1: 529-533.

Wong-Riley M. 1978. Reciprocal connections between striate and prestriate cortex in squirrel monkey as demonstrated by combined peroxidase histochemistry and autoradiography. Brain Res. 147: 159-164.

Wurtz RH. 1969. Visual receptive fields of striate cortex neurons in awake monkeys. J Neurophysiol. 32: 727-742.

Xiao Y, Felleman DJ. 2004. Projections from primary visual cortex to cytochrome oxidase thin stripes and interstripes of macaque visual area 2. Proc Natl Acad Sci USA. 101: 7147-7151.

Xiao Y, Zych A, Felleman DJ. 1999. Segregation and convergence of functionally defined V2 thin stripe and interstripe compartment projections to area V4 of macaques. Cereb Cortex. 9: 792-804.

Yeterian EH, Pandya DN. 1997. Corticothalamic connections of extrastriate visual areas in rhesus monkeys. J Comp Neurol. 378: 562-585.

Yoshioka T, Levitt JB, Lund JS. 1994. Independence and merger of thalamocortical channels within macaque monkey primary visual cortex: anatomy of interlaminar projections. Vis Neurosci. 11: 467-489.

Youakim M, Bender DB, Baizer JS. 2001. Vertical meridian representation on the prelunate gyrus in area V4 of macaque. Brain Res Bull. 56: 93-100.

Yukie M, Iwai E. 1981. Direct projection from the dorsal lateral geniculate nucleus to the prestriate cortex in macaque monkeys. J Comp Neurol. 201: 81-97.

Yukie M, Iwai E. 1985. Laminar origin of direct projection from cortex area V1 to V4 in the rhesus monkey. Brain Res. 346: 383-386.

Zeki S. 1980a. A direct projection from area V1 to area V3A of rhesus monkey visual cortex. Proc R Soc Lond B Biol Sci. 207: 499-506.

Zeki S. 1980b. The representation of colours in the cerebral cortex. Nature. 284: 412-418.

Zeki S. 1983a. Abnormal callosal connections of macaque monkey visual cortex. Proceedings of the Physiological Society. 341: 78p.

Zeki S. 1983b. Colour coding in the cerebral cortex: the reaction of cells in monkey visual cortex to wavelengths and colours. Neuroscience. 9: 741-765.

Zeki S. 1983c. Colour coding in the cerebral cortex: the responses of wavelength-selective and colour-coded cells in monkey visual cortex to changes in wavelength composition. Neuroscience. 9: 767-781.

Zeki S. 1983d. The distribution of wavelength and orientation selective cells in different areas of monkey visual cortex. Proc R Soc Lond B Biol Sci. 217: 449-470.

Zeki S. 1993. A vision of the brain. Oxford ; Boston: Blackwell Scientific Publications.

Zeki S. 2003. Improbable areas in the visual brain. Trends Neurosci. 26: 23-26.

Zeki S, Shipp S. 1988. The functional logic of cortical connections. Nature. 335: 311-317.

Zeki S, Shipp S. 1989. Modular connections between areas V2 and V4 of macaque monkey visual cortex. Eur J Neurosci. 1: 494-506.

Zeki SM. 1969a. Representation of central visual fields in prestriate cortex of monkey. Brain Res. 14: 271-291.

Zeki SM. 1969b. The secondary visual areas of the monkey. Brain Res. 13: 197-226.

Zeki SM. 1970. Interhemispheric connections of prestriate cortex in monkey. Brain Res. 19: 63-75.

Zeki SM. 1971a. Convergent input from the striate cortex (area 17) to the cortex of the superior temporal sulcus in the rhesus monkey. Brain Res. 28: 338-340.

Zeki SM. 1971b. Cortical projections from two prestriate areas in the monkey. Brain Res. 34: 19-35.

Zeki SM. 1973. Colour coding in rhesus monkey prestriate cortex. Brain Res. 53: 422-427.

Zeki SM. 1977a. Colour coding in the superior temporal sulcus of rhesus monkey visual cortex. Proc R Soc Lond B Biol Sci. 197: 195-223.

Zeki SM. 1977b. Simultaneous anatomical demonstration of the representation of the vertical and horizontal meridians in areas V2 and V3 of rhesus monkey visual cortex. Proc R Soc Lond B Biol Sci. 195: 517-523.

Zeki SM. 1978a. The cortical projections of foveal striate cortex in the rhesus monkey. J Physiol. 277: 227-244.

Zeki SM. 1978b. The third visual complex of rhesus monkey prestriate cortex. J Physiol. 277: 245-272.

Zeki SM. 1978c. Uniformity and diversity of structure and function in rhesus monkey prestriate visual cortex. J Physiol. 277: 273-290.

Zeki SM, Sandeman DR. 1976. Combined anatomical and electrophysiological studies on the boundary between the second and third visual areas of rhesus monkey cortex. Proc R Soc Lond B Biol Sci. 194: 555-562.

Zilles K, Clarke S. 1997. Architecture, connectivity and transmitter receptors of human extrastriate visual cortex. Comparison with non-human primates. New York.: Plenum.

Zimmermann-Schlatter A, Schuster C, Puhan MA, Siekierka E, Steurer J. 2008. Efficacy of motor imagery in post-stroke rehabilitation: a systematic review. J Neuroeng Rehabil. 5: 8.

Zipser K, Lamme VA, Schiller PH. 1996. Contextual modulation in primary visual cortex. J Neurosci. 16: 7376-7389.